

Text-to-Image Synthesis: A Decade Survey

Nonghai Zhang Hao Tang*

Abstract—When humans read a specific text, they often visualize the corresponding images, and we hope that computers can do the same. Text-to-image synthesis (T2I), which focuses on generating high-quality images from textual descriptions, has become a significant aspect of Artificial Intelligence Generated Content (AIGC) and a transformative direction in artificial intelligence research. Foundation models play a crucial role in T2I. In this survey, we review over 440 recent works on T2I. We start by briefly introducing how GANs, autoregressive models, and diffusion models have been used for image generation. Building on this foundation, we discuss the development of these models for T2I, focusing on their generative capabilities and diversity when conditioned on text. We also explore cutting-edge research on various aspects of T2I, including performance, controllability, personalized generation, safety concerns, and consistency in content and spatial relationships. Furthermore, we summarize the datasets and evaluation metrics commonly used in T2I research. Finally, we discuss the potential applications of T2I within AIGC, along with the challenges and future research opportunities in this field.

Index Terms—Text-to-Image Synthesis (T2I), Artificial Intelligence Generated Content (AIGC), Foundation Models, Generative Adversarial Networks (GAN), Autoregressive Models (AR), Diffusion Models (DM), Survey



1 INTRODUCTION

Text and images are fundamental means of recording the objective world. As the saying goes, “A picture is worth a thousand words”. When we read pure text, our minds often create corresponding images to help us better understand the content. In computing, text-to-image generation (T2I) [1], [2], [3], [4], [5], [6], [7], [8], [9], [10], [11], [12], [13], [14], [15] combines the fields of natural language processing (NLP) [16], [17], [18] and computer vision (CV) [19], [20], [21], referring to the process of generating realistic images from textual descriptions using specific models. Due to its potential to revolutionize content creation in various domains, T2I has received significant attention. By converting textual descriptions into visual content, this technology bridges the gap between language and imagery, opening new possibilities for art, design, and multimedia applications. Moreover, T2I plays a key role in AI-generated content (AIGC) [22] and represents an important milestone on the path towards general artificial intelligence [23], [24], [25]. Figure 1 shows a series of representative works in the T2I field.

With the advancement of deep learning [48], T2I models have become capable of generating more refined images that closely match textual descriptions. Looking back at the evolution of T2I models, AlignDRAW [1], proposed by Elman Mansimov’s team, is considered a pioneering work in this field. This model effectively demonstrated the relationship between generated images and text descriptions by introducing attention mechanisms [49], although the quality

of the generated images still needed improvement in certain cases.

The introduction of Generative Adversarial Networks (GANs) [50] brought significant progress to T2I. Inspired by conditional GAN (cGAN) [51], Reed et al. designed the GAN-CLS and GNA-INT models [2], which were the first to apply GAN to T2I tasks, demonstrating the advantages of GAN in generating high-quality, detail-rich images. This phase marks an important milestone for the use of GANs in T2I [3], [4], [34].

Using the Transformer architecture [17] from NLP, OpenAI introduced the DALL-E model [7]. This model was the first to employ an autoregressive (AR) for image generation, utilizing large-scale datasets to produce diverse images. Although the AR approach has demonstrated high-quality generation capabilities [9], [35], [45], its substantial computational cost limits its practicality in certain application scenarios.

In recent years, diffusion models (DM) [52], [53], inspired by nonequilibrium thermodynamics, have gradually become the most advanced approach in the T2I field. GLIDE [8] was the first work to apply diffusion models to T2I tasks, demonstrating exceptional generative capabilities by operating in pixel space. The introduction of the Latent Diffusion Model (LDM) [33] highlighted the importance of latent space in diffusion models, significantly improving the quality of the generated images. As research has progressed, diffusion models have demonstrated unparalleled effectiveness [12], [13], [15], making them one of the most popular research directions in T2I.

The continuous advancement of T2I technology has sparked enthusiastic discussions within the community [54]. Various research teams are consistently publishing new papers, and the rapid pace of technological updates poses significant challenges for newcomers trying to get started and stay up to date. Current studies have explored the development of GANs in T2I [55], [56], the progress of DM

- Nonghai Zhang is with the School of Software & Microelectronics, Peking University, Beijing 102600, China. Beijing 100871, China. E-mail: znh@stu.pku.edu.cn
- Hao Tang is with the School of Computer Science, Peking University, Beijing 100871, China. E-mail: haotang@pku.edu.cn

*Corresponding author: Hao Tang.

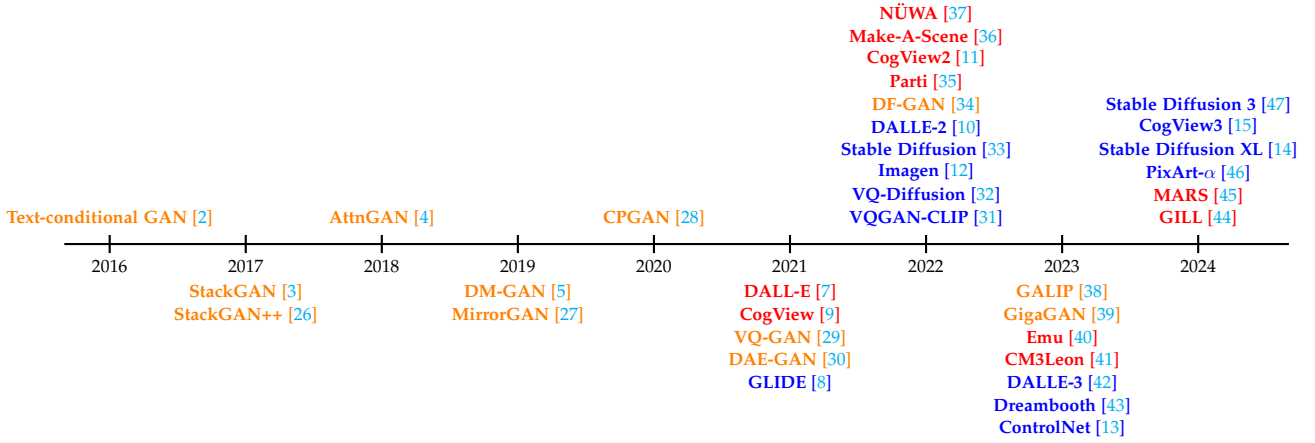


Fig. 1: Representative works on the text-to-image synthesis task over time are shown. The GAN-based methods, autoregressive methods, and diffusion-based methods are highlighted in orange, blue, and red, respectively.

models [57], and relevant work on controllable generation modules [58]. However, comprehensive reviews of the latest directions in T2I remain limited. To help researchers understand the latest advances in T2I, this paper will introduce the basic principles of the GAN, AR, and DM models and provide a detailed review of their progress. Furthermore, this paper will conduct a comprehensive survey of cutting-edge research directions in T2I, with the aim of providing researchers with a clear roadmap and valuable references for further exploration.

The structure of this paper is as follows. Section 2 introduces the mathematical principles and model structures of GANs, AR models, and diffusion models. Section 3 discusses the history of development of these three models, highlighting representative works from different periods, and providing explanations to illustrate their technological evolution. Section 4 explores the latest research directions in T2I, including detailed control, controllable T2I generation, personalized image generation, consistency issues, and concerns related to safety and copyright protection. Section 5 describes the datasets and evaluation metrics currently used in the T2I research and compares the effectiveness of various models using these metrics. Section 6 presents the latest applications of T2I, highlighting its significance and potential impact on AIGC. Finally, Section 7 summarizes the research achievements in T2I, reviews past challenges, and discusses future development directions and recommendations for further research.

2 BASIC MODELS OF T2I

The currently recognized mainstream foundational models for T2I include GANs, autoregressive models, and diffusion models. In this section, we will explore the mathematical principles and underlying mechanisms of these models to understand why they are effective and why they serve as the foundation for T2I research.

2.1 Generative Adversarial Networks (GAN)

GAN was introduced in 2014 [50] and has since been widely applied in various fields of CV [59], [60] and NLP [61] fields, achieving remarkable results. A GAN consists of two main components: a Generator and a Discriminator.

The Generator is responsible for creating samples, while the Discriminator’s role is to distinguish between real samples and those generated by the Generator. Specifically, the Generator creates samples from noise (i.e., random values), and the optimization problem of a GAN is formulated as a minimax problem, with its objective function shown in Equation (1). Given the Generator G , the optimal solution for the Discriminator D is to maximize $V(D)$.

$$\min_G \max_D V(D, G) = \mathbb{E}_{x \sim p_{\text{data}}(x)} [\log D(x)] + \mathbb{E}_{z \sim p_z(z)} [\log(1 - D(G(z)))] \quad (1)$$

In T2I tasks, the GAN working mechanism is more complex and sophisticated [2], [38], [62], [63]. As illustrated in Figure 2, the Generator produces corresponding images by transforming text descriptions into latent vectors [64]. This process often involves Conditional GAN (cGAN) techniques [51], where the Discriminator not only evaluates the quality of the generated images, but also takes into account the related textual information. The feedback from the Discriminator helps the Generator continuously refine its generation strategy, resulting in images that become increasingly realistic and consistent.

2.2 Autoregressive Models (AR)

Autoregressive models were initially used for NLP tasks [65], and their capabilities were further expanded with the introduction of the Transformer architecture [17]. The Image Generative Pre-trained Transformer (iGPT) [66] is a significant work that brought Transformers into the realm of image generation, showcasing their potential in this area. Equation (2) illustrates how the model relies on previously generated parts and the input text prompt when generating each pixel or feature.

$$P(X|T) = \prod_{t=1}^T P(X_t | X_{<t}, T) \quad (2)$$

Inspired by iGPT, DALL-E [7] and CogView [9] were among the first models to apply Transformers to T2I. By generating sequences step by step, these models effectively capture the complex semantic relationships between text and images, achieving results comparable to the state-of-the-art GAN models [4], [5], [34] of their time. As illustrated

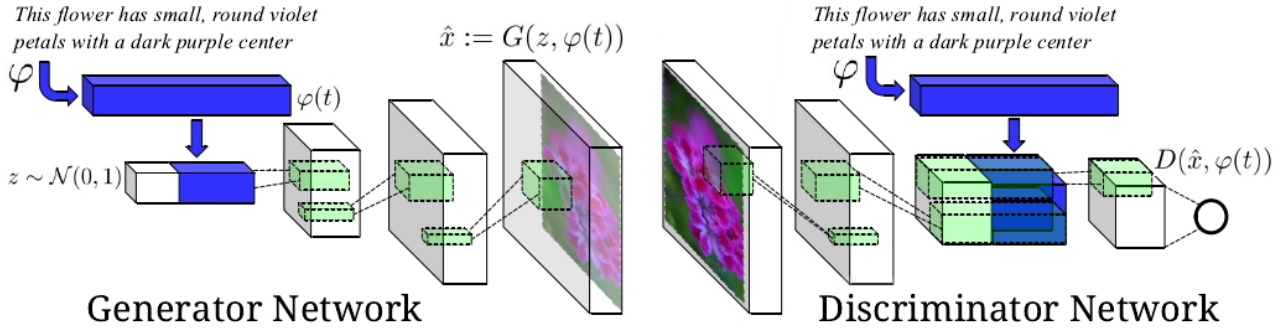


Fig. 2: The text-conditional convolutional GAN architecture [2]. Text encoding $p(t)$ is used by both generator and discriminator. It is projected to lower dimensions and depth concatenated with image feature maps for further stages of convolutional processing.

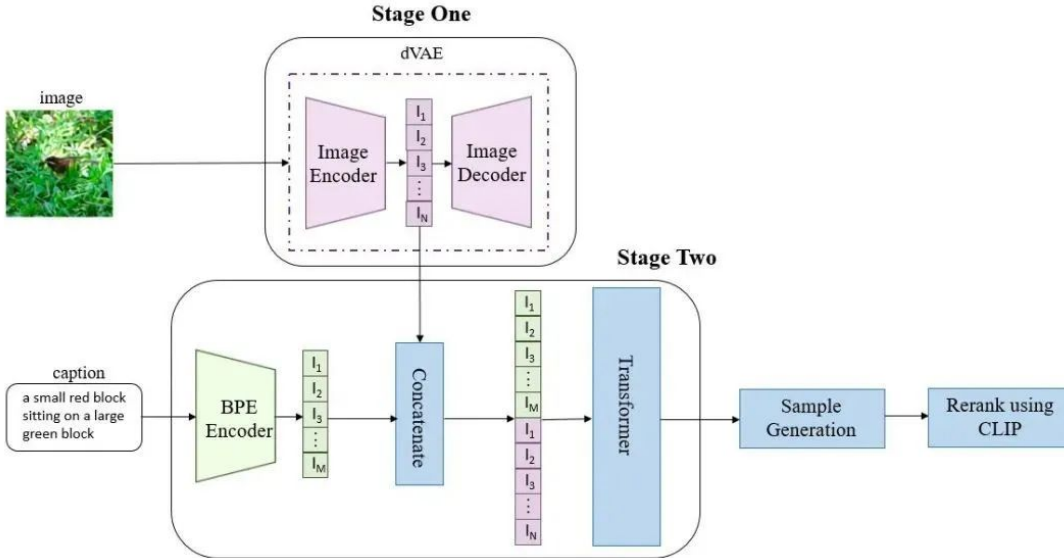


Fig. 3: The training of DALL-E [7] is divided into two stages. The first stage trains the codebook of VQ-VAE, while the second stage trains the Transformer, corresponding to Stage One and Stage Two indicated in the figure.

in Figure 3, DALL-E uses a two-stage Transformer architecture that maps text and image features into a shared latent space and progressively generates each pixel of the image. In the first stage, DALL-E employs a discrete variational autoencoder (dVAE) [67] to compress images. In the second stage, it concatenates 256 text tokens encoded by byte pair encoding (BPE) with 1024 image tokens (32×32) to train an autoregressive Transformer that models the joint distribution of text and image tokens. For the generated series of images, DALL-E utilizes a pretrained CLIP model [68] to evaluate the correspondence between the generated images and the text captions, scoring and ranking them accordingly.

As illustrated in Figure 4, CogView combines text descriptions with image generation employing an autoregressive approach to progressively generate images. First, text and images are converted to tokens using SentencePiece [69] for text and a discrete autoencoder, similar to stage 1 of VQ-VAE [70], for images. The text and image tokens are then concatenated and entered into a unidirectional GPT [65] model to learn image generation. During the T2I generation process, the trained model uses CLIP to rank the generated images by calculating a Caption Score [71], ultimately selecting the image that best matches the input text.

2.3 Diffusion Models (DM)

Building on the fundamental concept of diffusion models [52], Denoising Diffusion Probabilistic Models (DDPM) [53] were introduced in 2020, representing a major milestone in the field. In the forward diffusion process, DDPM gradually adds noise to the data, ultimately resulting in a Gaussian noise distribution. The transformation of data x_0 into x_t at each time step t can be described by Equation (3).

$$x_t = \sqrt{\alpha_t}x_0 + \sqrt{1 - \alpha_t}\epsilon_t. \quad (3)$$

In the denoising diffusion process, the model learns to recover the original data from noise. The generation process is described by Equation (4):

$$p_\theta(x_{t-1}|x_t) = \mathcal{N}(x_{t-1}; \mu_\theta(x_t, t), \Sigma_\theta(x_t, t)), \quad (4)$$

where μ_θ and Σ_θ are the mean and variance parameters learned by the model.

In T2I, the generation process is also conditioned on the text prompt, which can be represented by Equation (5): where T is the input text prompt, and the model generates images related to the text through conditional diffusion.

$$p_\theta(x_0|T) = \int p_\theta(x_0|x_1)p_\theta(x_1|T) dx_1. \quad (5)$$

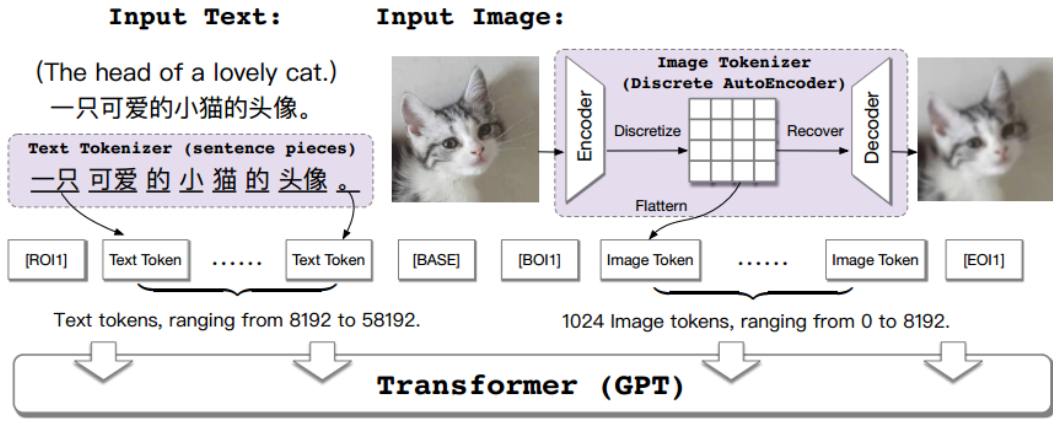


Fig. 4: The framework of CogView [9]. [ROI1], [BASE1], etc., are separator tokens.

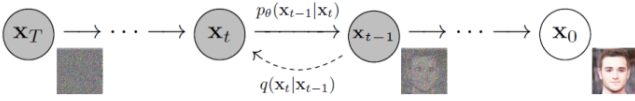


Fig. 5: DDPM [53] generates new images by adding noise and then denoising.

As illustrated in Figure 5, the diffusion process gradually adds Gaussian noise to the original image in a fixed Markov chain, ultimately transforming the image into Gaussian noise. The reverse process then restores the original image step by step through denoising, achieving image generation. This approach is known for its excellent generative performance [72], which offers new insights for T2I tasks by progressively transforming text descriptions into high-quality images using the diffusion process.

GLIDE [8] is considered the first work to explore T2I using DDPM. This study compared two different guidance strategies: CLIP guidance [68] and classifier-free guidance [73]. The latter achieved more realistic and detailed images by replacing original category labels with text. The results of GLIDE are shown in Figure 7.

Stable Diffusion was the first to apply diffusion models in the latent space of a powerful pretrained autoencoder, serving as a demonstration of the Latent Diffusion Model (LDM) [33]. As illustrated in Figure 6, it follows a two-stage approach: in the first stage, the image is compressed into a latent representation [64] to reduce computational complexity; in the second stage, a DDPM structure is used. In addition, a cross-attention mechanism [17] was introduced, which allows text or image sketches to influence the diffusion model and generate the desired images.

3 DEVELOPMENT OF GAN, AR, AND DM IN T2I

In Section 2, we introduce the foundational work on GAN [2], AR [7], and DM [8] in the field of T2I. In this section, we will discuss the development of these three models in T2I, providing a comprehensive overview of their evolution from their inception to the present, in order to illustrate the ongoing advancement of foundational models in T2I.

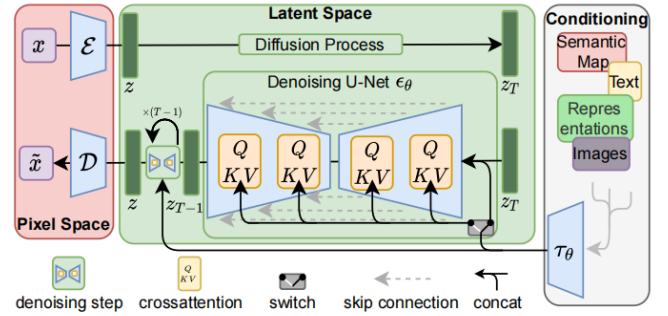


Fig. 6: The condition LDM [33] either via concatenation or by a more general cross-attention mechanism.

3.1 Developments of GAN Models in T2I

As shown in Table 1, the application of GANs in the T2I field has seen significant advances. The work of Reed et al. [2] in 2016 marked the first application of GANs in T2I, utilizing a conditional GAN (cGAN) structure [51], which laid the foundation for subsequent research.

The following year, StackGAN [3] was introduced, which generates images in a two-stage manner. In the first stage, basic shapes and colors were drawn on the basis of the given text description to produce low-resolution images. In the second stage, the output from the first stage was refined by combining it with the text description to generate high-resolution images, significantly improving the quality of the generated images. Building on this, StackGAN++ [26] adopted a tree structure with multiple generators and discriminators to improve image generation. The images were progressively refined from low to high resolution through different branches of the tree, further improving image details and consistency, while enhancing the model's ability to understand text descriptions. Meanwhile, TACGAN [74] introduced an adaptive control mechanism that incorporated auxiliary classification tasks into the discriminator, allowing it to more accurately identify text categories and thereby produce images that better align with text descriptions.

In 2018, AttnGAN [4] built on StackGAN++ by integrating attention mechanisms into a multistage optimization pipeline. This integration allowed the model to focus more on the key elements of the text, thereby enhancing semantic consistency in the generated images. Beyond using global

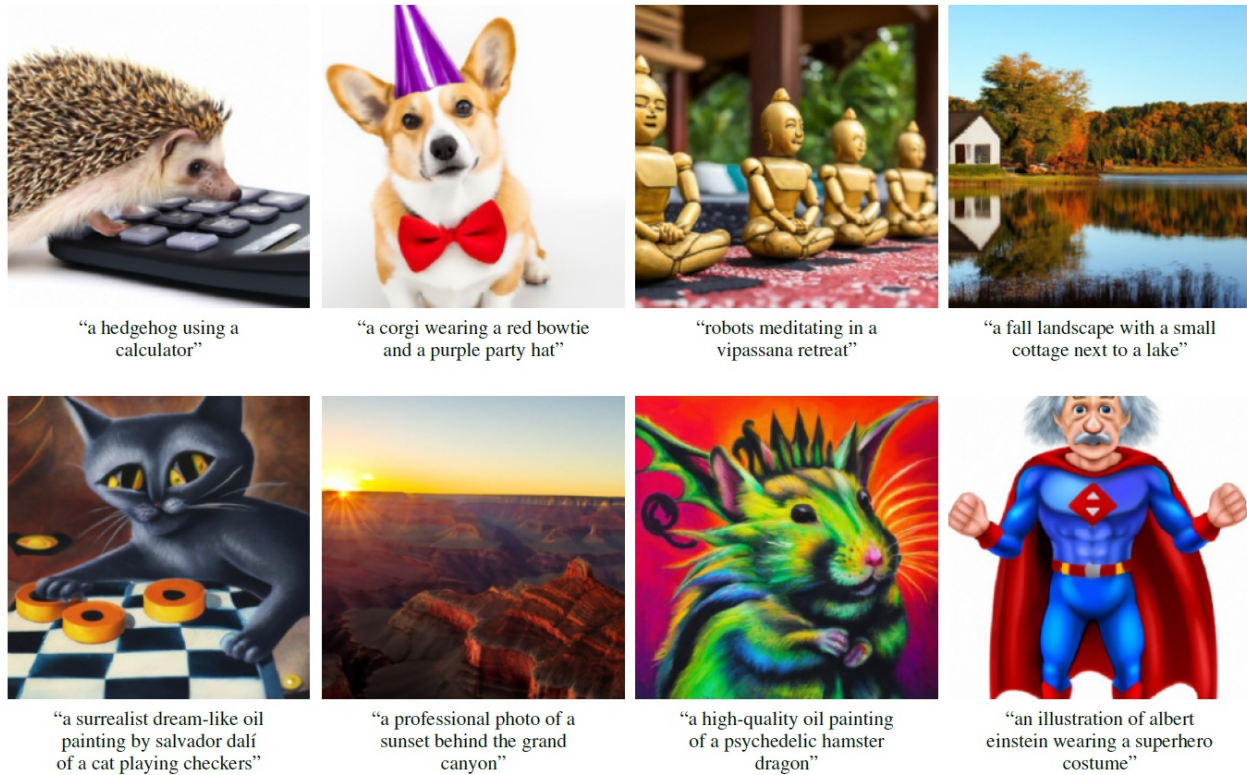


Fig. 7: Selected samples from GLIDE [8] using classifier-free guidance. We observe that the model can produce photorealistic images with shadows and reflections, can compose multiple concepts in the correct way, and can produce artistic renderings of novel concepts.

sentence vectors, the attention mechanism also enabled the synthesis of fine-grained details based on relevant words. Fused GAN [75] combined multimodal information from both images and text, using two generators for conditional and unconditional image synthesis. These generators partially shared a common latent space, allowing one generator to perform both types of synthesis simultaneously. HDGAN [76] focused on generating high-resolution images, with a generator designed to capture complex image features. Using a deep generative model architecture, HDGAN improved the detail representation of images, resulting in more coherent output.

In 2019, the development of GANs in the T2I field flourished. ControlGAN [80] enabled users to control specific attributes of generated images, allowing manipulation of visual properties such as categories, textures, and colors. DM-GAN [5] integrated diffusion model concepts and introduced a dynamic memory module to refine blurred image content, helping to prevent poor results during initial image generation. GauGAN [79] was noted for generating realistic images from user-drawn sketches, using semantic layouts to produce photorealistic effects, thereby providing an interactive image generation experience. MirrorGAN [27] employed a bidirectional generation mechanism to map text to images and back, improving semantic coherence in the outputs. This model introduced a new framework that combined global and local attention with semantic preservation, redefining text-to-image generation. Obj-GAN [78] focused on generating images with specific objects and attributes, enhancing the targeted nature of generation and enabling the synthesis of complex scenes from textual descriptions through attention-driven multistage optimiza-

tion. Text-SeGAN [77] utilized sequential generation to improve coherence in generated images, allowing the synthesis of diverse images from text descriptions.

In 2020, CookGAN [81] focused on image generation in specific domains, optimizing the generation process to simulate visual effects within causal chains, thus demonstrating the flexibility of GANs. CPGAN [28] enhanced semantic consistency between text and images by delving deeply into their content. RiFeGAN [6] adopted a fine-grained control strategy, becoming a T2I model with novel and rich features. SegAttnGAN [82] integrated additional segmentation information with attention mechanisms, further improving the realism of generated images.

In 2021, VQ-GAN [29] achieved efficient image generation by compressing continuous data and using vector quantization. XMC-GAN [62] enhanced the complementarity between text and images through cross-modal learning, employing intermodal and intramodal contrastive learning to maximize mutual information, thus addressing the cross-modal contrastive loss issue in T2I generation. DAE-GAN [30] incorporated the concepts of denoising autoencoders to improve the robustness of generated images. CI-GAN [83] focused on diversifying image content and style, enhancing the artistic quality of the generated output. R-GAN [84] generated coherent images in a human-like manner, demonstrating naturalness and consistency in its generation process.

In 2022, DF-GAN [34] directly generated high-resolution images in the first stage and introduced a novel target-aware discriminator in the second stage to improve the consistency between text and images. LAFITE [87] used CLIP to guide the generation process, enhancing the quality and inter-

TABLE 1: Overview of GAN models in T2I by year.

Year	Source	Model and Description
2016	ICML	Text-conditional GAN [2]: The first GAN used for T2I tasks.
2017	arXiv ICCV TPAMI	TAC-GAN [74]: Incorporated auxiliary classification tasks into the discriminator. StackGAN [3]: 1. Generate Stage-I low-resolution images; 2. Generate high-resolution images using text descriptions. StackGAN++ [26]: Composed of multiple generators and discriminators in a tree-like structure.
2018	ECCV CVPR CVPR	Fused GAN [75]: Two generators for conditional and unconditional image synthesis. HDGAN [76]: Accompanying hierarchical-nested adversarial objectives inside the network hierarchies. AttnGAN [4]: Integrates attention mechanisms into a multi-stage optimization pipeline.
2019	AAAI CVPR CVPR SIGGRAPH CVPR Access	Text-SeGAN [77]: Modify the discriminator to regress semantic relevance between text and image. Obj-GANs [78]: Using a novel object-wise discriminator based on the Fast R-CNN. MirrorGAN [27]: Focuses on global and local attention and semantic preservation. GauGAN [79]: Using spatially-adaptive normalization. DM-GAN [5]: Refines blurry images using a dynamic storage module. ControlGAN [80]: Manipulates visual attributes in T2I generation.
2020	CVPR ECCV CVPR arXiv	RiFeGAN [6]: Enriching the given caption from prior knowledge, formed by the training dataset. CPGAN [28]: Design a memory mechanism in text and encode the generated image in an object-aware manner. CookGAN [81]: Simulates visual effects in the causal chain. SegAttnGAN [82]: Utilizes segmentation information for synthesis.
2021	CVPR CVPR ICCV ACM MM ACM MM	XMC-GAN [62]: Addresses cross-modal contrastive loss. VQ-GAN [29]: Discrete vector representations in VQ space. DAE-GAN [30]: Comprehensively represents information from sentence-level, word-level, and aspect-level. CI-GAN [83]: Learns similarity between text representations and latent encodings. R-GAN [84]: Constructing a scene graph to capture the monolithic structural representation of the text.
2022	ECCV TMM CVPR CVPR CVPR ECCV	VQGAN-CLIP [31]: Guides VQGAN using CLIP. VLMGAN [85]: Enhances image quality and consistency through a dual vision-language matching mechanism. DF-GAN [34]: Novel one-stage text-to-image backbone, Target-Aware Discriminator and deep text-image fusion block. SSA-GAN [86]: a Semantic-Spatial Aware block learns semantic-adaptive transformations and generates semantic masks. LAFITE [87]: The first work enables the language-free training using pretrained CLIP model. AttnGAN++ [63]: Adding the spectral normalization layers to the discriminator based on AttnGAN.
2023	CVPR ICML CVPR TMM CVPR SIGGRAPH	GigaGAN [39]: The first GAN-based method trains a billion-scale model on billions of real-world complex Internet images. StyleGAN-T [88]: Using Fourier features, a second-order style mechanism, and improved text conditioning mechanisms. GALIP [38]: Leverages the powerful pretrained CLIP model both in the discriminator and generator. RAT-GAN [89]: Propose a recurrent affine transformation (RAT) connects all the CAT blocks. Layout-VQGAN [90]: Propose an object-guided joint-decoding module. DragGAN [91]: An interactive point-based image editing framework.
2024	CVPR CVPR	UFOGen [92]: Hybrid approach integrating diffusion with GAN objectives. HyperCGAN [93]: Represents 2D images as implicit neural representations.

pretability of the generated images. SSA-GAN [86] introduced an adaptive selection mechanism to refine generation details based on different text descriptions. VLMGAN [85] combined visual and language models to improve semantic understanding capabilities in image generation. VQGAN-CLIP [31] integrated VQGAN and CLIP models to allow efficient T2I generation. AttnGAN++ [63] expanded on AttnGAN by employing spectral normalization to stabilize training.

In 2023, RAT-GAN [89] adopted recursive affine transformations to incorporate conditional information during generation. GALIP [38] improved the quality of the generated images by combining image generation with language understanding, integrating CLIP into both the discriminator and generator. GigaGAN [39] achieved high-quality image generation through large-scale data training, surpassing the state-of-the-art performance of diffusion models. GigaGAN is considered to produce results comparable to those of diffusion models while offering faster generation speeds. Some of its results are illustrated in Figure 8. StyleGAN-T [88] focused on style transfer, increasing the diversity of generated images. Layout-VQGAN [90] used layout information to generate complex scenes, enhancing the structural representation of the generated images. Meanwhile, DragGAN [91] introduced a point-based interactive image editing method, allowing pixel-level precision in the editing

results.

In recent research, UFOGen [92] aims at ultra-fast one-step T2I using a hybrid approach that combines diffusion models with GAN objectives. HyperCGAN [93] addresses the T2I task from a different perspective, representing two-dimensional images as implicit neural representations (INRs) [94] and controlling the INR-GAN generation process using weight modulation operators based on word-level attention, through the use of a supernet.

These evolving GAN models not only improve the quality of T2I generation but also broaden their application scope, driving rapid advancements in the T2I field. With ongoing technological innovations, future research is expected to focus more on the accuracy and controllability of generation, providing users with an increasingly rich generation experience.

3.2 Developments of AR Models in T2I

The latest advances in autoregressive models in the field of T2I demonstrate their strong generative capabilities and remarkable flexibility.

As shown in Table 2, DALL-E [7], based on the Transformer architecture [17], became the first large-scale autoregressive T2I model, demonstrating the tremendous potential of autoregressive models in T2I tasks. Building on this foundation, CogView [9] further improved generation quality

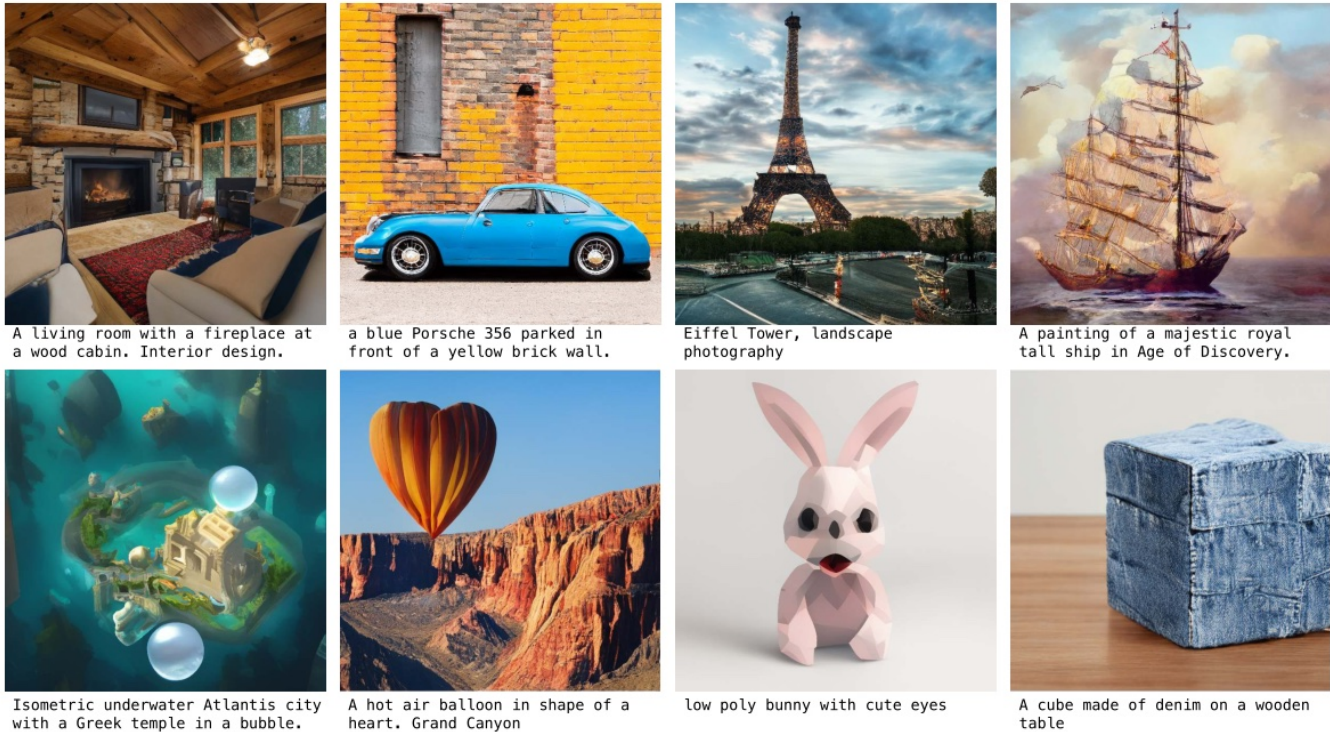


Fig. 8: The model, GigaGAN [39], shows GAN frameworks can also be scaled up for general T2I synthesis and superresolution tasks, generating a 512px output at an interactive speed of 0.13s, and 4096px within 3.7s. Selected examples at 2K resolution.

by combining VQ-VAE with autoregressive strategies, producing diverse images, and improving the user-interaction experience. Meanwhile, M6 [95] provided a large dataset for multimodal pre-training in Chinese, and Parti [35] enhanced the detail representation of generated images through image patch processing, similar to machine translation, where image token sequences are used as target outputs.

CogView2 [11], an upgraded version of CogView, not only improved generation quality but also supported text-based interactive image editing. Make-A-Scene [36] introduced scene understanding capabilities, allowing users to specify elements in the generated images more precisely, thus enhancing control and accuracy. NUWA [37] combined autoregressive generation with multimodal information, allowing the creation of new visual data or the manipulation of existing visual data (such as images and videos) to meet various visual synthesis tasks. Emu [40] proposed a quality tuning method that effectively guides the pretrained model to generate visually appealing images while maintaining generality with respect to visual concepts. CM3Leon [41] used an improved autoregressive mechanism and became the first multimodal model trained using an approach adapted from text-specific language models, including a large-scale retrieval-augmented pretraining phase followed by a multitask supervised fine-tuning (SFT) phase.

GILL [44] integrated frozen text-only large language models (LLMs) [65], [101] with pretrained image encoder and decoder models through autoregressive modeling, mapping between their embedding spaces. MARS [45] retained the NLP capabilities of LLMs while also providing them with enhanced visual understanding. Unified-IO 2 [96] consolidated autoregressive generative capabilities across

multiple tasks, including T2I generation, image understanding, and image-to-image generation, demonstrating broad applications in T2I. STAR [97] adopted a scale-wise autoregressive paradigm for T2I modeling, enhancing the coherence of the generated images and improving alignment with the text descriptions. HART [98] introduced a hybrid tokenizer to achieve efficient high-resolution visual synthesis, combining autoregressive models with adversarial generation to enhance the diversity and realism of the generated images.

Recently, the SJD method used in AR [99] enhanced the richness of generated content by integrating autoregressive strategies with structured data and introducing Jacobi techniques to accelerate the autoregressive model. On the other hand, DART [100] utilized a denoising autoregressive encoder, incorporating a dynamic adjustment mechanism into the generation process, thus improving the adaptability to complex text descriptions and increasing the diversity of generated outputs.

These continuously evolving autoregressive models not only enhance the quality of T2I but also drive rapid advancements in the field, demonstrating the unique advantages of autoregressive methods in multimodal generation. With ongoing technological innovations, future research is expected to focus more on the accuracy and controllability of generation, providing users with an increasingly rich generative experience.

3.3 Rapid Rise of Diffusion Models in T2I

As noted by OpenAI, diffusion models have significant advantages in image generation [72]. In recent years, diffusion models have rapidly gained prominence in the field of T2I,

TABLE 2: Overview of AR models in T2I by year.

Year	Source	Model and Description
2021	ICML	DALL-E [7]: The first to use AR for generation in T2I.
	NeurIPS arXiv	CogView [9]: A 4-billion-parameter Transformer with a VQ-VAE tokenizer. M6 [95]: The largest dataset for Chinese multimodal pre-training.
2022	TMLR NeurIPS ECCV ECCV	Parti [35]: Uses image token sequences as the target output instead of text tokens. CogView2 [11]: A solution based on hierarchical transformers and local parallel autoregressive generation. Make-A-Scene [36]: Control mechanism complementary to text in the form of a scene. NÜWA [37]: Using a 3D transformer encoder-decoder framework.
	arXiv NeurIPS	Emu [40]: Quality-tuning to effectively guide a pretrained model. CM3Leon [41]: The first multimodal model trained using a recipe adapted from text-specific language models.
2024	arXiv CVPR arXiv arXiv arXiv NeurIPS arXiv	MARS [45]: Retains NLP capabilities of LLMs while endowing specialized visual understanding. Unified-IO 2 [96]: The first model trained on a diverse and extensive skill set, unifying three generative abilities. STAR [97]: Employs a scale-wise autoregressive paradigm for text-to-image modeling. HART [98]: Introduces a hybrid tokenizer for efficient high-resolution visual synthesis. SJD+AR [99]: Integrating Jacobi to accelerate the autoregressive model. GILL [44]: Combining frozen large language models (LLMs) with pretrained image encoder and decoder models. DART [100]: Utilizes a denoising autoregressive encoder.

sparkling widespread interest and inspiring new research that reflects the enthusiasm of the scientific community. The development of Denoising Diffusion Probabilistic Models (DDPM) in T2I is summarized in Table 3. GLIDE [8] was the pioneering application of diffusion models in T2I, marking an important milestone and highlighting the potential of diffusion models for T2I tasks.

VQ-Diffusion [32] uses vector quantization technology for efficient generation, while Imagen [12] combines the strengths of Transformer language models and high-fidelity diffusion models by using a pretrained language model to encode text. Stable Diffusion (LDMs) [33] offers strong generative capabilities through latent space optimization. DALL-E 2 [10] is a two-stage model: first, a prior model generates CLIP image embeddings based on text descriptions, and then a decoder generates images conditioned on these embeddings.

Additionally, Blended Diffusion [102] uses natural language guidance to generate realistic and diverse images. PixArt- α [46], based on the Transformer T2I diffusion model, excels in artistic style generation. DALL-E 3 [42] combines an image encoder with the GPT-4 language model [126], allowing it to generate detailed textual descriptions for each image, further enhancing text understanding and generation quality. Stable Diffusion XL [14] is an upgraded version of Stable Diffusion, featuring a backbone network [127] that is three times larger. DreamBooth [43] allows users to customize image generation with a few examples, while ControlNet [13] introduces additional control parameters into the generation process, enhancing flexibility.

Specialist Diffusion [103] extends the existing single-stream diffusion process into a multi-task, multi-modal network called Versatile Diffusion (VD), which can handle multiple streams such as text-to-image, image-to-text, and their variants within a unified model. UniDiffuser [104] integrates various generative capabilities based on a Transformer framework that accommodates multimodal data distributions, allowing it to process text-to-image, image-to-text, and joint image-text tasks simultaneously. Multimodal-CoT [128] uses a chain-of-thought mechanism [129] to combine language (text) and visual (image) modalities in a two-stage framework that separates inference generation from answer reasoning. This approach allows answer reasoning

to build on a stronger inferential foundation generated from multi-modal information.

Versatile Diffusion [105] is the first unified multistream multimodal diffusion framework, while Custom Diffusion [106] is an efficient enhancement method for existing T2I models, allowing users to customize the generation process and achieve rapid fine-tuning. SVDiff [107] involves fine-tuning the singular values of weight matrices [130], creating a compact and efficient parameter space that reduces the risk of overfitting and language drift. ERNIE-ViLG 2 [108] is the first large T2I model in the Chinese language domain, integrating fine-grained textual knowledge and key visual elements, such as adding part-of-speech descriptions (verbs, nouns, adjectives) to the text and incorporating object recognition preprocessing for images.

Corgi [109] proposes an offset diffusion model that improves the generation of image embeddings from input text. Würstchen [110] develops a latent diffusion technique that uses a detailed yet compact semantic image representation to guide the diffusion process. ConPreDiff [113] improves diffusion-based image synthesis through context prediction, while ContextDiff [125] incorporates the cross-modal context, including interactions and alignment between text conditions and visual samples, into both forward and backward diffusion processes.

CogView3 [15] is the first model to implement relay diffusion [131] in T2I. Stable Diffusion 3 (SD3) [47] introduces a new Transformer-based architecture for T2I that assigns different weights to text and image modalities, allowing bidirectional information flow between images and text annotations. SD3 is currently considered the leading open source T2I model, with examples of its generated results shown in Figure 9. Ranni [111] provides a control panel for managing T2I, while RPG [112] uses a Multimodal Large Language Model (MLLM) [18] as a global planner. It breaks down the process of generating complex images into simple generation tasks across multiple subregions, using complementary regional diffusion to achieve region-level combinatorial generation. Additionally, RPG integrates text-guided image generation and editing in a closed-loop manner, enhancing the model’s generalization capabilities. DistriFusion [114] leverages parallelism across multiple GPUs, supports asynchronous communication, and can be

TABLE 3: Overview of DM models in T2I by year.

Year	Source	Model and Description
2021	arXiv	GLIDE [8]: The first diffusion work in T2I.
2022	CVPR NeurIPS CVPR arXiv CVPR	VQ-Diffusion [32]: Based on a vector quantization diffusion model. Imagen [12]: Combines Transformer language models and diffusion processes. Stable Diffusion [33]: Applies the diffusion model to the latent space of a powerful pretrained autoencoder. DALLE-2 [10]: A two-stage model generating CLIP image embeddings based on text. Blended Diffusion [102]: Using natural language guidance to produce realistic and diverse images.
2023	arXiv CVPR ICCV CVPR ICML ICCV CVPR ICCV CVPR CVPR	DALLE-3 [42]: Using diffusion based on DALLE-2 and using GPT-3. Dreambooth [43]: Fine-tunes a pretrained T2I model using a few images of an object. ControlNet [13]: Adds spatial conditional control to a large pretrained text-to-image diffusion model. Specialist Diffusion [103]: Handles multiple streams of text-to-image and image-to-text within a unified model. UniDiffuser [104]: Perturbs data in all modalities instead of a single modality. Versatile Diffusion [105]: Handles multiple flows of text-to-image, image-to-text, and variations in one unified model. Custom Diffusion [106]: Optimizing a few parameters in the text-to-image conditioning mechanism. SVDiff [107]: Fine-tunes singular values of weight matrices for a compact parameter space. ERNIE-ViLG 2 [108]: The first large T2I model in the Chinese field. Corgi [109]: Based on a shifted diffusion model.
2024	arXiv ICML ICLR ICLR ICLR CVPR ICML NeurIPS CVPR CVPR CVPR CVPR arXiv arXiv arXiv arXiv arXiv arXiv CVPR ICLR	CogView3 [15]: Implementing relay diffusion in text-to-image generation. Stable Diffusion 3 [47]: Uses different weights for modalities, enabling bidirectional information flow. Würstchen [110]: Develops a latent diffusion technique using a compact semantic image representation. Stable Diffusion XL [14]: Utilizes a three times larger UNet backbone network. PixArt-α [46]: By 1) Training strategy decomposition. 2) Efficient T2I Transformer. 3) High-informative data. Ranni [111]: Using a semantic panel as the middleware and incorporating visual concepts parsed by LLM. RPG [112]: Integrates text-guided image generation and editing through MLLMoRPG. ConPreDiff [113]: Improves diffusion-based image synthesis through context prediction. DistriFusion [114]: Uses parallelism across multiple GPUs for integration into computational pipelines. InstanceDiffusion [115]: Increases precise instance-level control by UniFusion, ScaleU and Multi-instance Sampler blocks. Instruct-Imagen [116]: Handling heterogeneous image generation tasks by multi-modal instruction. ElasticDiffusion [117]: Decouple the generation trajectory of a pretrained model into local and global signals. PIXART-δ [118]: Integration of LCM significantly accelerates inference speed. PixArt-Σ [119]: Evolves from the weaker 'baseline' to a stronger 'model' via incorporating higher quality data. SD3-Turbo [120]: Introduces latent adversarial diffusion distillation (LADD). StreamMultiDiffusion [121]: The first real-time region-based text-to-image generation framework. OmniGen [122]: Unifying image generation architecture, simplifying user workflows, enabling effective knowledge transfer. Hunyuan-DiT [123]: Using carefully designed transformer architecture and a MLLM. DragDiffusion [124]: Enhances interactive point-based editing for real and diffusion-generated images. ContextDiff [125]: Incorporating cross-modal context into both the forward and reverse diffusion processes.

integrated with computational pipelines for fast T2I generation. InstanceDiffusion [115] enhances precise instance-level control, while Instruct-Imagen [116] is designed to handle diverse image generation tasks and generalize to unseen tasks.

ElasticDiffusion [117] introduces a new decoding strategy that uses a pretrained diffusion model to generate images of arbitrary sizes while maintaining a constant memory footprint during inference. PIXART- δ [118] significantly accelerates inference speed through the integration of LCM [132], enabling high-quality image generation in just 2-4 steps. It also introduces an innovative ControlNet-Transformer [13] architecture specifically designed for transformers, providing explicit controllability and high-quality image generation. PixArt- Σ [119] offers significantly higher image fidelity and better alignment with text prompts.

Recently, SD3-Turbo [120] introduced Latent Adversarial Diffusion Distillation (LADD), a novel distillation method that overcomes the limitations of Adversarial Diffusion Distillation (ADD) [133]. Unlike the pixel-based ADD, LADD leverages the generative features of a pretrained latent diffusion model. StreamMultiDiffusion [121] is the first real-time region-based T2I generation framework. OmniGen [122] presents a new type of diffusion model for unified image generation, while Hunyuan-DiT [123] is a T2I diffusion transformer with fine-grained understanding capabilities. The results of the Hunyuan-DiT generation are shown in Figure 10. In terms of image generation in Chinese,

Hunyuan-DiT outperforms existing open source models, including SD3, in text-image consistency, elimination of AI artifacts, subject clarity and aesthetics. Its performance in subject clarity and aesthetics is comparable to that of leading closed-source models like DALLE-3. DragDiffusion [124] optimizes only the latent variables for a single time step, achieving efficient and precise spatial control, which significantly enhances the applicability of interactive point-based editing for both real and diffusion-generated images.

The rapid development of these models has not only advanced T2I generation technology but also created new opportunities for multimodal generation.

4 RECENT RESEARCH DIRECTIONS IN T2I

Research on T2I generation not only focuses on improving the performance metrics of various models [223], [228] but also requires deeper exploration of more specific topics. This section discusses key research directions in T2I based on the latest findings, including but not limited to controllable T2I generation [13], [163], personalized image generation [43], [139], consistency issues in generation [263], [264], [295], [296], safety concerns [245], [251], copyright protection [257], [262], incorporating human feedback [134], [135], style transfer [188], [194], fine-grained generation control [318], [323], and the supporting role of large language models (LLMs) in T2I [335], [337]. As shown in Table 4, these studies not only enhance the performance of generative models,

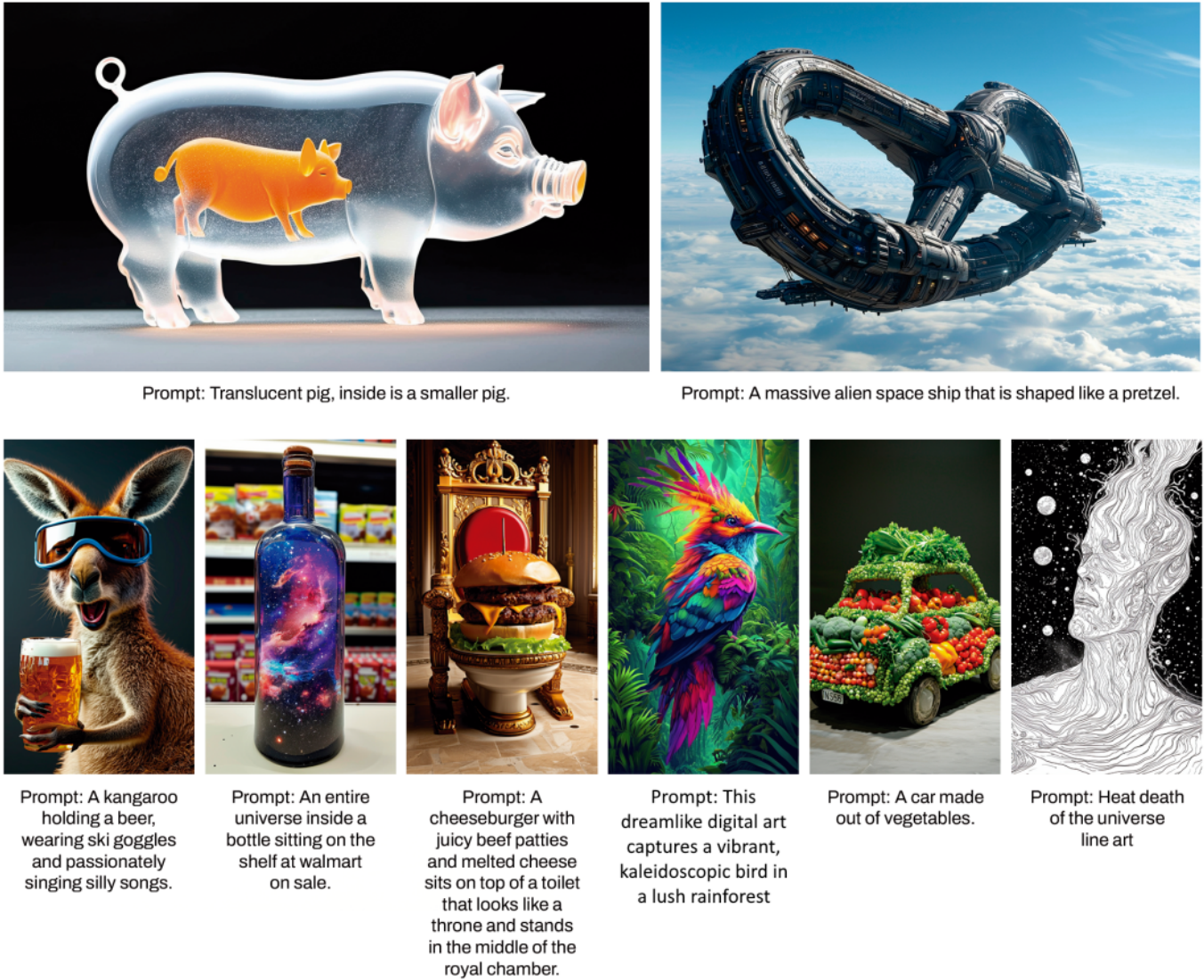


Fig. 9: Sampling is derived from Stable Diffusion 3 [47], generating fantastical pictures.



请将杞人忧天的样子画出来。
Please draw a man from Qi who was haunted by the fear that the sky might fall.

醉后不知天在水，满船清梦压星河。
After drinking I don't know the sky is in the water, the boat is full of clear dreams that presses the star river.

枯藤老树昏鸦，小桥流水人家。
Withered vines, old trees, there are some crows at dusk; A small bridge, flowing water, some huts.

Fig. 10: Hunyuan-DiT [123] can generate images containing Chinese elements. In this report, without further notice, all the images are directly generated using Chinese prompts.

but also provide greater flexibility and safety for practical applications.

4.1 Alignment and Human Feedback

In the field of T2I research, scholars face a range of challenges, including artifacts in generated images, inconsistencies with text descriptions, and deficiencies in aesthetic

quality. Ensuring alignment between generated images and text descriptions, as well as with human cognition, has consistently been a key area of focus in T2I research [343].

The ImageReward model [137], as the first general-purpose human preference reward model for T2I, effectively encodes human preferences and supports Reinforcement Learning from Human Feedback (ReFL). ReFL is a direct tuning algorithm that has shown advantages over other methods through both automatic and human evaluations.

Inspired by the success of human feedback learning [344] in large language models, Liang et al. [134] collected extensive human feedback and designed RAHF, a multimodal Transformer model. As illustrated in Figure 11, RAHF uses self-attention mechanisms to understand and predict human evaluations of generated images, significantly improving its ability to identify inconsistencies between text and images.

DiffAgent [135], an LLM-based model agent, adopts a novel two-stage training framework (SFTA), which enables it to accurately align T2I API responses with user input based on human preferences.

In terms of the impact of datasets on alignment research,

TABLE 4: Overview of T2I research directions.

Research Area	Model
Sec.4.1: Alignment and Human Feedback	RAHF [134], DiffAgent [135], HPS [136], ImageReward [137], Multi-dimensional Human Preference (MHP) [138], MPS [138]
Sec.4.2: Personalized Generation	Textual Inversion [139], PIA [140], Prompt-Free Diffusion [141], ADI [142], HyperDreamBooth [143], DreamBooth [43], Personalized Residuals [144], PALP [145], PhotoMaker [146], DreamTurner [147], ELITE [148], Tailored Visions [149], RealCustom [150], SAG [151], CoRe [152], Imagine Yourself [153], FastComposer [154], InstantID [155], Specialist Diffusion [103], ControlStyle [156], UniPortrait [157], TIGC [158], DETEX [159], FlashFace [160], IDAdapter [161], SSR-Encoder [162]
Sec.4.3: Controllable T2I Generation	ControlNet [13], T2I-Adapter [163], Custom Diffusion [106], SID [164], JeDi [165], ViCo [166], DreamMatcher [167], RealCustom [150], StyleGAN Meets Stable Diffusion [168], Uni-ControlNet [169], BLIP-Diffusion [170], LayerDiffusion [171], ReCo [172], SpaText [173], Codi [174], StyleTokenizer [175], P+ [176], IP-Adapter [177], ResAdapter [178], DetDiffusion [179], CAN [180], SceneDiffusion [181], Zero-Painter [182], FreeControl [183], PCDMs [184], ControlNet++ [185], ControlNeXt [186], Composer [154], MultiDiffusion [187]
Sec.4.4: T2I Style Transfer	Styleformer [188], InST [189], ArtAdapt [190], InstantBooth [191], OSASIS [192], DEADiff [193], Uncovering the Disentanglement Capability [194], InstantStyle [195], StyleAligned [196], FreeCustom [197]
Sec.4.5: Text-guided Image Generation	DisenDiff [198], Predicated Diffusion [199], LEDITS++ [200], PH2P [201], GSN [202], NMG [203], Imagic [204], SINE [205], AdapEdit [206], FISEdit [207], BARET [208], D-Edit [209], PromptCharm [210], RAPHAEL [211], SUR-Adapter [212], Prompt Diffusion [213], SDG [214], InfEdit [215], FPE [216], FoI [217], DiffEditor [218], Prompt Augmentation [219], TurboEdit [220], PPE [221], DE-Net [222]
Sec.4.6: Performance and Effectiveness	LowRank Adaptation (LoRA) [223], ECLIPSE [224], InstaFlow [225], SVDiff [107], LinFusion [226], Speculative Jacobi Decoding [99], Token-Critic [227], Null-text Inversion [228], DiffFit [229], Progressive Distillation [230], YOSO [231], SwiftBrush [232], StreamDiffusion [233], TiNO-Edit [234], On the Scalability of Diffusion-based T2I Generation [235], Muse [236], UFC-BERT [237], MarkovGen [238]
Sec.4.7: Reward Mechanism	Prompt AutoEditing (PAE) [239], AIG [240], IterComp [241], Powerful and Flexible [242], Optimizing Prompts for T2I Generation [243], ImageReward [137], SPIN-Diffusion [244],
Sec.4.8: Safety Issues	Self-Discovering [245], POSI [246], Detection-based Method [247], SteerDiff [248], MetaCloak [249], OpenBias [250], SPM [251], Guidance-based Methods [33], [246], [252], Fine-tuning-based Method [253], HFI [254], RECE [255], RIATIG [256]
Sec.4.9: Copyright Protection Measures	AdvDM [257], Mist [258], Anti-DreamBooth [259], InMark [260], VA3 [261], SimAC [262]
Sec.4.10: Consistency Between Text and Image Content	TokenCompose [263], Attention Refocusing [264], DPT [265], MIGC [266], INITNO [267], DiffusionCLIP [268], SDEdit [269], MasaCtrl [270], RIE [271], Scene TextGen [272], AnyText [273], SceneGenie [274], ZestGuide [275], Adma-GAN [276], AtHom [277], TL-Norm [278], GSN [202], DiffPNG [279], Compose and Conquer [280], StoryDiffusion [281], SynGen [282], ParaDiffusion [283], Token Merging (Tome) [284], Training-Free Structured Diffusion Guidance [285], StyleT2I [286], Bounded Attention [287], DAC [288], Attention Map Control [289], DDS [290], CDS [291], StableDrag [292], FreeDrag [293], RegionDrag [294]
Sec.4.11: Spatial Consistency Between Text and Image	SPRIGT [295], CoMat [296], CLIP [68], MULAN [297], TCTIG [298], PLACE [299], Backward Guidance [300], SSMG [301]
Sec.4.12: Specific Content Generation	CosmicMan [302], Text2Human [303], CAFE [304], ZS-SBIR [305], HanDiffuser [306], EmoGen [307], Cross Initialization for Face Personalization [308], HcP [309], PanFusion [310], StoryGen [311], Text2Street [312], SVGDreamer [313], Face-Adapter [314], StoryDALL-E [315], TextFit [316], EditWorld [317]
Sec.4.13: Fine-grained Control in Generation	Continuous 3D Words [318], FiVA [319], GLIGEN [320], InteractDiffusion [321], PreciseControl [322], Localizing Object-level Shape Variations [323], Motion Guidance [324], SingDiffusion [325], CFLD [326], NoiseCollage [327], Concept Weaver [328], Playground v2.5 [329], LayerDiffuse [330], ConForm [331]
Sec.4.14: LLM-assisted T2I	LayoutGPT [332], DiagrammerGPT [333], AutoStory [334], CAFE [304], LayoutLLM-T2I [335], MoMA [336], SmartEdit [337], RFNet [338], TIAC [339], RPG [112], ELLA [340], DialogGen [341], MGIE [342]

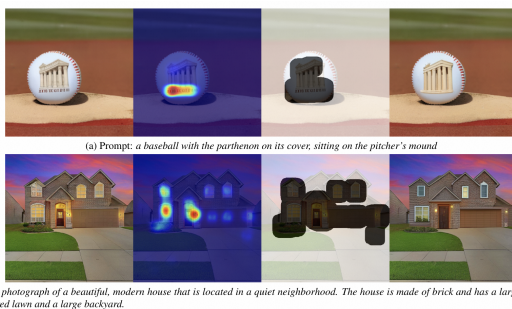


Fig. 11: RAHF [134] region inpainting with Muse [236] generative model. From left to right, original images with artifacts from Muse, predicted implausibility heatmaps from our model, masks by processing (thresholding, dilating) the heatmaps, and new images from Muse region inpainting with the mask, respectively.

HPS (Human Preference Score) [136] introduced the HPD dataset, which focuses on images generated by stable diffusion models. This dataset uses human preference annotations to train the HPS model to better align with human preferences. HPS v2 [345] further expanded the dataset to include eight generative models and incorporated titles from the COCO [346] dataset. Although HPS v2 primarily addresses overall human preferences, it does not yet fully account for the diversity of individual tastes.

The Multidimensional Human Preference (MHP) dataset [138] considers a wider range of human preference dimensions, with human annotators providing multidimensional labels for image pairs based on aesthetics, detail quality, semantic alignment, and overall scores. Furthermore, its MPS model aims to predict scores under different preference conditions and establishes a benchmark to evaluate existing T2I generation models.

4.2 Personalized Generation

Personalized T2I generation refers to the process of creating images based on specific user needs, preferences, or personal characteristics. In 2022, the DreamBooth model [43], developed by the Google research team, was widely recognized as a landmark achievement in this field, with its personalized generation capabilities illustrated in Figure 12.

DreamBooth fine-tunes diffusion models by incorporating custom subjects, focusing on the ability to generate images of specific entities while maintaining consistency across different scenes, poses, and perspectives. This approach not only expands the model’s language-vision dictionary, enhancing the association between new terms and subjects, but also effectively addresses common issues of overfitting and mode collapse typically encountered in traditional fine-tuning methods.

$$\mathbb{E}_{x,c,\epsilon,\epsilon',t}[w_t\|\hat{x}_\theta(\alpha_t x + \sigma_t \epsilon, c) - x\|_2^2 + \lambda w_{t'}\|\hat{x}_\theta(\alpha_{t'} x_{pr} + \sigma_{t'} \epsilon', c_{pr}) - x_{pr}\|_2^2]. \quad (6)$$

As illustrated in Figure 13, the model uses rare identifier tokens to represent given subjects and gradually optimizes the generation results through a staged fine-tuning process. Additionally, the proposed “autogenous class-specific prior preservation loss” function plays a crucial role in balancing the discrepancies between real images and the generated images of the specified subjects, as shown in Equation (6).

Complementing DreamBooth is Textual Inversion [139], which addresses the challenge of introducing new concepts in large models by learning new “words” to represent user-provided objects or styles, enabling personalized creation. Furthermore, PIA [140] provides a flexible solution for personalized image animation, ensuring controllable movement between images and text while integrating various personalized models.

Prompt-Free Diffusion [141] improves image generation quality by eliminating the need for prompts, thereby simplifying the personalized generation process. PALP [145] maintains consistency between text and generated images, even under complex prompting conditions, demonstrating excellent performance. PhotoMaker [146] efficiently encodes the input ID images using stacked ID embeddings, ensuring the retention of identity information.

Furthermore, ADI [142] introduces disentangled identifiers, which enable the generation of new images with shared actions through specific symbols, enhancing the diversity of output. DreamTurner [147] achieves theme-driven image generation through a theme encoder, allowing for more detailed preservation of subject identity.

In terms of encoding, ELITE [148] introduces a combination of global and local mapping networks to enable fast and accurate customized generation, while Tailored Visions [149] enhances personalization by rewriting user prompts based on historical interactions. LayoutDiffusion [347] focuses on layout-controlled image generation, overcoming the challenges of multimodal fusion between images and layouts, thus offering improved generation quality and controllability.

HyperDreamBooth [143] uses a hypernetwork to generate personalized weights from a single image, allowing for efficient style and context switching. SAG [151] employs

dual classifier-free guidance to ensure that generated outputs align with both themes and input text prompts, enhancing generation accuracy. Personalized Residuals [144] introduces a low-rank personalization method that improves effectiveness while maintaining generation speed.

FastComposer [154] is a multi-theme generation method that does not require fine-tuning, using an image encoder to extract theme embeddings for efficient personalized generation. InstantID [155] retains identity in a zero-shot manner, guiding generation through facial images and text prompts to ensure high fidelity. Specialist Diffusion [103] can be seamlessly integrated into existing models, learning complex styles and demonstrating efficient tuning capabilities with high-quality samples.

ControlStyle [156] focuses on text-driven stylized generation, aiming to enhance the editability of content creation, while UniPortrait [157] offers a unified framework for portrait image personalization, supporting customization for both single and multiple identities. Face-Diffuser [348] generates high-fidelity images by jointly learning scenes and characters, using a saliency-adaptive noise fusion mechanism to improve image quality.

TIGC [158] introduces a non-tuning image customization framework that modifies detailed attributes based on text descriptions while preserving key subject features. DETEX [159] enhances the flexibility of personalized generation using decoupled concept embeddings, and FlashFace [160] improves identity retention accuracy by encoding facial identity through feature maps. IDAdapter [161] and CoRe [152] enhance generation diversity and text alignment accuracy using non-tuning methods and contextual regularization techniques, respectively.

Finally, Imagine Yourself [153] represents an advanced model that requires no fine-tuning, pushing the boundaries of personalized image generation through a novel synthesis pairing mechanism and parallel attention architecture. Collectively, these research advances drive the development of personalized T2I generation technology, providing users with diverse and high-quality generation experiences.

4.3 Controllable T2I Generation

Advancements in controllable T2I generation technology allow users to exercise more precise control over the content and style of generated images.

ControlNet [13] is a key technology in this field, as illustrated in Figure 14. It works by introducing conditioning images, e.g., sketches, edge maps, and pose keypoints, to guide the generation process of pretrained image diffusion models, thereby enhancing the flexibility and customization of the generated content.

Specifically, ControlNet maps additional conditional information into the parameters of a fixed pretrained large model, such as Stable Diffusion [33]. As shown in Figure 15, the gray module on the left represents the pretrained Stable Diffusion model, whose parameters remain unchanged. ControlNet includes encoder blocks and middle blocks consistent with the Stable Diffusion model, with initialized parameters copied from the pretrained model.

Furthermore, Uni-ControlNet [169] offers a unified framework that simultaneously utilizes local controls (such



Fig. 12: With just a few images (typically 3-5) of a subject (left), DreamBooth [43], the AI-powered photo booth, can generate a myriad of images of the subject in different contexts (right), using the guidance of a text prompt. The results exhibit natural interactions with the environment, as well as novel articulations and variation in lighting conditions, all while maintaining high fidelity to the key visual features of the subject.

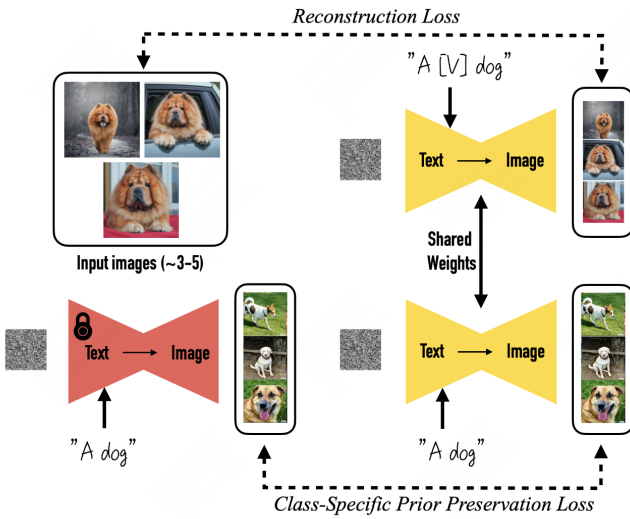


Fig. 13: Fine-tuning of DreamBooth [43]. Given approximately 3-5 images of a subject, we fine-tune a text-to-image diffusion model with the input images paired with a text prompt containing a unique identifier and the name of the class the subject belongs to (e.g., “A [V] dog”). In parallel, we apply a class-specific prior preservation loss, which leverages the semantic prior that the model has on the class and encourages it to generate diverse instances belonging to the subject’s class using the class name in a text prompt (e.g., “A dog”).

as edge maps, depth maps, and segmentation masks) and global controls (such as CLIP image embeddings), significantly reducing the cost of training from scratch. The T2I-Adapter [163] acts as a pluggable module, enhancing the control capabilities of T2I models by injecting additional conditional information, including text descriptions, image templates, and keypoints, into the generation process.

Additionally, Custom Diffusion [106] achieves rapid model adjustments to represent new concepts by optimizing a minimal number of parameters, with the ability to train multiple concepts concurrently. Jedi [165] generates personalized images based on an arbitrary number of reference images, constructing a synthetic dataset of related images to learn the shared distribution of multiple text-image pairs.

ViCo [166] provides a fast and lightweight solution for personalized generation, supporting plug-and-play features that avoid fine-tuning the original diffusion model while preserving the details of newly generated concepts.

DreamMatcher [167] introduces a semantically consistent masking strategy to more accurately replicate target attributes such as color and texture. RealCustom [150] improves alignment between text descriptions and generated content by gradually reducing the influence of real words using a cross-attention mechanism. Selectively Informative Description [164] serves as an innovative text description strategy that utilizes descriptions generated by multimodal GPT-4, integrating seamlessly into the optimized model to enhance flexibility and accuracy in generation.

Additionally, StyleGAN Meets Stable Diffusion [168] combines the identity-preserving capabilities of StyleGAN with diffusion models, enhancing semantic editing capabilities. LayerDiffusion [171] enables non-rigid editing and attribute modification of specific subjects through hierarchical control. ReCo [172] allows users to control arbitrary objects using open text by adding location markers and natural language region descriptions. Meanwhile, SpaText [173] employs open-vocabulary scene control, combining global text prompts and segmentation maps to generate high-fidelity images. BLIP-Diffusion [170] introduces a new multimodal encoder pretrained in BLIP-2 [349] to achieve improved controllable generation.

Regarding generation efficiency, Codi [174] presents a conditional diffusion model capable of producing high-quality results quickly. StyleTokenizer [175] enhances alignment between style and text representations through zero-shot style control [350] for image generation. P+ [176] improves reconstruction capacity and expressiveness by introducing extended text inversion, while IP-Adapter [177], as a lightweight adapter, facilitates efficient image prompting capabilities.

ResAdapter [178] enables the generation of images with unrestricted resolutions and is compatible with various diffusion models. DetDiffusion [179] improves the effectiveness of the generated data by leveraging the synergy between perceptual models and generative models. CAN [180] adds control over image generation by dynamically adjusting neural network weights, making the generation



Fig. 14: Controlling Stable Diffusion [33] with Learned Conditions. ControlNet [13] allows users to add conditions like Canny edges (top), human pose (bottom), etc., to control the image generation of large pretrained diffusion models. The default results use the prompt “a high-quality, detailed, and professional image”. Users can optionally give prompts like “chef in kitchen”.

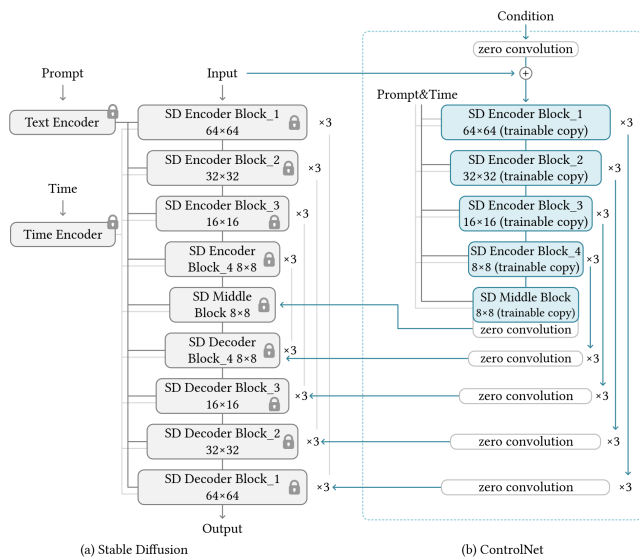


Fig. 15: Stable Diffusion [33]’s U-net architecture is connected with a ControlNet [13] on the encoder blocks and middle block. The locked, gray blocks show the structure of Stable Diffusion V1.5 (or V2.1, as they use the same U-net architecture). The trainable blue blocks and the white zero convolution layers are added to build a ControlNet.

process more flexible. SceneDiffusion [181] optimizes hierarchical scene representation during the diffusion sampling process, supporting a range of spatial editing operations.

Zero-Painter [182] is an innovative training-free framework that generates images based on text layout conditions, while FreeControl [183] serves as a general-purpose zero-training solution supporting controllable generation across different conditions and architectures. PCDMs [184] im-

prove generation accuracy by gradually reducing discrepancies in pose-guided image generation.

Lastly, ControlNet++ [185] and ControlNeXt [186] further enhance controllable generation, improving consistency between conditional controls and the resulting images. MultiDiffusion [187] provides a unified framework that leverages pretrained T2I diffusion models to achieve diverse and controllable image generation without requiring further training or fine-tuning. Composer [154] introduces a new approach for flexibly controlling spatial layouts and color palettes in generated images while maintaining synthesis quality and model creativity.

4.4 T2I Style Transfer

We need artistic images. T2I Style Transfer combines the benefits of T2I generation and style transfer, enabling users to create images in specific artistic styles by inputting text descriptions and style images. This area has a rich body of research, with various innovative methods developed to achieve effective style transfer.

First, InST [189] is a deep learning-based artistic style transfer framework capable of generating high-fidelity new artistic images while preserving the creative attributes of the original work. It does so by providing a single painting image and controlling the content using natural images or text descriptions, as illustrated in Figure 16.

Styleformer [188] is a deep learning project based on the Transformer architecture that can alter the writing style while preserving the original text content, allowing the style transfer of textual information in the T2I domain. Furthermore, research has shown that by fixing the Gaussian noise introduced during the denoising process and adjusting the text embeddings [194], it is possible to generate the target



Fig. 16: Style transfer results using the proposed method. Given only a single input painting, InST [189] can accurately transfer the style attributes such as semantics, material, object shape, brushstrokes and colors of the references to a natural image with a very simple learned textual description “[C]”.

style without changing the semantic content, laying the foundation for future lightweight algorithms.

Similarly, ArtAdapter [190] uses a multilevel style encoder and an explicit adaptation mechanism to ensure a balance between style and text semantics, enabling rapid style adaptation.

Additionally, InstantBooth [191] achieves personalized image generation without requiring test-time fine-tuning, effectively capturing both global and local features of the input image. OSASIS [192] demonstrates a one-shot stylization method that decouples the semantics and structure of images, allowing for flexible style application.

DEADiff [193] uses a mechanism to decouple style and semantics, employing Q-Formers to extract feature representations for optimal results in visual stylization. InstantStyle [195] introduces a simple mechanism to separate style and content, ensuring a balance between style control and visual quality.

StyleAligned [196] maintains style consistency among a series of generated images through a shared attention mechanism, allowing users to create stylistically consistent images with straightforward inversion operations. Finally, FreeCustom [197] offers a tuning-free approach that uses a multireference self-attention mechanism and weighted masking strategies to generate customized images based on multiconcept compositions from reference concepts.

4.5 Text-guided Image Generation

Text-guided Image Generation encompasses not only the ability to create entirely new images but also the editing and modification of existing ones. This technology allows users to make detailed adjustments and reconfigurations of existing images based on textual prompts. Imagic [204], as the first method aimed at semantic editing of a single image through text, significantly improves the precision of image editing by optimizing text embeddings and fine-tuning pretrained diffusion models, establishing itself as a benchmark in the field, as illustrated in Figure 17.

DisenDiff [198], on the contrary, uses a cross-attention mechanism to disentangle multiple concepts within a single image, allowing users to describe different elements independently, thus increasing the flexibility of image generation. Noise Map Guidance (NMG) [203] provides a context-rich inversion approach for editing real images, enhancing the naturalness of the editing results. SINE [205] introduces

a novel classifier-free guiding model that facilitates the extraction of knowledge from a single image for application to pretrained diffusion models, enabling effective content creation from a single image.

AdapEdit [206] addresses complex, continuity-sensitive image editing tasks by employing variable spatiotemporal guiding scales, which enhance the naturalness and contextual consistency of edits. FISEdit [207] integrates cache-supported sparse diffusion model inference, allowing users to perform efficient image editing through minor text modifications, thus reducing inference time.

BARET [208] enhances the flexibility of image editing by optimizing the image reconstruction process through target text inversion scheduling, progressive transition strategies, and balanced attention modules. D-Edit [209] decouples the interaction between images and prompts, supporting various image editing by manipulating learned prompts.

Predicated Diffusion [199] employs predicate logic to model the relationships between words in prompts, improving the fidelity of generated images. LEDITS++ [200] addresses the efficiency challenges associated with the processing of multiple text commands, allowing users to input several editing instructions simultaneously and generate realistic images, thus improving the user experience. PH2P [201] examines the impact of prompt conditions during the diffusion process and introduces an immediate inversion framework that does not require auxiliary tasks.

PromptCharm [210] advances T2I generation through multimodal prompt engineering and refinement, allowing users to explore different image styles within a large database. RAPHAEL [211] uses a mixture of expert layers to create highly artistic images that accurately reflect complex textual prompts.

SUR-Adapter [212] introduces a semantic understanding and reasoning adapter, enhancing the ability of pretrained diffusion models to handle concise narratives. Prompt Diffusion [213] establishes a contextual learning framework within diffusion generation models, enabling automatic comprehension of latent tasks and execution of corresponding operations.

SDG [214] provides a unified framework for guiding image generation through reference images and language, allowing effective generation on datasets without textual annotations. InfEdit [215] standardizes attention control mechanisms in text-guided editing, proposing an inversion-

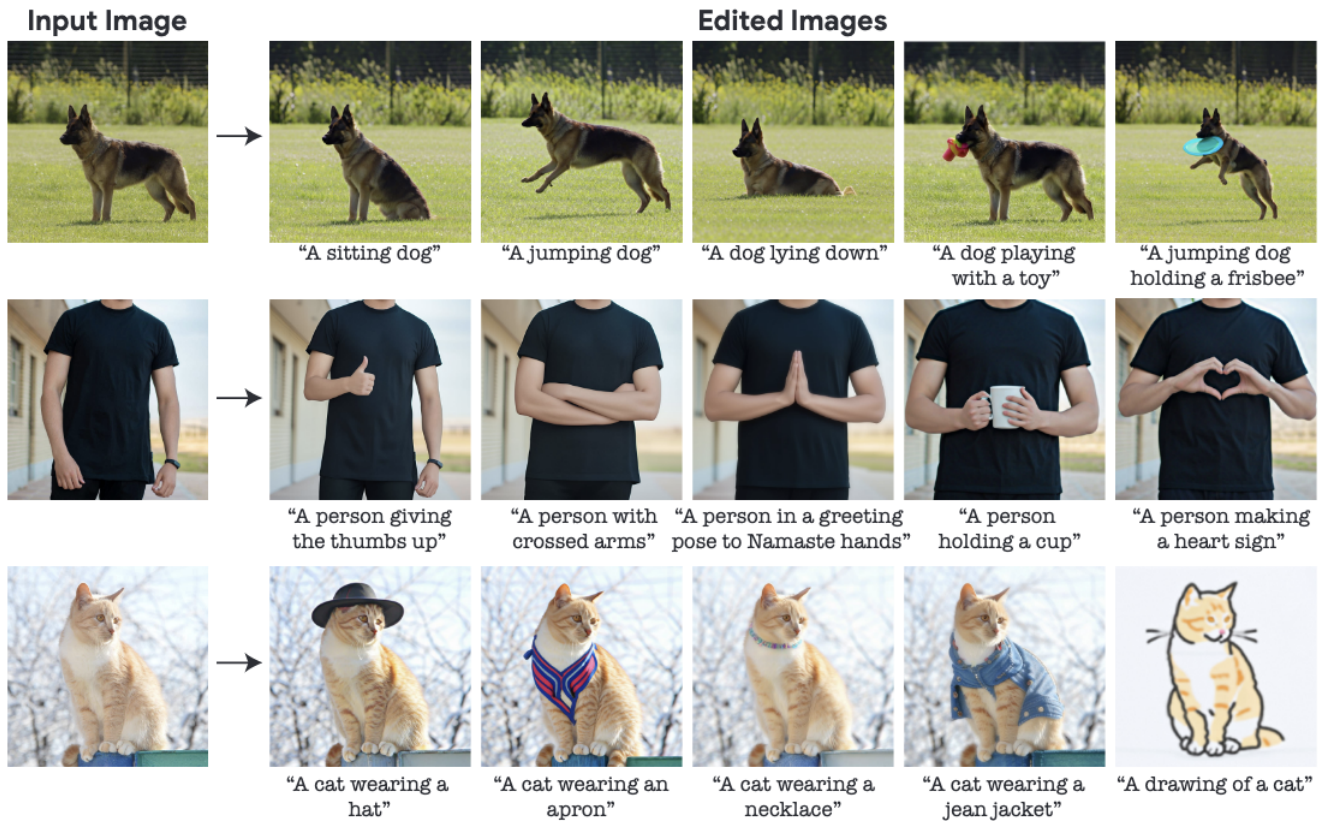


Fig. 17: Different target texts applied to the same image. Imagic [204] edits the same image differently depending on the input text.

free method to accommodate complex modifications.

FPE [216] examines the influence of attention layers on image editing outcomes and introduces free prompt editing to simplify the editing process. The FoI [217] method ensures precise and coordinated editing of multiple instructions without requiring additional training. DiffEditor [218] incorporates image prompts for fine-grained image editing, further improving the quality of edits.

Text-Driven Image Editing [351] via Learnable Regions introduces a new region generation model, enabling mask-based T2I models to perform local image editing without the need for user-provided masks. Prompt Augmentation [219] expands a single input prompt to multiple target prompts, enriching the textual context and facilitating localized image editing.

TurboEdit [220] employs iterative inversion techniques using encoders for fine-grained editing of input images, supporting decoupled control in low-step diffusion models.

The comprehensive application of these technologies is driving rapid progress in the field of text-guided image generation. In particular, the breakthroughs in semantic editing by Imagic [204] have laid a solid foundation for future advances in this domain.

UFC-BERT [237] differs from existing two-stage autoregressive methods (such as DALL-E [7] and VQ-GAN [29]) by employing non-autoregressive generation (NAR) in the second stage. This design enhances the overall consistency of the synthesized images, supports the retention of specific image segments, and improves the synthesis speed.

Muse [236] employs a masked generative transformer

architecture that randomly masks portions of the input image during training while designing pretraining text tasks for reconstruction learning. Compared to pixel-space diffusion models such as Imagen [12] and DALLE-2 [10], Muse is more efficient because it utilizes discrete tokens and requires fewer sampling iterations. Furthermore, in contrast to autoregressive models such as Parti [35], Muse achieves greater efficiency through parallel decoding. Using pretrained LLM, Muse improves fine-grained language understanding, resulting in high-fidelity image generation and a deeper comprehension of visual concepts.

MarkovGen [238] is the first study to utilize MRF to enhance the efficiency and quality of text-to-image models. This model achieves a 1.5-fold acceleration and quality improvement by replacing the final steps of Muse with the learned MRF layers, as validated by human evaluation and FID metrics. The parameters of the MRF model can be trained in a few hours, facilitating the rapid integration of the MRF model with the pretrained Muse model, further enhancing both efficiency and quality.

4.6 Performance and Effectiveness

In the field of T2I, balancing performance and efficiency is essential. Low-Rank Adaptation (LoRA) [223], initially used to fine-tune large models in natural language processing, was later introduced to SD models. Specifically, as shown in Equation (7), consider a weight matrix W that needs fine-tuning. LoRA represents the update to W as the product of two low-rank matrices:

$$W' = W + BA. \quad (7)$$

By decomposing the weight updates of a pretrained model into low-dimensional matrices, LoRA significantly enhances the efficiency of fine-tuning. Block-wise LoRA [352] further optimizes the fine-tuning strategy for U-Net, resulting in improved generation quality.

Latent variable models [33], [353] have seen remarkable success in T2I, allowing the production of high-quality images from text prompts or other modalities. SVDiff [107] introduces a compact parameter space approach that mitigates overfitting and language drift issues by fine-tuning the singular values of matrices. It also incorporates a cut-mix-decomposition data augmentation technique. The basic framework of SVDiff is illustrated in Figure 18.

Token-Critic [227], an auxiliary model, enhances the sampling capabilities of non-autoregressive generative transformers, thereby improving the quality of generated content. Null-text Inversion [228] enhances image editing by employing diffusion key inversion and optimizing empty text prompts.

The study [235] conducted a large-scale comparative analysis to explore the scalability of diffusion-based T2I generation methods. ECLIPSE [224] leverages pretrained visual language models for contrastive learning, significantly reducing data requirements while maintaining generation quality. InstaFlow [225] is the first one-step T2I generator capable of producing high-quality images.

The Progressive Distillation technique [230] greatly reduces the sampling time by distilling the behavior of pretrained diffusion models into new models, with minimal impact on sample quality. YOSO [231] achieves high-fidelity, one-step image synthesis with enhanced training stability. SwiftBrush [232] also focuses on one-step generation, producing images that are comparable in quality to those generated by stable diffusion models.

Speculative Jacobi Decoding (SJD) [99] accelerates the inference process in autoregressive T2I generation by allowing the model to predict multiple tokens simultaneously at each step. LinFusion [226] introduces a novel linear attention mechanism that significantly reduces both time and memory complexity while maintaining performance. DiffFit [229] adapts quickly to new domains by fine-tuning only specific layer parameters, thus reducing training time.

StreamDiffusion [233] is a real-time interactive generation pipeline that enhances speed through batch denoising. TiNO-Edit [234] focuses on optimizing the noise patterns and diffusion time steps during the editing process, proposing new loss functions to accelerate optimization.

The combined application of these technologies effectively balances performance and efficiency in T2I, driving the continued advancement of T2I technology.

4.7 Reward Mechanism

In T2I generation, designing an effective reward mechanism is crucial to optimize the generation process. By introducing effective reward functions [354], generative models can better align with human aesthetics and preferences.

ImageReward [137] is the first general-purpose reward model for T2I generation that effectively encodes human preferences. It can be used as a reward function in RLHF

(Reinforcement Learning from Human Feedback), thus further optimizing generative models' performance. ImageReward provides a clear scoring mechanism for the generation process and has had a significant impact in T2I.

[243] uses reinforcement learning to explore better prompting strategies that generate images more aligned with user expectations.

Prompt AutoEditing (PAE) [239] aims to transform user-provided raw prompts into refined, dynamic prompts for generating high-quality images. PAE adjusts the weights of each word and modifies the injection time steps through an online reinforcement learning strategy, establishing a multidimensional reward system that considers aesthetic scores, semantic consistency, and user preferences.

Annealed Importance Guidance (AIG) [240] is an inference-time regularization method that achieves a Pareto optimal trade-off between rewards and image diversity, allowing the model to optimize rewards while preserving diversity. This approach effectively mitigates issues related to indiscriminate regularization and reference mismatches.

IterComp [241] improves the generative capabilities of the base diffusion model by collecting composition-aware preferences from a model library and utilizing iterative feedback learning. The associated RL fine-tuning framework [355] further improves generation diversity by incorporating theoretically supported diversity rewards.

SPIN-Diffusion [244] introduces a self-play fine-tuning algorithm that fosters competition between the diffusion model and its earlier versions, encouraging an iterative self-improvement process. This approach serves as an alternative to traditional supervised fine-tuning and reinforcement learning strategies.

Lastly, Powerful and Flexible [242] presents a novel reinforcement learning framework that employs deterministic policy gradient methods for personalized T2I generation. This framework enables the integration of various objectives to enhance the quality of the generated images. Collectively, these works advance the development of reward mechanisms in the T2I field, providing effective strategies for achieving high-quality image generation.

4.8 Safety Issues

In the field of T2I generation, safety concerns are gaining increasing attention, especially since generated images can contain biases and unsafe elements, such as gender discrimination or depictions of violence that may be harmful to children. To address these issues, researchers have proposed various methods to ensure ethical and safe generation processes.

Recent studies have employed detection-based methods [247], guiding techniques [33], [246], [252], and fine-tuning approaches [253] to intervene in both text and image content, aiming to make T2I generation safer.

Structured Permeable Membrane (SPM) [251] introduces a conceptual structure into diffusion models to perform targeted erasure, effectively mitigating unwanted variations and preventing harmful content from appearing in generated images.

The Prompt Optimizer (POSI) [246] is an automated system that optimizes text prompts, guiding T2I models

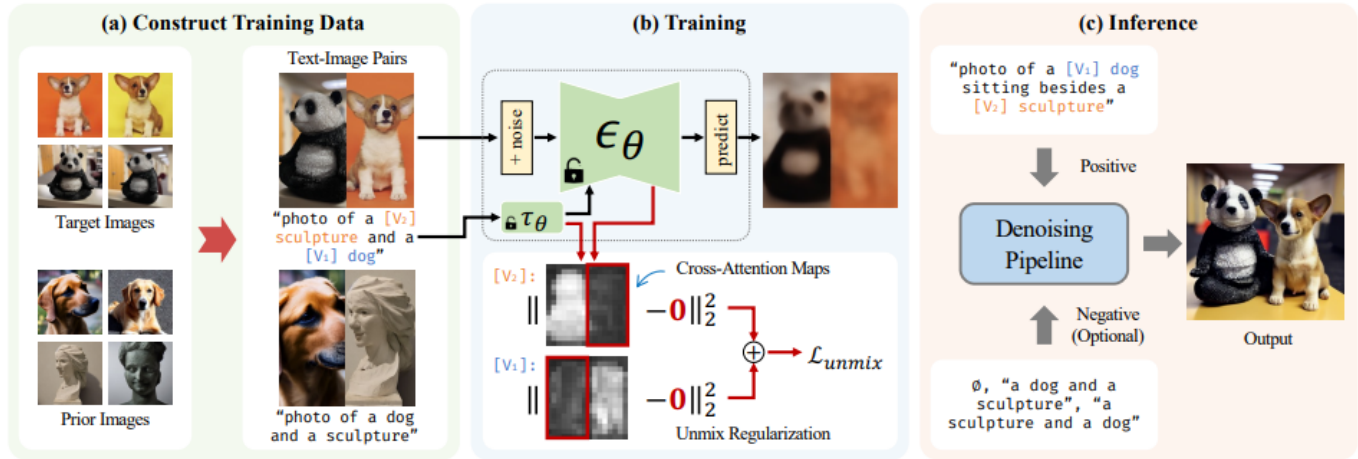


Fig. 18: SVDiff [107] proposes the Cut-Mix-Unmix data augmentation technique to enhance the quality of multi-subject image generation, which is a simple text-based image editing framework.

to generate images that are both safe and semantically aligned with the original prompts. This system preprocesses potentially toxic prompts using GPT [65] and applies fine-tuning based on datasets, thus enhancing the safety and reliability of T2I models.

SteerDiff [248] is a lightweight adapter module designed to serve as an intermediary between user input and the diffusion model, ensuring that generated images meet ethical and safety standards. This method identifies and adjusts inappropriate concepts within the text embedding space to guide the model away from harmful outputs.

Recently, the Self-Discovering method proposed by Li et al. [245] identifies ethically-related latent vectors by finding corresponding latent directions in the U-Net bottleneck layer and suppressing their activation, thereby reducing the likelihood of generating inappropriate content. This approach offers a new perspective by discovering and controlling ethical concepts in an interpretable latent space to achieve responsible generation.

Moreover, MetaCloak [249] prevents unauthorized subject-driven synthesis by creating perturbations using a pool of proxy diffusion models to generate transferable, model-agnostic perturbations that mitigate the harmfulness of personalized generation. OpenBias [250] tackles open-set bias detection in T2I generation models by using large language models to extract potential biases and quantify them through visual question-answering models.

HFI (Human Feedback Inversion) [254] proposes a framework that condenses guidance for generating images based on human feedback, enhancing the model's alignment with human judgment, and significantly reducing the generation of inappropriate content. RECE (Reliable and Efficient Concept Erasure) [255] provides an innovative approach to rapidly modify models without additional fine-tuning, employing closed-form solutions to derive new target embeddings that mitigate inappropriate content generation.

Finally, RIATIG [256] introduces a reliable and stealth adversarial attack method for T2I models using subtle examples. This approach formulates the example creation process as an optimization problem to generate prompts that remain undetectable to the model.

Together, these studies and methods contribute to ad-

vancements in addressing safety issues within the T2I field, offering effective solutions to generate ethically sound and high-quality images.

4.9 Copyright Protection Measures

As T2I models continue to advance, concerns about copyright infringement are becoming more prominent. To address this challenge, researchers have proposed various technologies and methods to protect artists' rights.

AdvDM [257] effectively disrupts the fine-tuning process of models by adding pixel-level micro watermarks to artworks, preventing them from replicating artistic styles. After fine-tuning, the model generates new artworks based on learned style concepts. As illustrated in Figure 19, images generated after AdvDM processing generally display lower quality, chaotic textures, and a loss of artistic usability. This shows that AdvDM can effectively prevent artistic style transfer in diffusion models.

Mist [258] employs adversarial attacks to inject imperceptible noise into generative models, preserving the uniqueness of the original artistic style. Anti-DreamBooth [259] applies subtle perturbations to user images to actively protect users from unauthorized personalized generators, thereby safeguarding privacy.

Furthermore, InMark [260] introduces a robust watermarking technique to protect images from unauthorized use, ensuring that personal semantics remain intact even if the images are modified. VA3 [261], a new online attack framework, exposes vulnerabilities in probabilistic copyright protection mechanisms and proposes effective strategies to enhance attack stability. Lastly, SimAC [262] addresses the issue of generating fake news featuring celebrity photos by designing a feature-based optimization framework to protect user privacy.

Together, these studies and technologies provide effective solutions for copyright protection and promote responsible use of T2I technology.

4.10 Consistency Between Text and Image Content

In the field of T2I, ensuring consistency between generated images and input text is a crucial research focus. To address

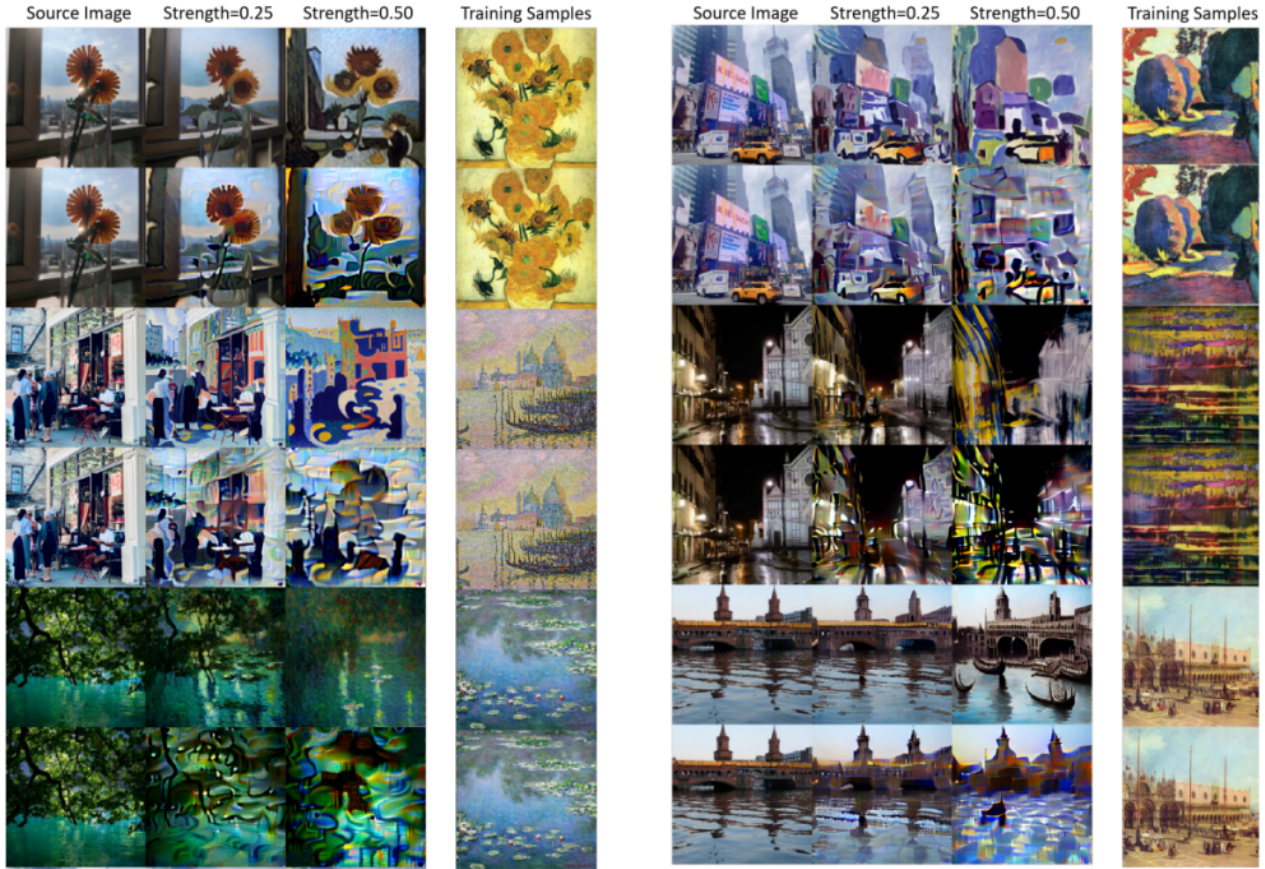


Fig. 19: Images shown in each group share the same source image. AdvDm [257] use textual inversion [139] to extract the style of training samples from WikiArt, shown in a separate column. For each group, the top row shows the generated images based on the style extracted from the clean examples. The bottom row shows the generated images based on the style extracted from the adversarial examples. Strength is a hyper-parameter that indicates how much the style of the source image is covered by the target style. LDM fails to capture the style from adversarial examples, compared to clean images.

this challenge, several studies have employed various methods and techniques. Recent research on GSN (Generative Semantic Nursing) [202], as shown in Figure 20, highlights that T2I models can sometimes overlook the main subject of the text during generation or incorrectly assign attributes to the wrong subject. GSN addresses these issues by adjusting latent codes during the denoising process, thereby improving the model’s semantic understanding of the input text and reducing semantic errors in the generated output.

TokenCompose [263] introduces a token consistency term that enhances the correlation between user-specified text prompts and generated images during fine-tuning, making it particularly effective for images containing multiple objects. Attention Refocusing [264] utilizes large language models to generate layouts, thus improving the controllability of the generated images and reducing the likelihood of errors.

DiffusionCLIP [268] proposes a method for text-driven image manipulation using diffusion models, enabling zero-shot image operations in unseen domains and increasing text-image consistency. Additionally, SDEdit [269] applies image denoising using stochastic differential equations, maintaining the realism and fidelity of the generated images while ensuring that the content aligns with the input text.

MasaCtrl [270] achieves consistent image generation

and complex image editing through a mutual self-attention mechanism, ensuring coordination between the foreground and background elements. DPT [265] proposes a method to enhance T2I alignment by improving the alignment between text and images using discriminative detection and adjustments, effectively addressing misalignment issues.

In the domain of object recognition and editing, Referring Image Editing [271] provides a framework that allows users to identify and edit specific objects in images using text prompts, thereby enhancing text-image consistency. Scene TextGen [272] integrates character and word-level models to ensure accurate and coherent text rendering in images, improving overall consistency. AnyText [273] focuses on multilingual visual text generation, ensuring that the rendered text is accurate and coherent across different languages.

SceneGenie [274] utilizes bounding boxes and segmentation information to ensure accurate scene representation when generating high-resolution images. ZestGuide [275] introduces a zero-shot segmentation guidance method that effectively aligns the generation process with input masks, further enhancing text-image consistency. DiffPNG [279] employs panoramic narrative positioning to handle multiple noun phrases within text prompts, thereby boosting text-image consistency.



Fig. 20: Given a pretrained text-to-image diffusion model (e.g., Stable Diffusion [33]) method in GSN [202], Attend-and-Excite, guides the generative model to modify the cross-attention values during the image synthesis process to generate images that more faithfully depict the input text prompt. Stable Diffusion alone (top row) struggles to generate multiple objects (e.g., a horse and a dog). However, by incorporating Attend-and-Excite (bottom row) to strengthen the subject tokens (marked in blue), we achieve images that are more semantically faithful with respect to the input text prompts.

In terms of generating layouts and ensuring detailed fidelity, TL-Norm [278] redefines the text-to-layout process by combining background and object layouts, which enhances the fidelity and consistency of generated images. INITNO [267] improves the consistency between prompts and generated images by employing initial noise optimization methods.

Compose and Conquer [280] incorporates three-dimensional object positioning control to ensure strict consistency between generated content and input prompts. StoryDiffusion [281] introduces a consistency-driven self-attention mechanism, significantly enhancing the consistency among generated images.

SynGen [282] improves attribute binding consistency by aligning attention maps, thereby reducing semantic errors. Training-Free Structured Diffusion Guidance [285] enhances T2I synthesis with structured representations, improving the accuracy of attribute binding. ParaDiffusion [283] focuses on generating images from long paragraphs, using the semantic understanding capabilities of large language models to enhance alignment between text and image feature spaces.

StyleT2I [286] uses a contrastive loss guided by CLIP to enhance the compositionality of T2I synthesis. Bounded Attention [287] limits the flow of information to prevent theme leakage, ensuring consistency across multiple themes during generation.

DAC [288] introduces an editability recovery framework using a dual counterfactual inference approach, enhancing text-image consistency. DDS [290] employs a text-based image editing scoring function to guide images towards the intended direction of text descriptions, ensuring alignment. CDS [291] uses a contrastive denoising scoring method to achieve structural correspondence during image translation and editing, ensuring content controllability.

MIGC (Multi-Instance Generation Controller) [266] ensures global alignment among multiple instances by managing controls such as instance quantity, position, attributes, and interactions. Adma-GAN [276] introduces an attribute-

driven memory-augmented GAN, which enhances generation quality by incorporating attribute information. AtHom [277] utilizes two attention modules to extract relationships between independent and unified modalities. DSE-GAN [356] reorganizes text features within an adversarial multistage architecture to improve the coherence of generated outputs. Phung et al. [264] propose a method to generate more semantically accurate compositions by restricting the attention area of each token in the prompt to the corresponding image section. Token Merging (Tome) [284] enhances semantic binding by merging related tokens into a single composite token, ensuring that the object, its attributes, and subobjects share the same cross-attention map.

Lastly, StableDrag [292] offers a stable and precise point-dragging editing framework, enhancing stability for long-distance manipulations. FreeDrag [293] is a feature-dragging method that reduces the complexity of point tracking, while RegionDrag [294] is a region-based editing technique that allows users to control the editing process with greater precision.

With these diverse technical approaches, researchers have made significant progress in improving text-image consistency, driving advances in T2I generation technology.

4.11 Spatial Consistency Between Text and Image

In the current field of T2I generation models, maintaining spatial consistency is a significant research focus. Although models like Stable Diffusion [33] and DALL-E [7] have made substantial progress in generating high-resolution, realistic images, they still struggle to accurately represent the spatial relationships described in text prompts. This limitation often results in generated images that do not reflect the correct positions and relative relationships of objects as described in the input text.

To address this issue, researchers have developed various methods aimed at enhancing spatial consistency through improvements in datasets, model architectures, and training strategies. For example, the SPRIGHT dataset [295]

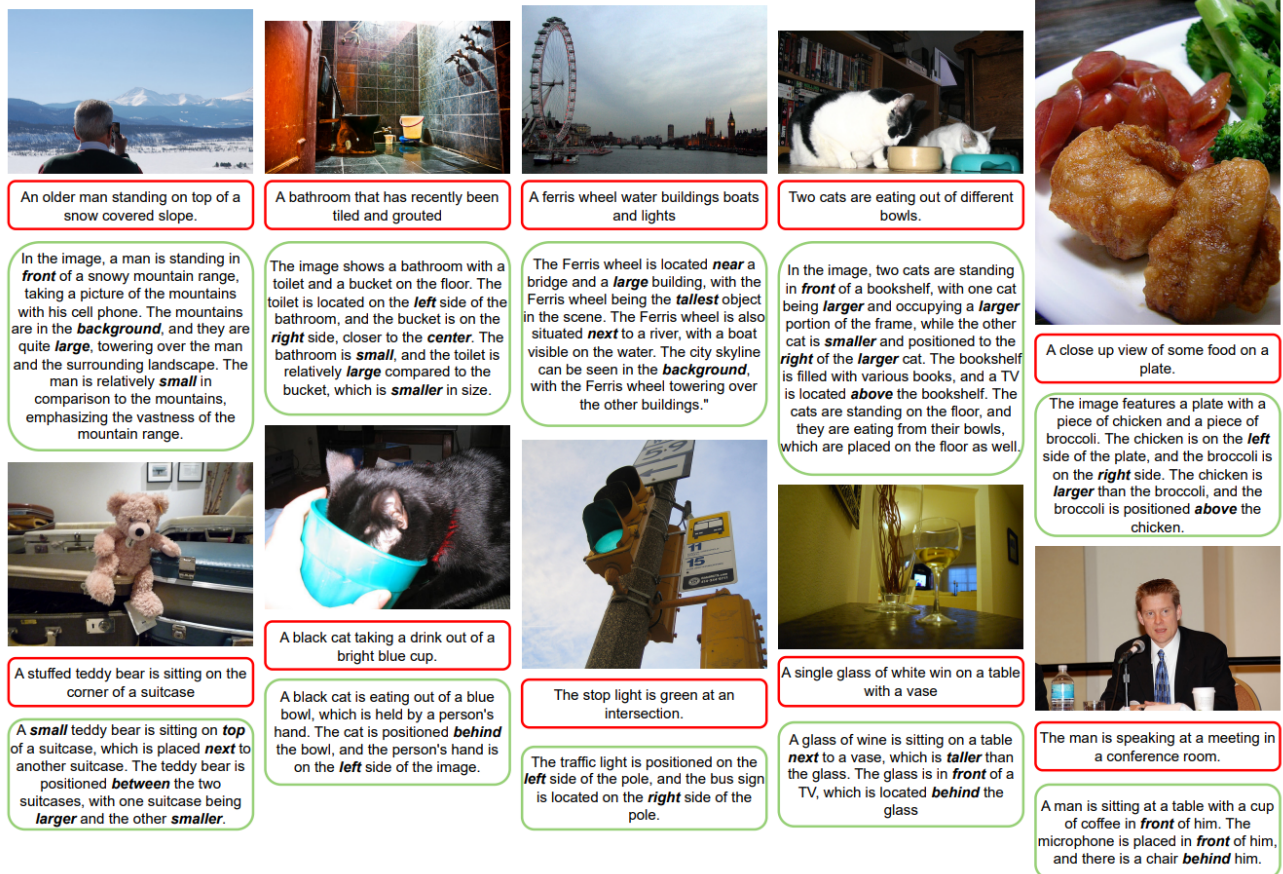


Fig. 21: The existing vision-language datasets do not capture spatial relationships well. To alleviate this shortcoming, we synthetically re-caption 6M images with a spatial focus, and create the SPRIGHT (SPatially RIGHT) [295] dataset. Shown above are samples from the COCO Validation Set, where text in denotes ground-truth captions and text in are corresponding captions from SPRIGHT.

provides detailed descriptions of spatial relationships, helping models learn how to transform text into images with accurate spatial layouts. As illustrated in Figure 21, these descriptions not only include basic spatial vocabulary but also detail the relative sizes of objects and other relationships, significantly advancing the research on spatial consistency in models.

Additionally, CoMat [296] improves the activation of text tokens by introducing the adversarial loss Fidelity Preservation, thereby encouraging the correct activation of image regions.

For user interaction, TCTIG [298] offers users a new way to control the generation process through mouse trajectory control, allowing them to draw paths while describing images, thus improving spatial control during generation. Meanwhile, the instance decomposition and occlusion information provided by the MULAN dataset [297] introduces new possibilities for image generation research.

The PLACE module [299] introduces an adaptive layout-semantic fusion mechanism that ensures the effective integration of layout information and semantic features, enhancing both the quality and consistency of generated images. Using backward guidance [300], researchers can leverage user-specified inputs to better control layouts, uncovering various factors that influence layout during the image generation process.

Finally, the SSMG diffusion model [301] improves generation quality and controllability through spatial-semantic map guidance, combined with relationship-sensitive and position-sensitive attention mechanisms. These studies and methods have made significant progress in improving T2I spatial consistency, advancing T2I model research, while providing crucial foundations and insights for future studies. By continuously improving models and datasets, researchers aim to achieve higher levels of text-image consistency to meet real-world application needs.

4.12 Specific Content Generation

In the field of T2I generation, specialized content generation is a key research direction that includes applications such as high-fidelity human imagery, emotional expression, and personalized image generation. To address these challenges, researchers have proposed various innovative methods. One of these is EmoGen [307], which introduces emotional image content generation (EICG), a novel task that focuses on creating images with clear semantic meaning and faithful emotional expression based on specified emotional categories. EmoGen ensures accurate emotional depiction by constructing an emotional space and aligning it with the CLIP space, as shown in Figure 22.

The CosmicMan model [302] targets high-fidelity human image generation, effectively capturing the requirements of

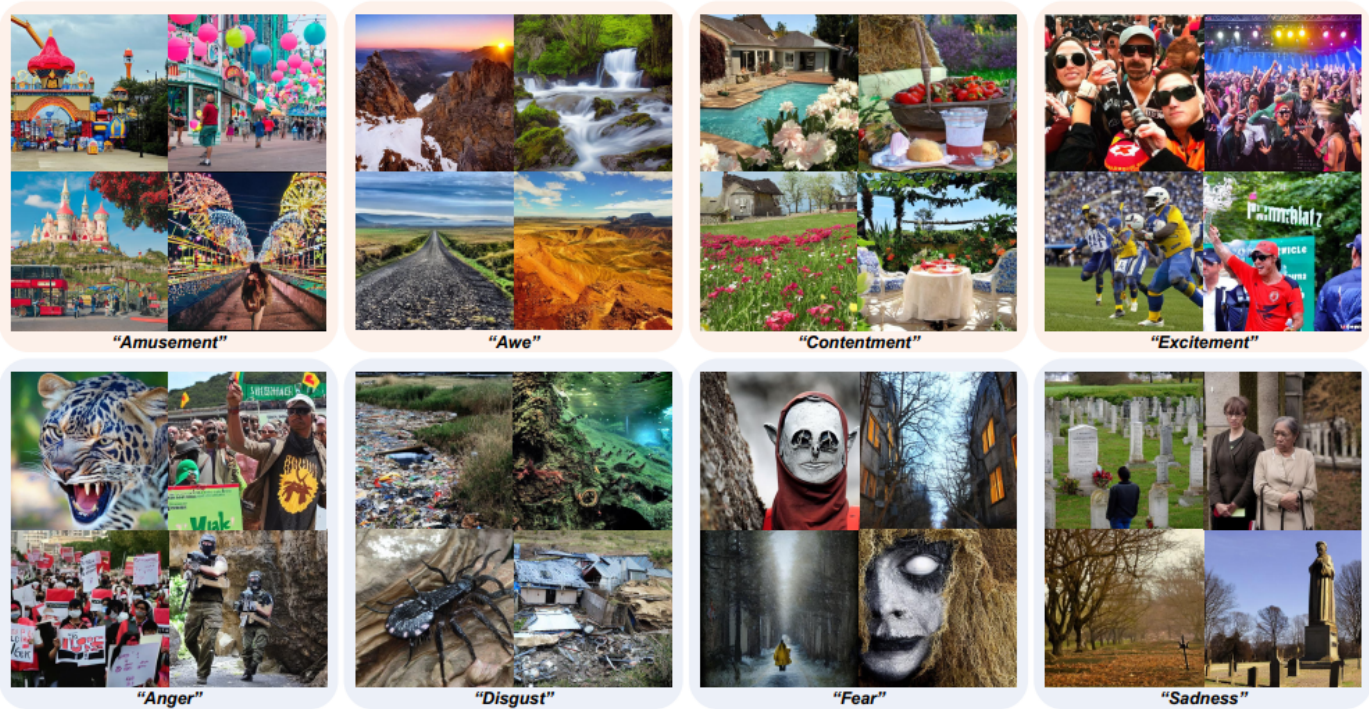


Fig. 22: Emotional Image Content Generation (EICG). Given an emotion category, The network EmoGen [307] produces images that exhibit unambiguous meanings (semantic-clear), reflect the intended emotion (emotion-faithful) and incorporate varied semantics (semantic-diverse).

text descriptions. Text2Human [303] uses a text-driven, controllable framework to synthesize complete human images by converting body poses into parsing maps. In contrast, Cross Initialization for Face Personalization [308] focuses on personalized face generation through cross-initialization, thereby improving visual fidelity. The HanDiffuser model [306] excels in generating realistic human hand images by incorporating hand embeddings during the generation process. Furthermore, Wang et al. [309] proposed a human-centric priors (HcP) layer to improve the alignment between cross-attention maps and human-related textual information in prompts. This approach strengthens human structure information within cross-attention maps derived from text prompts, thereby improving the quality of generated images. The Face-Adapter [314] offers high-precision facial editing capabilities for pretrained diffusion models.

The ZS-SBIR method [305] uses diffusion models as feature extractors to tackle challenges in zero-shot sketch-based image retrieval. Text2Street [312] allows controllable street view generation by combining road topology and object layout generation strategies. PanFusion [310] generates 360-degree images from text prompts by integrating stable diffusion models with panoramic branches to achieve cohesive image generation. StoryGen [311] creates current frames using text prompts and previous images, allowing the production of sequential images and story-like visuals. SVGDreamer [313] improves image editability by employing a semantic image vectorization process and introduces a scoring distillation method based on vector particles to enhance aesthetic appeal. StoryDALL-E [315] focuses on story continuation by generating visual stories from source images and enhancing pretrained models for sequential image generation.

Finally, TexFit [316] and EditWorld [317] have made

notable progress in fashion image editing and world instruction-based image editing, respectively. These studies illustrate how T2I generation technology has made significant advances in specialized content generation, offering new opportunities for various future applications.

4.13 Fine-grained Control in Generation

In the field of fine-grained attention generation, several innovative methods have been proposed to improve the ability of T2I generation models to control details and allow personalization.

Playground v2.5 [329] aims to improve the aesthetic quality of the generated images by addressing key challenges such as improving color and contrast, generating different aspect ratios, and refining human-centered details. Playground v2.5 highlights the importance of noise scheduling in achieving realism and visual fidelity in generated images. It also suggests that preparing a balanced bucketed dataset can help handle different aspect ratios during image generation and ensure that model outputs align with human aesthetic preferences, ultimately meeting perceptual expectations (as shown in Figure 23).

Continuous 3D Words [318] introduces a new three-dimensional perception method that learns continuous attribute control, allowing adaptation to various new conditions and improving object viewpoint changes. Localizing Object-level Shape Variations with T2I Diffusion Models [323] achieves object-level shape exploration by generating variations in specific object shapes, using self-attention and cross-attention layers to precisely localize operations on these shapes. FiVA is the first fine-grained visual attribute dataset. Building on FiVA, FiVA-Adapter [319] decomposes image aesthetics into specific visual attributes, enabling



A portrait of an African American woman on a black background at night, photo realistic, ultra realistic

Black UFO in front of a rising sun at the dawn, vibrant colours, dark surroundings, photorealistic

A black obelisk in front of a white background

A town square lit only by torchlight

Fig. 23: Colors and contrast. The top row is SDXL [14], bottom row is Playground v2.5. The model Playground v2.5 [329] can generate samples with more vibrant colors and contrast.

users to apply features like lighting, texture, and dynamics from different images. This approach allows decoupling visual attributes from one or more source images and adapting them to the generated image, thereby controlling fine-grained visual attributes during generation.

To address challenges in editing object layout, position, pose, and shape, Motion Guidance [324] employs a zero-shot technique that allows users to specify complex motion fields, guiding the diffusion model to achieve the desired effects. GLIGEN [320] introduces multimodal inputs, supporting not only textual prompts but also bounding boxes and reference images for more precise concept localization and generation control.

InteractDiffusion [321] incorporates interaction information into existing T2I models as an additional training condition, improving the accuracy of interactions in generated images, and improving the representation of complex relationships. NoiseCollage [327] independently estimates noise for objects using a noise collage technique, involving cropping and merging during the denoising process to optimize control over object layouts. Concept Weaver [328] employs a two-step approach to customized T2I generation, enhancing identity fidelity by generating personalized targets.

ConForm [331] proposes a contrastive framework to address challenges related to high-fidelity generation, focusing on comparing object attributes to improve image quality. LayerDiffuse [330] allows pretrained latent diffusion models to generate transparent images by adjusting latent transparency while maintaining overall quality.

SingDiffusion [325] addresses the issue of initial singularities in time steps within diffusion models, improving performance during generation, and reducing FID scores.

CFLD [326] introduces a new training paradigm that controls the generation process using images, gradually refining learnable queries to separate fine-grained appearance and pose information. Finally, PreciseControl [322] combines large T2I models with StyleGAN2 to achieve fine-grained attribute editing in the $W+$ latent space, allowing rough edits through text prompts.

4.14 LLM-assisted T2I

In the field of LLM-assisted T2I, several significant research efforts have been made to improve the accuracy and flexibility of generative models. MGIE [342] explores how multimodal large language models (MLLM) [357] can facilitate editing instructions, providing clear guidance to enhance image editing results, as shown in Figure 24.

LLM-grounded Diffusion [358] and VPGen [359] leverage large language models (LLMs) to infer object positions using carefully crafted system prompts. LayoutGPT [332] integrates language understanding with graphic generation technologies, utilizing pretrained language models like GPT-4 [126] to interpret complex layout instructions and generate the required 2D and 3D layouts. It also incorporates GLIGEN [320] for image layout generation, GLIP [360] for image evaluation, and ATISS for 3D scene synthesis, forming a complete end-to-end process.

LayoutLLM-T2I [335] is the first to explore layout planning in complex natural scenes using large language models and diffusion models. It proposes a feedback-based sampler learning paradigm and a layout-guided object interaction scheme. DiagrammerGPT [333] uses GPT-4 as a “planner” to generate layout information for diagrams and as an “auditor” for detail optimization. SmartEdit [337] improves

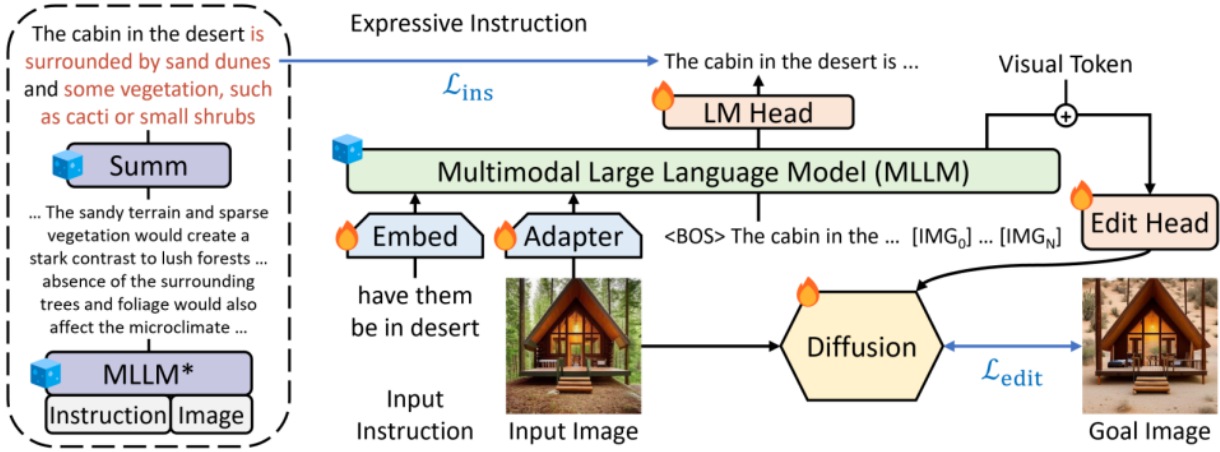


Fig. 24: Overview of MLLM-Guided Image Editing (MGIE) [342], which leverages MLLMs to enhance instruction-based image editing. MGIE learns to derive concise and expressive instructions while providing explicit visual-related guidance for the intended goal. The diffusion model jointly trains and achieves image editing with latent imagination through the edit head in an end-to-end manner, showing that the module is trainable or frozen, respectively.

the understanding and reasoning abilities for complex instructions using MLLM [357]. It introduces a bidirectional interaction module (BIM) to facilitate comprehensive information exchange between input images and MLLM outputs.

AutoStory [334] aims to generate story images that meet specific user needs with minimal human input, align text, and produce high-quality story visuals by combining LLM with diffusion models. CAFE [304] offers rapid customization without additional tuning, handling diverse inputs and inferring user intentions. Ranni [111] introduces a semantic panel as middleware to enhance the T2I generation process, improving the model’s ability to follow instructions.

RFNet [338] explores generating images from complex prompts that require artistic creativity by presenting a Reality-Fantasy Network. This network combines diffusion models with large language models (LLMs) without requiring additional training. TIAC [339] transforms abstract concepts into tangible physical objects by integrating information to generate prompts for T2I models. RPG [112] uses multimodal LLMs to enhance the combinatorial capacity of T2I generation, breaking the generation process into multiple simpler tasks. ELLA [340] introduces an efficient LLM adapter to improve text alignment without the need to train additional models.

DialogGen [341] establishes a multimodal interactive dialogue system for multi-turn T2I generation, ensuring effective prompt alignment and data organization. Lastly, MoMA [336] utilizes multimodal LLMs as feature extractors and generators, enhancing the similarity of target objects in the generated images. These studies provide significant theoretical foundations and practical insights for LLM-assisted T2I generation, advancing the development of the field.

5 DATASETS AND EVALUATION CRITERIA

5.1 Datasets

In the field of T2I, the construction and selection of datasets play a crucial role in the training, evaluation, and ensuring the fairness of the model. Enhancing image generation

capabilities requires large amounts of data [361], [362]. Fortunately, numerous datasets are available for the T2I tasks [363], as summarized in Table 5.

The COCO (Common Objects in Context) dataset [346] contains a diverse collection of more than 300,000 images, each paired with five human-generated descriptions that capture a wide variety of objects and scenes. This dataset is widely used in tasks related to image annotation, generation, and retrieval. Images are collected through crowd-sourcing, and the descriptions are authored by professionals, ensuring both diversity and accuracy.

COCO Captions [370] is a dataset derived from the COCO dataset, which itself is a large-scale collection of images obtained from Flickr, showcasing multiple objects in natural environments. COCO Captions extends MS-COCO by providing 1,026,459 captions for 164,062 images. Each image in the MS-COCO dataset has five captions, and a subset of 5,000 images includes annotations with 40 reference sentences.

The Flickr30k dataset [369], [386] contains 30,000 images, each paired with five textual descriptions spanning various everyday scenarios. It is primarily used for image generation and image-to-text retrieval tasks, reflecting the diversity of real-world scenes. Images are sourced from the Flickr platform, with descriptions provided by users.

The Flickr8k dataset [367] includes 8,000 images, each accompanied by five distinct descriptions. It is commonly used for image annotation and generation tasks and is well-suited for training image-to-text generation models as well as assessing the descriptive capabilities of models.

The Oxford 102 Flower Dataset [364] includes images of 102 flower species, with 40 to 258 images per species, each accompanied by detailed descriptions. This dataset is commonly used for fine-grained image generation and classification tasks. The images are captured through field photography and manually annotated, ensuring accuracy and detail. It also serves as a benchmark for previous T2I studies.

The CelebA dataset [375] consists of 200,000 images of

TABLE 5: Datasets in the T2I task.

Dataset	Year	Size	Source
Oxford 102 Flower Dataset [364]	2008	8,189	University of Oxford
UIUC Pascal Sentence [365]	2010	1,000	VOC2008
SBU Captions [366]	2011	1,000,000	Flickr.com
Flickr8K [367]	2013	8,092	Flickr.com
COCO [346]	2014	330,000+	Microsoft
ABSTRACT-50S [368]	2015	500	ASD
Flickr30k [369]	2015	31,783	Flickr.com
COCO Captions [370]	2015	204,721	Microsoft
PASCAL-50S [368]	2015	1,000	VOC2008
vQA [371]	2015	254,721	MS COCO & Abstract Images
Pinterest40M [372]	2016	40,000,000	Pinterest.com
Visual Genome [373]	2017	108,000	Stanford University
vQAv2.0 [374]	2017	204,721	MS COCO
CelebA [375]	2018	202,599	Chinese University of Hong Kong
Nocaps [376]	2019	15,100	Open Images V4 (Flickr.com)
VCR [377]	2019	110	LSMDC & YT
Conceptual Captions [378]	2018	3,369,218	Google Research
LAION-400M [379]	2021	400,000,000	LAION (Large-scale AI Open Network)
CC-500 [285]	2022	500	Synthetic prompts
Conceptual 12M [380]	2021	12,423,374	World Wide Web
LAION-5B [381]	2022	5,000,000,000	LAION
DiffusionDB [382]	2022	2,000,000	Open-source contributions
Winoground [383]	2022	800	Getty Images API
DrawBench [12]	2022	200	DALL-E & Reddit
ABC-6K [285]	2022	6,400	MS COCO
I2P [252]	2023	4,703	User generated prompts
T2I-CompBench [384]	2023	6,000	Generated prompts by GPT
PaintSkills [385]	2023	65,535	Synthetic prompts
RichHF-18K [134]	2024	18,000	Pick-a-Pic

celebrity faces, each tagged with 40 attribute labels. It is suitable for generating face images with specific features. The dataset is created by collecting and manually annotating celebrity images from the Internet, ensuring diversity and reliability of the attributes.

The Conceptual Captions dataset [378] contains three million images, each paired with a natural language description. It focuses on conceptual understanding and aims to promote multimodal learning. The images are gathered from the web and the descriptions are generated by computational algorithms, reflecting the contextual information of the images. Additionally, the Conceptual 12M dataset [380] includes 12 million images with concept-related descriptions.

LAION-400M [379] is a large-scale multimodal dataset comprising 400 million image-text pairs, primarily sourced from the Internet. This dataset is used for training large-scale image generation models, such as CLIP. The data is collected through web scraping, which automatically matches images with relevant text. LAION-5B [381] is used to assess gender bias in occupational contexts, generated by filtering relevant data from LAION-400M to help analyze gender bias in images related to various occupations.

The Visual Genome dataset [373] includes images along with detailed regional descriptions, supporting tasks such as object detection and image generation. The dataset provides detailed annotations generated through a combination of manual annotation and CV techniques, aiding in the understanding of complex image content.

The SBU Captions dataset [366] contains over one million images paired with corresponding descriptions, primarily used to train and evaluate image generation models. The images in this dataset are collected from Flickr, and the descriptions are generated based on the context of the images, ensuring diversity and comprehensiveness.

DiffusionDB [382] is a large-scale prompt gallery dataset that provides extensive prompt data for T2I generation models, primarily gathered through automated collection and organization. PaintSkills [385] is a dataset focused on painting skills, emphasizing object recognition, quantity, and spatial relationships between objects in images and text. It is mainly used for researching models that generate artistic works and provides a wealth of painting samples to enhance the model’s artistic capabilities.

The Pinterest40M dataset [372] contains 40 million images along with associated texts, such as user comments and tags. It is intended for multimodal learning and recommendation systems, supporting tasks related to image content understanding and the training of recommendation algorithms. The dataset helps models learn associations between images and text, making it suitable for image retrieval, personalized recommendations, and advertising optimization tasks.

Nocaps [376], developed by Facebook AI Research, is designed to evaluate a model’s ability to generate image descriptions without relying on contextual information. It includes question-and-answer tasks related to images, aiming to enhance the model’s understanding of visual content and enable it to generate accurate descriptions even without additional context. This is crucial for developing AI systems capable of independently understanding and describing images.

The UIUC Pascal Sentence Dataset [365] combines images with corresponding sentences and is primarily used for research in image understanding and description generation. Each image is accompanied by multiple sentence descriptions, supporting diverse generation tasks and NLP applications.

PASCAL-50S [368] contains 50 object categories with their descriptions, mainly used for image understanding

and generation tasks. This dataset supports object recognition and classification, making it suitable for training and evaluating CV models.

ABSTRACT-50S [368] focuses on abstract concepts, providing images and their descriptions. It is suitable for researching image understanding and generation, which presents challenging tasks that require models to generate descriptions at a higher conceptual level.

The Visual Question Answering (VQA) dataset [126], [349], [371] allows users to ask questions about images and receive corresponding responses. It supports the training and evaluation of models, helping to improve their visual understanding and reasoning capabilities. VQAv2.0 [374] is an updated version of the VQA dataset, featuring a wider range of question types and more diverse image data, increasing thus the complexity of the questions. This dataset is used to train and evaluate the performance of question-answering models.

The VCR (Visual Commonsense Reasoning) dataset [377] combines visual and textual information to support complex reasoning tasks, evaluating a model's reasoning capabilities based on visual input. Winoground [383] is also used to assess a model's reasoning ability in understanding the relationship between images and text, with an emphasis on contextual understanding and relevance. It provides complex tasks to evaluate the model's reasoning skills, featuring 1,600 image-text pairs: 800 correct and 800 incorrect, covering 400 examples and showcasing 800 unique titles and images.

DrawBench [12], developed alongside the Imagen model, includes 200 challenging prompts designed to assess the performance of various T2I models, covering 11 different categories. DrawBench serves as a valuable tool for T2I research, promoting the development of generative models in a variety of application scenarios.

ABC-6K [285] contains 6,000 images with descriptions, suitable for image generation and understanding tasks, facilitating rapid experimentation. This dataset provides a straightforward environment for testing and validating image processing algorithms. Similarly, the CC-500 [285] dataset includes 500 images with descriptions, mainly used for quick experimentation and validation, making it suitable for developing and testing preliminary models.

I2P [252] is a dataset for image-to-image translation that focuses on transforming one image into another. It supports a variety of generation tasks and is useful for research in image transformation and processing.

RichHF-18K [134] contains 18,000 images with detailed descriptions and is primarily used for multimodal learning and evaluation. It offers complex annotations to support the fine-tuning of scoring models based on human feedback, providing valuable resources for evaluating generative models through detailed annotations and intricate feedback mechanisms.

T2I-CompBench [384] is a dataset designed to investigate complex prompt combinations in image generation models. It is used to evaluate the performance of different models when handling complex textual prompts and provides various evaluation criteria to help researchers analyze the generative capabilities of the models.

These datasets enable researchers to comprehensively evaluate and optimize the performance of T2I generation models, advancing research in this field.

5.2 Data Augmentation

In T2I generation tasks, data augmentation is an important technique to improve model performance and generation quality. Common image enhancement techniques include rotation, translation, cropping, resizing, flipping, adding noise, and adjusting brightness, contrast, saturation, and random erasure. These techniques help maintain visual consistency and improve model robustness. For text data augmentation, common methods include synonym replacement (replacing words in text descriptions to increase the diversity of training samples), text reconstruction (modifying sentence structures or using different descriptions while preserving the original meaning to enrich the dataset) and random insertion or deletion (randomly inserting or deleting words in the text to generate variations) [55].

In multimodal tasks, T2I data can be augmented by generating new images based on existing text descriptions and creating new text descriptions from existing images [387]. Additionally, combining these data augmentation methods can lead to even better results.

Label smoothing [388] is also widely used to improve the robustness and accuracy of models during training. The Mixup technique [389] involves using convex combinations of samples and their labels to train neural networks. However, because interpolated samples do not introduce new information, relying solely on this method may not effectively address data scarcity. Therefore, retrieving relevant training data from external databases for re-imaging is crucial to further enhance model performance.

LAFITE [87] is the first work to implement language-free training for T2I generation. This approach leverages the powerful pretrained CLIP model [68] to use its multimodal semantic space, thus reducing the reliance on explicit text conditions by generating text features from image features.

In recent T2I research, linear extrapolation has been used to enhance text features in small datasets. This means that new image data can be retrieved from search engines using text descriptions to expand the existing dataset [390]. Furthermore, K-means clustering [391] and fine-grained classifiers can be used to identify and remove irrelevant images, ensuring the quality of the new data. Furthermore, introducing a NULL condition guidance mechanism [75], [392], [393] improves the score estimation for image generation by using prompts with no physical meaning. These methods are effective in increasing data volume for small datasets.

The Semantic-aware Data Augmentation (SADA) framework [394] is a new data augmentation approach specifically designed for T2I synthesis. It introduces an implicit text semantic preservation enhancement method to improve text representation in the semantic space and combines it with a specially designed image semantic regularization loss to ensure semantic consistency in the generated images. This approach effectively addresses issues such as semantic mismatches and collapse. Theoretically, it has been shown that implicit text semantic preservation enhancement can

improve text-image consistency, while image semantic regularization loss helps maintain semantic integrity in generated images, preventing semantic collapse, and enhancing image quality.

5.3 Evaluation Metrics

Evaluating T2I is a highly challenging task. Effective evaluation metrics for T2I models must not only assess the realism of generated images, but also consider the semantic relevance between the textual descriptions and the generated images. In addition, the diversity of the generated content is a critical factor. A comprehensive evaluation framework should integrate these dimensions to ensure that the generated images accurately reflect the textual content while also demonstrating richness and variability in expression [363].

Several important evaluation metrics for T2I tasks are summarized in Table 6. Among them, C2ST (Cumulative 2-Sample Test) [395] uses statistical methods to assess the similarity between generated images and real images, focusing primarily on comparing the distributions of the two samples. KPR (Kernel Precision Recall) [396] combines kernel methods with precision and recall to analyze the comprehensiveness of the generated content. SSIM (Structural Similarity Index) [397] evaluates image quality by analyzing the similarity between generated and reference images in terms of luminance, contrast, and structural information. PSNR (Peak Signal-to-Noise Ratio) [398] assesses image quality by calculating the mean squared error, providing a measure of the signal-to-noise ratio. The Inception Score (IS) [399] employs a pretrained Inception model to evaluate the quality of generated images by calculating their class distribution and diversity, focusing on the recognizability of the images. The Fréchet Inception Distance (FID) [400] is widely used in image generation tasks and measures quality by calculating the distance between generated images and real images in the feature space. Modified FID (MiFID) [401] improves FID by incorporating multiple indicators to assess image quality, including diversity and structural features. The Kernel Inception Distance (KID) [402] enhances the robustness of FID through the use of kernel methods, making it particularly suitable for small sample scenarios. R-Precision [403] is a classic metric used in information retrieval, evaluating the accuracy of image and text matching by examining the proportion of correct matches. PickScore [404] is commonly used for GAN models to assess the diversity and quality of generated images, usually achieved through feature extraction and comparison.

The Holistic Evaluation of Text-to-Image Models (HEIM) [405] combines self-curated prompts with MS-COCO data [346] to propose an evaluation benchmark that includes biases and fairness subcategories, providing a comprehensive assessment of text-to-image generation models.

Using OpenAI’s CLIP model, CLIPScore [413] calculates the similarity between images and text by embedding them in the same feature space and evaluating their relevance using cosine similarity. CLIP-R-Precision [403] assesses the quality of generated content by calculating the matching accuracy between images and text. NegCLIP [414] introduces negative samples for contrastive learning, enhancing image-text alignment. MosaiCLIP [419] evaluates overall

TABLE 6: Evaluation metrics in T2I task.

Metric	Year	Human Evaluated	Positive Correlation
SSIM [397]	2004	✓	✓
PSNR [398]	2010	✓	✓
CIDEr [368]	2015	✓	✓
IS [399]	2016	×	✓
C2ST [395]	2016	×	✓
FID [400]	2017	×	×
KID [402]	2018	×	✓
PRD [406]	2018	×	×
LEIC [407]	2018	×	×
GMM-GIOA [408]	2018	×	×
KPR [396]	2019	×	✓
VIFIDEL [409]	2019	✓	✓
TIGer [410]	2019	✓	✓
I-PRD [396]	2019	×	×
ViLBERTScore [411]	2020	✓	✓
SOA [412]	2020	✓	✓
MiFID [401]	2021	×	×
R-Precision [403]	2021	✓	✓
CLIPScore [413]	2021	✓	✓
CLIP-R-Precision [403]	2021	✓	✓
NegCLIP [414]	2022	×	×
BLIP-ITC [415]	2022	×	✓
BLIP-ITM [415]	2022	×	✓
vISORcond [416]	2022	✓	✓
vISOR [416]	2022	✓	×
vISORN [416]	2022	✓	×
MID [417]	2022	✓	✓
PA [63]	2022	✓	✓
CA [63]	2022	✓	×
Aesthetic Predictor [381]	2022	×	✓
PAL4InPaint [418]	2022	×	×
PickScore [404]	2023	✓	✓
MosaiCLIP [419]	2023	×	✓
CLIP-IOA [420]	2023	✓	×
BLIP2-ITC [349]	2023	×	✓
BLIP2-ITM [349]	2023	×	✓
HPSv1 [136]	2023	✓	✓
HPSv2 [136]	2023	✓	✓
ViCE [421]	2023	✓	✓
DINO Metric [43]	2023	×	✓
DreamSim [422]	2023	✓	✓
DA-Score [423]	2023	×	✓
3-in-1 [384]	2023	✓	✓
TIFA [424]	2023	×	×
VIEScore [425]	2023	×	✓
UniDet [384]	2023	×	×
COBRA [426]	2024	✓	✓
VNLI [427]	2024	✓	×
MINT-IQA [428]	2024	✓	✓
TIAM [343]	2024	✓	✓
CLove [429]	2024	×	×
HEIM [405]	2024	✓	✓
MQ [430]	2024	×	✓

performance by concatenating and comparing multimodal features. CLove [429] quantifies the similarity between generated images and their textual descriptions, while CLIP-IOA (CLIP Image Output Assessment) [420] measures the degree of alignment between generated images and text descriptions.

The BLIP model also provides evaluation metrics. BLIP-

ITC [415] uses contrastive learning in image-text pairs to calculate similarity and consistency. BLIP-ITM [415] focuses on direct image-text matching, evaluating alignment using a contrastive learning framework. BLIP2-ITC [349] is an improved version of BLIP, designed to enhance image-text matching performance by optimizing contrastive learning for more efficient similarity scoring. BLIP2-ITM [349] uses enriched image and text features to match, assessing the relevance and consistency of the generated content.

ImageReward [137] evaluates the quality of generated images through a reward mechanism, often integrating human evaluations or feedback from pretrained models. RAHF (Relevance-Aware Hybrid Framework) [134] combines image-text relevance employing various features for comprehensive scoring while incorporating human feedback. PAL4VST [431] emphasizes perceptual evaluation, focusing on the subjective quality of the generated content.

COBRA [426] evaluates the alignment between objects in images and text using contrastive learning. HPSv1 [136] and its improved version, HPSv2 [136], assess the consistency and quality of generated content through multimodal contrastive learning, with HPSv2 offering enhanced evaluation accuracy. vISORcond [416] uses conditional contrastive learning to understand the dependencies between images and text, thus assessing the quality of the generated content. VIFIDEL [409] integrates visual and textual features, using contrastive learning to analyze the relationship between images and text while calculating similarity scores. ViCE [421] uses contrastive learning to evaluate the embedding space of images and text, optimizing similarity through a contrastive loss function.

ViLBERTScore [411], based on the ViLBERT model, assesses the correlation between images and text by calculating joint embeddings to evaluate the match between generated content and its descriptions, using contrastive learning to optimize scores. vISOR [416] evaluates generation quality by comparing the similarity between images and text, calculating matching scores that combine visual and linguistic features, making it well-suited for analyzing complex image-text relationships. vISORN [416] is an enhanced version of vISOR that incorporates negative sample contrastive learning to improve understanding of image-text relationships, strengthening its ability to distinguish between correct and incorrect matches.

VNLI [427] emphasizes reasoning capabilities by assessing the relationships between images and text through natural language inference, analyzing whether the image content supports the text description, typically using inference models to generate evaluation results. The DINO Metric [43], based on self-supervised learning, evaluates generation quality by comparing image and text features, using the DINO model to extract features and compute similarity scores. MID [417] assesses the relevance between multimodal features by extracting and comparing them. MINT-IQA [428] evaluates the quality of images and text using inference methods, combining multimodal information to analyze the consistency of generated content.

DreamSim [422] simulates the evaluation process to calculate the correlation between generated images and their textual descriptions. TIGER [410] analyzes the generation processes of text and images, assessing the quality

of generated content by integrating various features and models to provide a comprehensive score. DA-Score [423] evaluates both the diversity and accuracy of generated content, quantifying how well the generated results match the textual descriptions. The 3-in-1 metric [384] combines three aspects—generation quality, relevance, and diversity—to provide a holistic assessment.

PA [63] is a metric for evaluating precision and recall in multimodal tasks, focusing on the relevance of generated content. PRD [406] combines precision and recall to assess performance by calculating the overlap between generated content and reference content. I-PRD [396] enhances PRD, aiming to improve the accuracy and robustness of the evaluation.

CA [63] examines how well the generated content covers the textual description, determining whether the generated images include all significant elements mentioned in the text by calculating feature coverage. LEIC [407] assesses the similarity between images and text by comparing their embedded features using cosine similarity. CIDEr [368] computes weighted TF-IDF values of N-Grams to evaluate the similarity between generated descriptions and reference descriptions, with a particular emphasis on the consensus of the descriptions.

TIAM [343] evaluates the alignment between textual descriptions and images by calculating feature similarity and analyzing semantic consistency. TIFA [424] focuses on the consistency of textual and visual features, ensuring that the generated content aligns with the input text by calculating feature vector similarity. GMM-GIOA [408] uses a Gaussian mixture model to evaluate the quality of the generated images by analyzing the distributional differences between the generated and reference images.

VIEScore [425] calculates the similarity between visual and linguistic features by analyzing the embedded characteristics of images and text, providing matching scores suitable for fine-grained assessments in multimodal learning. MQ [430] integrates image quality and text quality, consolidating various features to provide a comprehensive evaluation. UniDet [384] assesses the relationship between images and text using unified feature extraction and comparison methods, yielding an overall matching score.

The Aesthetic Predictor [381] evaluates the quality of generated content by analyzing the aesthetic characteristics of images, typically using a pretrained aesthetic model to compute aesthetic scores. PAL4InPaint [418] specializes in image inpainting tasks, combining multiple features to assess the quality of generated images, including semantic consistency and visual quality. Semantic Object Accuracy (SOA) [412] metric is employed for the quantitative evaluation of T2I tasks, utilizing a pre-trained object detector to assess whether the generated images contain the objects mentioned in the corresponding captions.

These advancements in evaluation metrics for T2I tasks will allow for a more comprehensive assessment of the quality and applicability of generated content, ultimately promoting further progress in T2I generation technology.

6 APPLICATIONS

In this digital age, artificial intelligence (AI) has become a major driving force behind technological innovation. In



Fig. 25: Example storytelling images generated by the method AutoStory [334]. It can generate text-aligned, identity-consistent, and high-quality story images from user-input stories and characters (the dog and cat on the left, specified by about 5 images per character), without additional inputs like sketches.

particular, T2I tools have emerged as a crucial element of AI-generated content (AIGC) [22]. Section 4 discusses the latest advancements in T2I technology. Based on this research, T2I technology has shown broad practical applications in various fields, significantly improving creativity and production efficiency.

6.1 T2I for Artistic Creation

2022 is often referred to as the year of AIGC. In the field of artistic creation, artists can use models like DALL-E [7], Stable Diffusion [33], Imagen [12], DALL-E-2 [10], DreamBooth [43] to generate unique art pieces based on specific descriptions. For example, by inputting “a cat playing golf on the moon”, the model can quickly produce an image that matches this description, helping artists spark their creativity and explore different styles.

In story creation, tools like TaleCraft [432], Custom Diffusion [106], Paint-by-Example [433], Make-a-Story [434] and AutoStory [334] enable creators to adapt their written texts into specific narratives, allowing for the rapid generation of continuous animations. As illustrated in Figure 25, AutoStory can generate a series of stories for a given animal based on text descriptions. This approach significantly reduces labor costs.

In game development, tools like DeepArt, Artbreeder and appsmith allow developers to generate concept art for characters and scenes. Designers can input “mysterious forest creature”, and the model will generate various visual styles for character designs, greatly saving time and costs associated with manual drawing.

In virtual reality and augmented reality applications, DeepAI can generate personalized environments based on user input. For instance, if a user wishes to experience a “sunset beach scene”, the model can generate images for use in virtual reality experiences, enhancing the user’s sense of immersion.

6.2 T2I for E-Commerce

Companies use tools like Stable Diffusion [33] and DALL-E [7] to quickly create appealing visual content based on product descriptions, enabling brands to publish creative ads on social media and attract more customer attention. For example, a beverage company might input “refreshing summer juice drink”, and the model would generate a variety of creative images that effectively enhance marketing impact. Here we use the Kolors [435] platform for generation, as illustrated in Figure 26.

In the context of cross-border women’s fashion e-commerce, it is essential to consider how customers from different countries perceive the fitting effects of clothing on models when launching advertisements. Many brands hire models from various countries to showcase the same clothing, aiming to cater to diverse customer preferences. Generative AI can play a crucial role here by utilizing the in-paint mask function in combination with the Stable Diffusion model [33] and relevant prompts to generate fitting effect images of different virtual models. This approach not only reduces the costs associated with hiring models, but also significantly reduces the time required for photoshoots.

Beyond fitting images in the women’s fashion industry, typical advertising scenarios in e-commerce also include product packaging design. Product packaging directly influences consumer appeal and attention, often impacting sales. For design purposes, T2I tools like ControlNet [13] can be used to generate diverse packaging designs by combining specific design templates. This approach not only enhances design efficiency, but also allows designers to quickly iterate and optimize their designs.

Overall, the application of T2I technology in advertising and marketing not only improves creative efficiency, but also enables brands to respond more flexibly to market demands, driving innovation in marketing strategies. Using specific models and tools, companies can stand out in a competitive market.



Fig. 26: Example images generated by Kolors [435], with the text description “refreshing summer juice drink”. Kolors can produce a variety of clear image results.

6.3 T2I for Education and Healthcare

OpenAI’s CLIP model [68] is widely used to generate vivid teaching materials. Teachers can input prompts like “explain the process of photosynthesis”, and the model such as Kolors generates relevant images that help students better understand complex concepts, thus improving learning outcomes, such as Figure 27.

GANs [3], [82], [436] can be used to create visualizations of medical images, helping doctors in diagnosis and treatment planning. For example, by inputting “abnormalities in lung CT scans”, the model generates images that provide important visual references to doctors.

6.4 T2I for Social Media

Users can leverage RunwayML and Kolors to transform text content into personalized images, creating eye-catching social media posts. They can also use powerful tools such as Stable Diffusion 3 [47], DALL-E-3 [42], and CogView2 [11] to generate these images. For instance, by inputting “a sunny day”, the model generates images that enhance visual appeal and boost user engagement. Similarly, content creators can quickly generate images to complement articles or videos using technologies such as Stable Diffusion [33]. For example, a blogger might input “a futuristic city”, and the resulting images can significantly increase the visual appeal of the content, as illustrated in Figure 28, capturing the audience’s interest.

The widespread application of T2I is reshaping creative practices in various fields: from artistic creation to advertising, marketing, game development, and education. This technology not only improves creative efficiency and enhances visual expression, but also provides new flexibility and opportunities for innovation for both businesses and creators. As generative AI continues to evolve, T2I technology is expected to play an increasingly important role in future commercial and artistic environments, driving innovation and development across industries. Through specific models and tools, T2I technology helps brands and individuals stand out in a competitive market by creating more engaging content.

7 CHALLENGES AND OUTLOOK

7.1 Challenges

Despite the significant potential of T2I technology in various fields, it still faces several challenges.

7.1.1 Data and Computational Resource Challenges

Training large models relies heavily on the collection of text-image pair data, which inevitably introduces biases, such as imbalances in racial and gender representation. [245], [250] These biases often originate from the datasets themselves, which can predominantly include images and descriptions that reflect certain demographics more than others. As a result, models trained on these datasets may exhibit biased behaviors, such as underrepresenting minority groups or generating stereotypical representations. This can lead to unfair performance when models are applied across different demographic groups, failing to provide equal representation or accurate outcomes for underrepresented communities. For example, when asked to generate images of professionals, a model might predominantly depict men, reflecting the societal biases present in the training data. This lack of fairness not only affects the accuracy of the generated results but also raises ethical concerns regarding the inclusivity of such AI technologies [254], [437], [438].

Additionally, most current models are designed with English as the default input language, putting non-English speakers at a significant disadvantage. This language barrier limits the accessibility and usability of these models globally, excluding a large portion of the population from fully benefiting from AI advances. Moreover, cultural nuances embedded in non-English texts are often lost, resulting in outputs that lack cultural relevance or misinterpret local contexts. To address these challenges, it is crucial to create more diverse and inclusive datasets [381], [439], [440] that represent a wide range of cultural, linguistic, and demographic variations. This would involve actively collecting data that includes minority groups, diverse languages, and different social contexts. It is equally important to explore new methods to mitigate the impact of these dataset biases on model performance [441], such as incorporating bias correction techniques, ensuring equitable representation, and using adversarial training to identify and reduce discriminatory tendencies in generated output.

The success of deep learning largely depends on the availability of rich labeled data, which is especially important for T2I generation models. Many major frameworks, such as DALL-E 2 [10], GLIDE [8], and Imagen [12], are trained on hundreds of millions of image-text pairs. This reliance on extensive datasets results in significant computational overhead, as training requires substantial computational resources and access to large-scale data infrastruc-



Fig. 27: Given Kolors [435] the content “explain the process of photosynthesis”, it can generate a series of images related to photosynthesis to enhance educational significance.

ture. Consequently, the costs associated with training such models are prohibitively high, limiting the opportunities for small and medium enterprises (SMEs) and research institutions to participate. Only large technology companies such as OpenAI, Google, and Baidu have the resources to afford such high training costs, leading to a concentration of power and technological capabilities in the hands of a few. This disparity creates a barrier for smaller players, preventing them from contributing to or benefiting from advancements in AI, and ultimately slowing the democratization of AI technology.

Furthermore, the large scale of these models makes their deployment in resource-constrained environments, such as edge devices or mobile platforms, particularly challenging. These models typically require substantial computational power and memory, making them impractical for real-time applications where lightweight and efficient inference is essential. As AI applications increasingly move toward edge computing, it becomes crucial to develop efficient model compression techniques, such as pruning, quantization, and knowledge distillation, to reduce the computational and memory requirements of these large models. This would enable their deployment in various environments, including those with limited resources, thus expanding their applicability and accessibility [46], [224].

To address these challenges, the research community needs to focus on a few key areas. First, more effort should be directed toward creating and curating balanced and diverse datasets that include a wide variety of cultural and linguistic contexts [405], [442], [443], which would reduce bias and improve model inclusion. Second, innovation in algorithm design is needed to create models that can learn effectively from smaller, high-quality datasets, rather than relying solely on massive data collection. This would make model training more accessible to smaller institutions and

researchers who may not have access to vast computational resources.

In addition, there is a need for increased collaboration between academia, industry, and policy makers to establish standards and guidelines that promote fairness, transparency, and accessibility in model training and deployment. Creating open and collaborative platforms for data sharing and model development can also help to distribute the benefits of AI more equitably, ensuring that advances in technology are not concentrated in the hands of a few, but are accessible to a broader community.

By addressing these data and computational challenges, the AI community can help create more equitable and inclusive technologies, making AI-generated content beneficial for users of all backgrounds and across different sectors. This will ensure that the development and use of AI models is more sustainable, fair, and accessible, ultimately fostering a more inclusive technological future.

7.1.2 Copyright and Ethical Issues

Although considerable progress [260], [262] has been made in addressing copyright and safety concerns, the issue of copyright infringement remains a significant challenge for T2I models [261], [444]. Generated images can still potentially infringe upon copyrights, especially when models are trained on content without proper authorization or when copyrighted works are used without clear attribution. The lack of transparency with respect to the sources of training data can further complicate the legal landscape, raising questions about intellectual property rights and the ownership of generated images. Researchers and developers must establish guidelines and implement mechanisms that respect the rights of original creators to avoid unintended copyright violations.



Fig. 28: Given the text description “a futuristic city”, a series of images can be generated to capture users’ attention. This example was generated by Kolors [435].

Moreover, ensuring the ethicality and nonmisleading nature of generated content is an ongoing critical issue. T2I models can sometimes generate misleading or harmful content, such as Deepfakes, which can be used for malicious purposes, including spreading misinformation or violating individuals’ privacy. This raises concerns about accountability and the responsible use of AI technologies. To address these issues, it is necessary to develop stricter ethical guidelines and implement safeguards, such as content moderation and transparent usage policies, to minimize misuse.

Another ethical concern involves biases in the generated content. Since models are trained on large datasets that may contain biased information, they can inadvertently produce biased or harmful images, leading to unfair representation of certain groups or reinforcing harmful stereotypes. Addressing these biases requires efforts to create more balanced training datasets and develop techniques that actively detect and reduce biased output [248], [250]. This is especially important as T2I models become more integrated into various applications, including media, education, and entertainment.

7.1.3 Understanding Complex Text, Generative Diversity, and Representation

Models may struggle to accurately understand context and implicit meanings when processing complex or abstract text, which can significantly impact the accuracy and relevance of the generated results. For example, when dealing with idiomatic expressions, nuanced phrases, or cultural references, the model might misinterpret the intended meaning, leading to outputs that do not match the original intent. This limitation is especially problematic in scenarios that require a deep understanding of the text, such as generating artwork based on literary descriptions or creating visuals that align with abstract themes.

Furthermore, generative models often exhibit inherent biases that result in a lack of diversity and representation in the generated images. These biases typically arise from imbalances in training data, where certain demographic groups or cultural contexts are underrepresented. As a consequence, the generated outputs may reinforce stereotypes or exclude diverse perspectives, limiting the applicability of these models to a broader audience. For example, when asked to generate images of professionals, the model may produce predominantly male figures, reflecting the biases present in the dataset. This lack of fairness and inclusivity

can have real-world implications, perpetuating stereotypes, and reducing the utility of the model for diverse users.

To address these challenges, significant improvements are needed in both the training data [295], [381] and algorithm [134] design. For training data, it is crucial to incorporate more diverse and balanced datasets that accurately represent different cultures, genders, and social contexts. This will help mitigate the biases present in the generated outputs and ensure that the models are more inclusive. Additionally, adopting techniques such as data augmentation, bias correction, and active learning can further enhance the model’s ability to handle diverse inputs effectively.

On the algorithmic side, more sophisticated approaches are required to improve contextual understanding and reduce biases. This may involve incorporating advanced natural language understanding techniques, such as context-aware embeddings, or leveraging reinforcement learning to guide the model toward fairer and more accurate outputs. Researchers are also exploring methods such as adversarial training to detect and correct biases during the model training process, ensuring that the generated results are not only relevant but also ethical and inclusive.

Ultimately, by addressing these challenges through more diverse data and advanced algorithmic solutions, generative models can produce a more accurate, fair, and representative output. This will not only enhance their usability across a wide range of applications but also promote equitable access to AI-generated content for users of different backgrounds and perspectives.

7.2 Outlook

7.2.1 Social Responsibility and Ethical Considerations

As image generation technology becomes more widely adopted, it is crucial to consider its potential social impacts and ethical issues. Researchers and developers should actively work to ensure that technological advancements do not result in bias, discrimination, or other negative consequences. In addition, establishing transparent usage standards and ethical frameworks is essential to guide the responsible and sustainable development of this technology.

7.2.2 Cross-Field Applications

T2I technology is expected to find broader applications in various fields, including education, healthcare, and game

development, driving innovation and growth in these areas. With the rapid advancement of deep learning, exploring collaborations between T2I diffusion models and other advanced technologies, such as the latest developments in NLP, presents an exciting opportunity. Applying these cutting-edge technologies to T2I could lead to new breakthroughs. For example, incorporating self-supervised learning techniques into T2I generation or using the latest dialogue systems to enhance user interaction are promising areas for further research.

7.2.3 Popularization and Accessibility

As technology advances and computational resources improve, T2I tools are expected to become more accessible, allowing more creators and small businesses to use them in their projects. In addition, clearer and more diverse evaluation standards, such as quantitative metrics and subjective assessments, will be developed, allowing fair comparisons between different research efforts. By integrating various evaluation methods, a more comprehensive assessment of model performance can be achieved.

7.2.4 Higher Generation Quality and Enhanced Context Understanding

In the context of ongoing technological advancements, focusing on emerging algorithms and model architectures will be crucial to improving the quality of T2I generation. Researchers should actively explore new network structures, optimization algorithms, and training methods to address the limitations of current models. Recent studies indicate that models such as Mamba [445] and TTT [446] can achieve better results as alternatives to the Transformer architecture. T2I technology can also benefit from similar iterations and upgrades to achieve superior performance. These efforts will not only enhance the quality of generated images, but may also advance the entire field. Future T2I tools are expected to generate higher quality, more refined images that meet increasingly complex creative demands. Moreover, future models are likely to better understand the context and emotions expressed in the text, allowing them to produce images that more closely align with the intent of the user.

As technology serves humanity, by addressing current challenges and seizing future opportunities, T2I technology is set to play an even more significant role in various fields, driving the continuous development and innovation of the creative industry.

REFERENCES

- [1] E. Mansimov, E. Parisotto, J. L. Ba, and R. Salakhutdinov, "Generating images from captions with attention," *arXiv preprint arXiv:1511.02793*, 2015. **1**
- [2] S. Reed, Z. Akata, X. Yan, L. Logeswaran, B. Schiele, and H. Lee, "Generative adversarial text to image synthesis," in *ICML*, 2016. **1, 2, 3, 4, 6**
- [3] H. Zhang, T. Xu, H. Li, S. Zhang, X. Wang, X. Huang, and D. N. Metaxas, "Stackgan: Text to photo-realistic image synthesis with stacked generative adversarial networks," in *ICCV*, 2017. **1, 2, 4, 6, 30**
- [4] T. Xu, P. Zhang, Q. Huang, H. Zhang, Z. Gan, X. Huang, and X. He, "Attngan: Fine-grained text to image generation with attentional generative adversarial networks," in *CVPR*, 2018. **1, 2, 4, 6**
- [5] M. Zhu, P. Pan, W. Chen, and Y. Yang, "Dm-gan: Dynamic memory generative adversarial networks for text-to-image synthesis," in *CVPR*, 2019. **1, 2, 5, 6**
- [6] J. Cheng, F. Wu, Y. Tian, L. Wang, and D. Tao, "Rifegan: Rich feature generation for text-to-image synthesis from prior knowledge," in *CVPR*, 2020. **1, 5, 6**
- [7] A. Ramesh, M. Pavlov, G. Goh, S. Gray, C. Voss, A. Radford, M. Chen, and I. Sutskever, "Zero-shot text-to-image generation," in *ICML*, 2021. **1, 2, 3, 4, 6, 8, 16, 20, 29**
- [8] A. Nichol, P. Dhariwal, A. Ramesh, P. Shyam, P. Mishkin, B. McGrew, I. Sutskever, and M. Chen, "Glide: Towards photorealistic image generation and editing with text-guided diffusion models," *arXiv preprint arXiv:2112.10741*, 2021. **1, 2, 4, 5, 8, 9, 30**
- [9] M. Ding, Z. Yang, W. Hong, W. Zheng, C. Zhou, D. Yin, J. Lin, X. Zou, Z. Shao, H. Yang *et al.*, "Cogview: Mastering text-to-image generation via transformers," in *NeurIPS*, 2021. **1, 2, 4, 6, 8**
- [10] A. Ramesh, P. Dhariwal, A. Nichol, C. Chu, and M. Chen, "Hierarchical text-conditional image generation with clip latents," *arXiv preprint arXiv:2204.06125*, vol. 1, no. 2, p. 3, 2022. **1, 2, 8, 9, 16, 29, 30**
- [11] M. Ding, W. Zheng, W. Hong, and J. Tang, "Cogview2: Faster and better text-to-image generation via hierarchical transformers," in *NeurIPS*, 2022. **1, 2, 7, 8, 30**
- [12] C. Saharia, W. Chan, S. Saxena, L. Li, J. Whang, E. L. Denton, K. Ghasemipour, R. Gontijo Lopes, B. Karagol Ayan, T. Salimans *et al.*, "Photorealistic text-to-image diffusion models with deep language understanding," in *NeurIPS*, 2022. **1, 2, 8, 9, 16, 25, 26, 29, 30**
- [13] L. Zhang, A. Rao, and M. Agrawala, "Adding conditional control to text-to-image diffusion models," in *ICCV*, 2023. **1, 2, 8, 9, 11, 12, 14, 29**
- [14] D. Podell, Z. English, K. Lacey, A. Blattmann, T. Dockhorn, J. Müller, J. Penna, and R. Rombach, "Sdxl: Improving latent diffusion models for high-resolution image synthesis," *arXiv preprint arXiv:2307.01952*, 2023. **1, 2, 8, 9, 23**
- [15] W. Zheng, J. Teng, Z. Yang, W. Wang, J. Chen, X. Gu, Y. Dong, M. Ding, and J. Tang, "Cogview3: Finer and faster text-to-image generation via relay diffusion," *arXiv preprint arXiv:2403.05121*, 2024. **1, 2, 8, 9**
- [16] Y. Bengio, R. Ducharme, and P. Vincent, "A neural probabilistic language model," in *NeurIPS*, 2000. **1**
- [17] A. Vaswani, "Attention is all you need," in *NeurIPS*, 2017. **1, 2, 4, 6**
- [18] T. B. Brown, "Language models are few-shot learners," *arXiv preprint arXiv:2005.14165*, 2020. **1, 8**
- [19] D. Marr, *Vision: A computational investigation into the human representation and processing of visual information*. MIT press, 2010. **1**
- [20] A. Krizhevsky, I. Sutskever, and G. E. Hinton, "Imagenet classification with deep convolutional neural networks," in *NeurIPS*, 2012. **1**
- [21] A. Dosovitskiy, "An image is worth 16x16 words: Transformers for image recognition at scale," *arXiv preprint arXiv:2010.11929*, 2020. **1**
- [22] J. Wu, W. Gan, Z. Chen, S. Wan, and H. Lin, "Ai-generated content (aigc): A survey," *arXiv preprint arXiv:2304.06632*, 2023. **1, 29**
- [23] B. Goertzel and C. Pennachin, *Artificial general intelligence*. Springer, 2007, vol. 2. **1**
- [24] B. Goertzel, "Artificial general intelligence: concept, state of the art, and future prospects," *Journal of Artificial General Intelligence*, vol. 5, no. 1, p. 1, 2014. **1**
- [25] J. Pei, L. Deng, S. Song, M. Zhao, Y. Zhang, S. Wu, G. Wang, Z. Zou, Z. Wu, W. He *et al.*, "Towards artificial general intelligence with hybrid tianjic chip architecture," *Nature*, vol. 572, no. 7767, pp. 106–111, 2019. **1**
- [26] H. Zhang, T. Xu, H. Li, S. Zhang, X. Wang, X. Huang, and D. N. Metaxas, "Stackgan++: Realistic image synthesis with stacked generative adversarial networks," *IEEE TPAMI*, vol. 41, no. 8, pp. 1947–1962, 2018. **2, 4, 6**
- [27] T. Qiao, J. Zhang, D. Xu, and D. Tao, "Mirrorgan: Learning text-to-image generation by redescription," in *CVPR*, 2019. **2, 5, 6**
- [28] J. Liang, W. Pei, and F. Lu, "Cpgan: Content-parsing generative adversarial networks for text-to-image synthesis," in *ECCV*, 2020. **2, 5, 6**

- [29] P. Esser, R. Rombach, and B. Ommer, "Taming transformers for high-resolution image synthesis," in *CVPR*, 2021. **2, 5, 6, 16**
- [30] S. Ruan, Y. Zhang, K. Zhang, Y. Fan, F. Tang, Q. Liu, and E. Chen, "Dae-gan: Dynamic aspect-aware gan for text-to-image synthesis," in *ICCV*, 2021. **2, 5, 6**
- [31] K. Crowson, S. Biderman, D. Kornis, D. Stander, E. Hallahan, L. Castricato, and E. Raff, "Vgan-clip: Open domain image generation and editing with natural language guidance," in *ECCV*, 2022. **2, 6**
- [32] S. Gu, D. Chen, J. Bao, F. Wen, B. Zhang, D. Chen, L. Yuan, and B. Guo, "Vector quantized diffusion model for text-to-image synthesis," in *CVPR*, 2022. **2, 8, 9**
- [33] R. Rombach, A. Blattmann, D. Lorenz, P. Esser, and B. Ommer, "High-resolution image synthesis with latent diffusion models," in *CVPR*, 2022. **1, 2, 4, 8, 9, 11, 12, 14, 17, 20, 29, 30**
- [34] M. Tao, H. Tang, F. Wu, X.-Y. Jing, B.-K. Bao, and C. Xu, "Df-gan: A simple and effective baseline for text-to-image synthesis," in *CVPR*, 2022. **1, 2, 5, 6**
- [35] J. Yu, Y. Xu, J. Y. Koh, T. Luong, G. Baid, Z. Wang, V. Vasudevan, A. Ku, Y. Yang, B. K. Ayan *et al.*, "Scaling autoregressive models for content-rich text-to-image generation," *TMLR*. **1, 2, 7, 8, 16**
- [36] O. Gafni, A. Polyak, O. Ashual, S. Sheynin, D. Parikh, and Y. Taigman, "Make-a-scene: Scene-based text-to-image generation with human priors," in *ECCV*, 2022. **2, 7, 8**
- [37] C. Wu, J. Liang, L. Ji, F. Yang, Y. Fang, D. Jiang, and N. Duan, "Nüwa: Visual synthesis pre-training for neural visual world creation," in *ECCV*, 2022. **2, 7, 8**
- [38] M. Tao, B.-K. Bao, H. Tang, and C. Xu, "Galip: Generative adversarial clips for text-to-image synthesis," in *CVPR*, 2023. **2, 6**
- [39] M. Kang, J.-Y. Zhu, R. Zhang, J. Park, E. Shechtman, S. Paris, and T. Park, "Scaling up gans for text-to-image synthesis," in *CVPR*, 2023. **2, 6, 7**
- [40] X. Dai, J. Hou, C.-Y. Ma, S. Tsai, J. Wang, R. Wang, P. Zhang, S. Vandenhende, X. Wang, A. Dubey *et al.*, "Emu: Enhancing image generation models using photogenic needles in a haystack," *arXiv preprint arXiv:2309.15807*, 2023. **2, 7, 8**
- [41] L. Yu, B. Shi, R. Pasunuru, B. Muller, O. Golovneva, T. Wang, A. Babu, B. Tang, B. Karrer, S. Sheynin *et al.*, "Scaling autoregressive multi-modal models: Pretraining and instruction tuning," *arXiv preprint arXiv:2309.02591*, vol. 2, no. 3, 2023. **2, 7, 8**
- [42] J. Betker, G. Goh, L. Jing, T. Brooks, J. Wang, L. Li, L. Ouyang, J. Zhuang, J. Lee, Y. Guo *et al.*, "Improving image generation with better captions," *Computer Science*. <https://cdn.openai.com/papers/dall-e-3.pdf>, vol. 2, no. 3, p. 8, 2023. **2, 8, 9, 30**
- [43] N. Ruiz, Y. Li, V. Jampani, Y. Pritch, M. Rubinstein, and K. Aberman, "Dreambooth: Fine tuning text-to-image diffusion models for subject-driven generation," in *CVPR*, 2023. **2, 8, 9, 11, 12, 13, 27, 28, 29**
- [44] J. Y. Koh, D. Fried, and R. R. Salakhutdinov, "Generating images with multimodal language models," in *NeurIPS*, 2024. **2, 7, 8**
- [45] W. He, S. Fu, M. Liu, X. Wang, W. Xiao, F. Shu, Y. Wang, L. Zhang, Z. Yu, H. Li *et al.*, "Mars: Mixture of auto-regressive models for fine-grained text-to-image synthesis," *arXiv preprint arXiv:2407.07614*, 2024. **1, 2, 7, 8**
- [46] J. Chen, J. Yu, C. Ge, L. Yao, E. Xie, Y. Wu, Z. Wang, J. Kwok, P. Luo, H. Lu *et al.*, "Pixart- α : Fast training of diffusion transformer for photorealistic text-to-image synthesis," *arXiv preprint arXiv:2310.00426*, 2023. **2, 8, 9, 31**
- [47] P. Esser, S. Kulal, A. Blattmann, R. Entezari, J. Müller, H. Saini, Y. Levi, D. Lorenz, A. Sauer, F. Boesel *et al.*, "Scaling rectified flow transformers for high-resolution image synthesis," in *ICML*, 2024. **2, 8, 9, 10, 30**
- [48] Y. LeCun, Y. Bengio, and G. Hinton, "Deep learning," *nature*, vol. 521, no. 7553, pp. 436–444, 2015. **1**
- [49] Z. Niu, G. Zhong, and H. Yu, "A review on the attention mechanism of deep learning," *Neurocomputing*, vol. 452, pp. 48–62, 2021. **1**
- [50] I. Goodfellow, J. Pouget-Abadie, M. Mirza, B. Xu, D. Warde-Farley, S. Ozair, A. Courville, and Y. Bengio, "Generative adversarial nets," in *NeurIPS*, 2014. **1, 2**
- [51] M. Mirza, "Conditional generative adversarial nets," *arXiv preprint arXiv:1411.1784*, 2014. **1, 2, 4**
- [52] J. Sohl-Dickstein, E. Weiss, N. Maheswaranathan, and S. Ganguli, "Deep unsupervised learning using nonequilibrium thermodynamics," in *ICML*, 2015. **1, 3**
- [53] J. Ho, A. Jain, and P. Abbeel, "Denoising diffusion probabilistic models," in *NeurIPS*, 2020. **1, 3, 4**
- [54] Y. Zhou and N. Shimada, "Vision+ language applications: A survey," in *CVPRW*, 2023. **1**
- [55] S. Frolov, T. Hinz, F. Raue, J. Hees, and A. Dengel, "Adversarial text-to-image synthesis: A review," *Elsevier Neural Networks*, vol. 144, pp. 187–209, 2021. **1, 26**
- [56] R. Zhou, C. Jiang, and Q. Xu, "A survey on generative adversarial network-based text-to-image synthesis," *Elsevier Neurocomputing*, vol. 451, pp. 316–336, 2021. **1**
- [57] C. Zhang, C. Zhang, M. Zhang, and I. S. Kweon, "Text-to-image diffusion models in generative ai: A survey," *arXiv preprint arXiv:2303.07909*, 2023. **2**
- [58] P. Cao, F. Zhou, Q. Song, and L. Yang, "Controllable generation with text-to-image diffusion models: A survey," *arXiv preprint arXiv:2403.04279*, 2024. **2**
- [59] H. Tang, D. Xu, N. Sebe, Y. Wang, J. J. Corso, and Y. Yan, "Multi-channel attention selection gan with cascaded semantic guidance for cross-view image translation," in *CVPR*, 2019. **2**
- [60] H. Tang, D. Xu, Y. Yan, P. H. Torr, and N. Sebe, "Local class-specific and global image-level generative adversarial networks for semantic-guided scene generation," in *CVPR*, 2020. **2**
- [61] D. Croce, G. Castellucci, and R. Basili, "Gan-bert: Generative adversarial learning for robust text classification with a bunch of labeled examples," in *Proceedings of the 58th annual meeting of the association for computational linguistics*, 2020, pp. 2114–2119. **2**
- [62] H. Zhang, J. Y. Koh, J. Baldridge, H. Lee, and Y. Yang, "Cross-modal contrastive learning for text-to-image generation," in *CVPR*, 2021. **2, 5, 6**
- [63] T. M. Dinh, R. Nguyen, and B.-S. Hua, "Tise: Bag of metrics for text-to-image synthesis evaluation," in *ECCV*, 2022. **2, 6, 27, 28**
- [64] D. P. Kingma, "Auto-encoding variational bayes," *arXiv preprint arXiv:1312.6114*, 2013. **2, 4**
- [65] A. Radford, "Improving language understanding by generative pre-training," 2018. **2, 3, 7, 18**
- [66] M. Chen, A. Radford, R. Child, J. Wu, H. Jun, D. Luan, and I. Sutskever, "Generative pretraining from pixels," in *ICML*, 2020. **2**
- [67] J. T. Rolfe, "Discrete variational autoencoders," *arXiv preprint arXiv:1609.02200*, 2016. **3**
- [68] A. Radford, J. W. Kim, C. Hallacy, A. Ramesh, G. Goh, S. Agarwal, G. Sastry, A. Askell, P. Mishkin, J. Clark *et al.*, "Learning transferable visual models from natural language supervision," in *ICML*, 2021. **3, 4, 11, 26, 30**
- [69] T. Kudo, "Sentencepiece: A simple and language independent subword tokenizer and detokenizer for neural text processing," *arXiv preprint arXiv:1808.06226*, 2018. **3**
- [70] A. Van Den Oord, O. Vinyals *et al.*, "Neural discrete representation learning," in *NeurIPS*, 2017. **3**
- [71] O. Vinyals, A. Toshev, S. Bengio, and D. Erhan, "Show and tell: A neural image caption generator," in *CVPR*, 2015. **3**
- [72] P. Dhariwal and A. Nichol, "Diffusion models beat gans on image synthesis," in *NeurIPS*, 2021. **4, 7**
- [73] J. Ho and T. Salimans, "Classifier-free diffusion guidance," *arXiv preprint arXiv:2207.12598*, 2022. **4**
- [74] A. Dash, J. C. B. Gamboa, S. Ahmed, M. Liwicki, and M. Z. Afzal, "Tac-gan-text conditioned auxiliary classifier generative adversarial network," *arXiv preprint arXiv:1703.06412*, 2017. **4, 6**
- [75] N. Bodla, G. Hua, and R. Chellappa, "Semi-supervised fusedgan for conditional image generation," in *ECCV*, 2018. **5, 6, 26**
- [76] Z. Zhang, Y. Xie, and L. Yang, "Photographic text-to-image synthesis with a hierarchically-nested adversarial network," in *CVPR*, 2018. **5, 6**
- [77] M. Cha, Y. L. Gwon, and H. Kung, "Adversarial learning of semantic relevance in text to image synthesis," in *Proceedings of the AAAI conference on artificial intelligence*, vol. 33, no. 01, 2019, pp. 3272–3279. **5, 6**
- [78] W. Li, P. Zhang, L. Zhang, Q. Huang, X. He, S. Lyu, and J. Gao, "Object-driven text-to-image synthesis via adversarial training," in *CVPR*, 2019. **5, 6**
- [79] T. Park, M.-Y. Liu, T.-C. Wang, and J.-Y. Zhu, "Gaugan: semantic image synthesis with spatially adaptive normalization," in *ACM SIGGRAPH 2019 Real-Time Live!*, 2019, pp. 1–1. **5, 6**
- [80] M. Lee and J. Seok, "Controllable generative adversarial network," *Ieee Access*, vol. 7, pp. 28 158–28 169, 2019. **5, 6**
- [81] B. Zhu and C.-W. Ngo, "Cookgan: Causality based text-to-image synthesis," in *CVPR*, 2020. **5, 6**

- [82] Y. Gou, Q. Wu, M. Li, B. Gong, and M. Han, "Segattnan: Text to image generation with segmentation attention," *arXiv preprint arXiv:2005.12444*, 2020. 5, 6, 30
- [83] H. Wang, G. Lin, S. C. Hoi, and C. Miao, "Cycle-consistent inverse gan for text-to-image synthesis," in *ACM MM*, 2021. 5, 6
- [84] Y. Qiao, Q. Chen, C. Deng, N. Ding, Y. Qi, M. Tan, X. Ren, and Q. Wu, "R-gan: Exploring human-like way for reasonable text-to-image synthesis via generative adversarial networks," in *ACM MM*, 2021. 5, 6
- [85] Q. Cheng, K. Wen, and X. Gu, "Vision-language matching for text-to-image synthesis via generative adversarial networks," *IEEE Transactions on Multimedia*, vol. 25, pp. 7062–7075, 2022. 6
- [86] W. Liao, K. Hu, M. Y. Yang, and B. Rosenhahn, "Text to image generation with semantic-spatial aware gan," 2022. 6
- [87] Y. Zhou, R. Zhang, C. Chen, C. Li, C. Tensmeyer, T. Yu, J. Gu, J. Xu, and T. Sun, "Towards language-free training for text-to-image generation," 2022. 5, 6, 26
- [88] A. Sauer, T. Karras, S. Laine, A. Geiger, and T. Aila, "Stylegan-t: Unlocking the power of gans for fast large-scale text-to-image synthesis," in *ICML*, 2023. 6
- [89] S. Ye, H. Wang, M. Tan, and F. Liu, "Recurrent affine transformation for text-to-image synthesis," *IEEE TMM*, vol. 26, pp. 462–473, 2023. 6
- [90] F. Wu, L. Liu, F. Hao, F. He, and J. Cheng, "Text-to-image synthesis based on object-guided joint-decoding transformer," in *CVPR*, 2022. 6
- [91] X. Pan, A. Tewari, T. Leimkühler, L. Liu, A. Meka, and C. Theobalt, "Drag your gan: Interactive point-based manipulation on the generative image manifold," in *ACM SIGGRAPH 2023 Conference Proceedings*, 2023, pp. 1–11. 6
- [92] Y. Xu, Y. Zhao, Z. Xiao, and T. Hou, "Ufogen: You forward once large scale text-to-image generation via diffusion gans," in *CVPR*, 2024. 6
- [93] K. Haydarov, A. Muhamed, X. Shen, J. Lazarevic, I. Skorokhodov, C. J. Galappaththige, and M. Elhoseiny, "Adversarial text to continuous image generation," in *CVPR*, 2024. 6
- [94] V. Sitzmann, J. Martel, A. Bergman, D. Lindell, and G. Wetzstein, "Implicit neural representations with periodic activation functions," in *NeurIPS*, 2020. 6
- [95] J. Lin, R. Men, A. Yang, C. Zhou, M. Ding, Y. Zhang, P. Wang, A. Wang, L. Jiang, X. Jia *et al.*, "M6: A chinese multimodal pretrainer," *arXiv preprint arXiv:2103.00823*, 2021. 7, 8
- [96] J. Lu, C. Clark, S. Lee, Z. Zhang, S. Khosla, R. Marten, D. Hoiem, and A. Kembhavi, "Unified-io 2: Scaling autoregressive multimodal models with vision language audio and action," in *CVPR*, 2024. 7, 8
- [97] X. Ma, M. Zhou, T. Liang, Y. Bai, T. Zhao, H. Chen, and Y. Jin, "Star: Scale-wise text-to-image generation via auto-regressive representations," *arXiv preprint arXiv:2406.10797*, 2024. 7, 8
- [98] H. Tang, Y. Wu, S. Yang, E. Xie, J. Chen, J. Chen, Z. Zhang, H. Cai, Y. Lu, and S. Han, "Hart: Efficient visual generation with hybrid autoregressive transformer," *arXiv preprint arXiv:2410.10812*, 2024. 7, 8
- [99] Y. Teng, H. Shi, X. Liu, X. Ning, G. Dai, Y. Wang, Z. Li, and X. Liu, "Accelerating auto-regressive text-to-image generation with training-free speculative jacobi decoding," *arXiv preprint arXiv:2410.01699*, 2024. 7, 8, 11, 17
- [100] J. Gu, Y. Wang, Y. Zhang, Q. Zhang, D. Zhang, N. Jaitly, J. Susskind, and S. Zhai, "Dart: Denoising autoregressive transformer for scalable text-to-image generation," *arXiv preprint arXiv:2410.08159*, 2024. 7, 8
- [101] J. Devlin, "Bert: Pre-training of deep bidirectional transformers for language understanding," *arXiv preprint arXiv:1810.04805*, 2018. 7
- [102] O. Avrahami, D. Lischinski, and O. Fried, "Blended diffusion for text-driven editing of natural images," in *CVPR*, 2022. 8, 9
- [103] H. Lu, H. Tunanyan, K. Wang, S. Navasardyan, Z. Wang, and H. Shi, "Specialist diffusion: Plug-and-play sample-efficient fine-tuning of text-to-image diffusion models to learn any unseen style," in *CVPR*, 2023. 8, 9, 11, 12
- [104] F. Bao, S. Nie, K. Xue, C. Li, S. Pu, Y. Wang, G. Yue, Y. Cao, H. Su, and J. Zhu, "One transformer fits all distributions in multi-modal diffusion at scale," in *ICML*, 2023. 8, 9
- [105] X. Xu, Z. Wang, G. Zhang, K. Wang, and H. Shi, "Versatile diffusion: Text, images and variations all in one diffusion model," in *ICCV*, 2023. 8, 9
- [106] N. Kumari, B. Zhang, R. Zhang, E. Shechtman, and J.-Y. Zhu, "Multi-concept customization of text-to-image diffusion," in *CVPR*, 2023. 8, 9, 11, 13, 29
- [107] L. Han, Y. Li, H. Zhang, P. Milanfar, D. Metaxas, and F. Yang, "Svdif: Compact parameter space for diffusion fine-tuning," in *ICCV*, 2023. 8, 9, 11, 17, 18
- [108] Z. Feng, Z. Zhang, X. Yu, Y. Fang, L. Li, X. Chen, Y. Lu, J. Liu, W. Yin, S. Feng *et al.*, "Ernie-vilg 2.0: Improving text-to-image diffusion model with knowledge-enhanced mixture-of-denoising-experts," in *CVPR*, 2023. 8, 9
- [109] Y. Zhou, B. Liu, Y. Zhu, X. Yang, C. Chen, and J. Xu, "Shifted diffusion for text-to-image generation," in *CVPR*, 2023. 8, 9
- [110] P. Pernias, D. Rampas, M. L. Richter, C. J. Pal, and M. Aubreville, "Würstchen: An efficient architecture for large-scale text-to-image diffusion models," *arXiv preprint arXiv:2306.00637*, 2023. 8, 9
- [111] Y. Feng, B. Gong, D. Chen, Y. Shen, Y. Liu, and J. Zhou, "Ranni: Taming text-to-image diffusion for accurate instruction following," in *CVPR*, 2024. 8, 9, 24
- [112] L. Yang, Z. Yu, C. Meng, M. Xu, S. Ermon, and C. Bin, "Mastering text-to-image diffusion: Recapturing, planning, and generating with multimodal llms," in *ICML*, 2024. 8, 9, 11, 24
- [113] L. Yang, J. Liu, S. Hong, Z. Zhang, Z. Huang, Z. Cai, W. Zhang, and B. Cui, "Improving diffusion-based image synthesis with context prediction," in *NeurIPS*, 2024. 8, 9
- [114] M. Li, T. Cai, J. Cao, Q. Zhang, H. Cai, J. Bai, Y. Jia, K. Li, and S. Han, "Distrifusion: Distributed parallel inference for high-resolution diffusion models," in *CVPR*, 2024. 8, 9
- [115] X. Wang, T. Darrell, S. S. Rambhatla, R. Girdhar, and I. Misra, "Instancediffusion: Instance-level control for image generation," in *CVPR*, 2024. 9
- [116] H. Hu, K. C. Chan, Y.-C. Su, W. Chen, Y. Li, K. Sohn, Y. Zhao, X. Ben, B. Gong, W. Cohen *et al.*, "Instruct-imagen: Image generation with multi-modal instruction," in *CVPR*, 2024. 9
- [117] M. Haji-Ali, G. Balakrishnan, and V. Ordonez, "Elasticdiffusion: Training-free arbitrary size image generation through global-local content separation," in *CVPR*, 2024. 9
- [118] J. Chen, Y. Wu, S. Luo, E. Xie, S. Paul, P. Luo, H. Zhao, and Z. Li, "Fast and controllable image generation with latent consistency models," *arXiv preprint arXiv:2401.05252*, 2024. 9
- [119] J. Chen, C. Ge, E. Xie, Y. Wu, L. Yao, X. Ren, Z. Wang, P. Luo, H. Lu, and Z. Li, "Weak-to-strong training of diffusion transformer for 4k text-to-image generation," *arXiv preprint arXiv:2403.04692*, 2024. 9
- [120] A. Sauer, F. Boesel, T. Dockhorn, A. Blattmann, P. Esser, and R. Rombach, "Fast high-resolution image synthesis with latent adversarial diffusion distillation," *arXiv preprint arXiv:2403.12015*, 2024. 9
- [121] J. Lee, D. S. Jung, K. Lee, and K. M. Lee, "Streammultidiffusion: Real-time interactive generation with region-based semantic control," *arXiv preprint arXiv:2403.09055*, 2024. 9
- [122] S. Xiao, Y. Wang, J. Zhou, H. Yuan, X. Xing, R. Yan, S. Wang, T. Huang, and Z. Liu, "Omnigen: Unified image generation," *arXiv preprint arXiv:2409.11340*, 2024. 9
- [123] Z. Li, J. Zhang, Q. Lin, J. Xiong, Y. Long, X. Deng, Y. Zhang, X. Liu, M. Huang, Z. Xiao *et al.*, "Hunyuan-dit: A powerful multi-resolution diffusion transformer with fine-grained chinese understanding," *arXiv preprint arXiv:2405.08748*, 2024. 9, 10
- [124] Y. Shi, C. Xue, J. H. Liew, J. Pan, H. Yan, W. Zhang, V. Y. Tan, and S. Bai, "Dragdiffusion: Harnessing diffusion models for interactive point-based image editing," in *CVPR*, 2024. 9
- [125] L. Yang, Z. Zhang, Z. Yu, J. Liu, M. Xu, S. Ermon, and C. Bin, "Cross-modal contextualized diffusion models for text-guided visual generation and editing," in *ICLR*, 2024. 8, 9
- [126] J. Achiam, S. Adler, S. Agarwal, L. Ahmad, I. Akkaya, F. L. Aleman, D. Almeida, J. Altenschmidt, S. Altman, S. Anadkat *et al.*, "Gpt-4 technical report," *arXiv preprint arXiv:2303.08774*, 2023. 8, 23, 26
- [127] O. Ronneberger, P. Fischer, and T. Brox, "U-net: Convolutional networks for biomedical image segmentation," in *MICCAI*, 2015. 8
- [128] Z. Zhang, A. Zhang, M. Li, H. Zhao, G. Karypis, and A. Smola, "Multimodal chain-of-thought reasoning in language models," *arXiv preprint arXiv:2302.00923*, 2023. 8
- [129] J. Wei, X. Wang, D. Schuurmans, M. Bosma, F. Xia, E. Chi, Q. V. Le, D. Zhou *et al.*, "Chain-of-thought prompting elicits reasoning in large language models," in *NeurIPS*, 2022. 8

- [130] J. Dodge, G. Ilharco, R. Schwartz, A. Farhadi, H. Hajishirzi, and N. Smith, "Fine-tuning pretrained language models: Weight initializations, data orders, and early stopping," *arXiv preprint arXiv:2002.06305*, 2020. **8**
- [131] J. Teng, W. Zheng, M. Ding, W. Hong, J. Wangni, Z. Yang, and J. Tang, "Relay diffusion: Unifying diffusion process across resolutions for image synthesis," *arXiv preprint arXiv:2309.03350*, 2023. **8**
- [132] P. Bachman, R. D. Hjelm, and W. Buchwalter, "Learning representations by maximizing mutual information across views," in *NeurIPS*, 2019. **9**
- [133] A. Sauer, D. Lorenz, A. Blattmann, and R. Rombach, "Adversarial diffusion distillation," in *ECCV*, 2024. **9**
- [134] Y. Liang, J. He, G. Li, P. Li, A. Klimovskiy, N. Carolan, J. Sun, J. Pont-Tuset, S. Young, F. Yang *et al.*, "Rich human feedback for text-to-image generation," in *CVPR*, 2024. **9, 10, 11, 25, 26, 28, 32**
- [135] L. Zhao, Y. Yang, K. Zhang, W. Shao, Y. Zhang, Y. Qiao, P. Luo, and R. Ji, "Diffagent: Fast and accurate text-to-image api selection with large language model," in *CVPR*, 2024. **9, 10, 11**
- [136] X. Wu, K. Sun, F. Zhu, R. Zhao, and H. Li, "Human preference score: Better aligning text-to-image models with human preference," in *ICCV*, 2023. **11, 27, 28**
- [137] J. Xu, X. Liu, Y. Wu, Y. Tong, Q. Li, M. Ding, J. Tang, and Y. Dong, "Imagereward: Learning and evaluating human preferences for text-to-image generation," in *NeurIPS*, 2024. **10, 11, 17, 28**
- [138] S. Zhang, B. Wang, J. Wu, Y. Li, T. Gao, D. Zhang, and Z. Wang, "Learning multi-dimensional human preference for text-to-image generation," in *CVPR*, 2024. **11**
- [139] R. Gal, Y. Alaluf, Y. Atzmon, O. Patashnik, A. H. Bermano, G. Chechik, and D. Cohen-Or, "An image is worth one word: Personalizing text-to-image generation using textual inversion," *arXiv preprint arXiv:2208.01618*, 2022. **9, 11, 12, 19**
- [140] Y. Zhang, Z. Xing, Y. Zeng, Y. Fang, and K. Chen, "Pia: Your personalized image animator via plug-and-play modules in text-to-image models," in *CVPR*, 2024. **11, 12**
- [141] X. Xu, J. Guo, Z. Wang, G. Huang, I. Essa, and H. Shi, "Prompt-free diffusion: Taking text out of text-to-image diffusion models," in *CVPR*, 2024. **11, 12**
- [142] S. Huang, B. Gong, Y. Feng, X. Chen, Y. Fu, Y. Liu, and D. Wang, "Learning disentangled identifiers for action-customized text-to-image generation," in *CVPR*, 2024. **11, 12**
- [143] N. Ruiz, Y. Li, V. Jampani, W. Wei, T. Hou, Y. Pritch, N. Wadhwa, M. Rubinstein, and K. Aberman, "Hyperdreambooth: Hypernetworks for fast personalization of text-to-image models," in *CVPR*, 2024. **11, 12**
- [144] C. Ham, M. Fisher, J. Hays, N. Kolkin, Y. Liu, R. Zhang, and T. Hinz, "Personalized residuals for concept-driven text-to-image generation," in *CVPR*, 2024. **11, 12**
- [145] M. Arar, A. Voynov, A. Hertz, O. Avrahami, S. Fruchter, Y. Pritch, D. Cohen-Or, and A. Shamir, "Palp: Prompt aligned personalization of text-to-image models," *arXiv preprint arXiv:2401.06105*, 2024. **11, 12**
- [146] Z. Li, M. Cao, X. Wang, Z. Qi, M.-M. Cheng, and Y. Shan, "Photomaker: Customizing realistic human photos via stacked id embedding," in *CVPR*, 2024. **11, 12**
- [147] M. Hua, J. Liu, F. Ding, W. Liu, J. Wu, and Q. He, "Dreamtuner: Single image is enough for subject-driven generation," *arXiv preprint arXiv:2312.13691*, 2023. **11, 12**
- [148] Y. Wei, Y. Zhang, Z. Ji, J. Bai, L. Zhang, and W. Zuo, "Elite: Encoding visual concepts into textual embeddings for customized text-to-image generation," in *ICCV*, 2023. **11, 12**
- [149] Z. Chen, L. Zhang, F. Weng, L. Pan, and Z. Lan, "Tailored visions: Enhancing text-to-image generation with personalized prompt rewriting," in *CVPR*, 2024. **11, 12**
- [150] M. Huang, Z. Mao, M. Liu, Q. He, and Y. Zhang, "Realcustom: Narrowing real text word for real-time open-domain text-to-image customization," in *CVPR*, 2024. **11, 13**
- [151] K. C. Chan, Y. Zhao, X. Jia, M.-H. Yang, and H. Wang, "Improving subject-driven image synthesis with subject-agnostic guidance," in *CVPR*, 2024. **11, 12**
- [152] F. Wu, Y. Pang, J. Zhang, L. Pang, J. Yin, B. Zhao, Q. Li, and X. Mao, "Core: Context-regularized text embedding learning for text-to-image personalization," *arXiv preprint arXiv:2408.15914*, 2024. **11, 12**
- [153] Z. He, B. Sun, F. Juefei-Xu, H. Ma, A. Ramchandani, V. Cheung, S. Shah, A. Kalia, H. Subramanyam, A. Zareian *et al.*, "Imagine yourself: Tuning-free personalized image generation," *arXiv preprint arXiv:2409.13346*, 2024. **11, 12**
- [154] G. Xiao, T. Yin, W. T. Freeman, F. Durand, and S. Han, "Fastcomposer: Tuning-free multi-subject image generation with localized attention," *Springer IJCV*, pp. 1–20, 2024. **11, 12, 14**
- [155] Q. Wang, X. Bai, H. Wang, Z. Qin, A. Chen, H. Li, X. Tang, and Y. Hu, "Instantid: Zero-shot identity-preserving generation in seconds," *arXiv preprint arXiv:2401.07519*, 2024. **11, 12**
- [156] J. Chen, Y. Pan, T. Yao, and T. Mei, "Controlstyle: Text-driven stylized image generation using diffusion priors," in *Proceedings of the 31st ACM International Conference on Multimedia*, 2023, pp. 7540–7548. **11, 12**
- [157] J. He, Y. Geng, and L. Bo, "Uniportrait: A unified framework for identity-preserving single-and multi-human image personalization," *arXiv preprint arXiv:2408.05939*, 2024. **11, 12**
- [158] P. Li, Q. Nie, Y. Chen, X. Jiang, K. Wu, Y. Lin, Y. Liu, J. Peng, C. Wang, and F. Zheng, "Tuning-free image customization with image and text guidance," in *ECCV*, 2024. **11, 12**
- [159] Y. Cai, Y. Wei, Z. Ji, J. Bai, H. Han, and W. Zuo, "Decoupled textual embeddings for customized image generation," in *AAAI*, 2024. **11, 12**
- [160] S. Zhang, L. Huang, X. Chen, Y. Zhang, Z.-F. Wu, Y. Feng, W. Wang, Y. Shen, Y. Liu, and P. Luo, "Flashface: Human image personalization with high-fidelity identity preservation," *arXiv preprint arXiv:2403.17008*, 2024. **11, 12**
- [161] S. Cui, J. Guo, X. An, J. Deng, Y. Zhao, X. Wei, and Z. Feng, "Idadapter: Learning mixed features for tuning-free personalization of text-to-image models," in *CVPR*, 2024. **11, 12**
- [162] Y. Zhang, Y. Song, J. Liu, R. Wang, J. Yu, H. Tang, H. Li, X. Tang, Y. Hu, H. Pan *et al.*, "Ssr-encoder: Encoding selective subject representation for subject-driven generation," in *CVPR*, 2024. **11**
- [163] C. Mou, X. Wang, L. Xie, Y. Wu, J. Zhang, Z. Qi, and Y. Shan, "T2i-adapter: Learning adapters to dig out more controllable ability for text-to-image diffusion models," in *AAAI*, 2024. **9, 11, 13**
- [164] J. Kim, J. Park, and W. Rhee, "Selectively informative description can reduce undesired embedding entanglements in text-to-image personalization," in *CVPR*, 2024. **11, 13**
- [165] Y. Zeng, V. M. Patel, H. Wang, X. Huang, T.-C. Wang, M.-Y. Liu, and Y. Balaji, "Jedi: Joint-image diffusion models for finetuning-free personalized text-to-image generation," in *CVPR*, 2024. **11, 13**
- [166] S. Hao, K. Han, S. Zhao, and K.-Y. K. Wong, "Vico: Plug-and-play visual condition for personalized text-to-image generation," *arXiv preprint arXiv:2306.00971*, 2023. **11, 13**
- [167] J. Nam, H. Kim, D. Lee, S. Jin, S. Kim, and S. Chang, "Dreammatcher: Appearance matching self-attention for semantically-consistent text-to-image personalization," in *CVPR*, 2024. **11, 13**
- [168] X. Li, X. Hou, and C. C. Loy, "When stylegan meets stable diffusion: a w+ adapter for personalized image generation," in *CVPR*, 2024. **11, 13**
- [169] S. Zhao, D. Chen, Y.-C. Chen, J. Bao, S. Hao, L. Yuan, and K.-Y. K. Wong, "Uni-controlnet: All-in-one control to text-to-image diffusion models," in *NeurIPS*, 2024. **11, 12**
- [170] D. Li, J. Li, and S. Hoi, "Blip-diffusion: Pre-trained subject representation for controllable text-to-image generation and editing," in *NeurIPS*, 2024. **11, 13**
- [171] P. Li, Q. Huang, Y. Ding, and Z. Li, "Layerdiffusion: Layered controlled image editing with diffusion models," in *SIGGRAPH Asia 2023 Technical Communications*, 2023, pp. 1–4. **11, 13**
- [172] Z. Yang, J. Wang, Z. Gan, L. Li, K. Lin, C. Wu, N. Duan, Z. Liu, C. Liu, M. Zeng *et al.*, "Reco: Region-controlled text-to-image generation," in *CVPR*, 2023. **11, 13**
- [173] O. Avrahami, T. Hayes, O. Gafni, S. Gupta, Y. Taigman, D. Parikh, D. Lischinski, O. Fried, and X. Yin, "Spatext: Spatio-textual representation for controllable image generation," in *CVPR*, 2023. **11, 13**
- [174] K. Mei, M. Delbracio, H. Talebi, Z. Tu, V. M. Patel, and P. Milanfar, "Codi: Conditional diffusion distillation for higher-fidelity and faster image generation," in *CVPR*, 2024. **11, 13**
- [175] W. Li, M. Fang, C. Zou, B. Gong, R. Zheng, M. Wang, J. Chen, and M. Yang, "Styletokenizer: Defining image style by a single instance for controlling diffusion models," *arXiv preprint arXiv:2409.02543*, 2024. **11, 13**
- [176] A. Voynov, Q. Chu, D. Cohen-Or, and K. Aberman, "p+: Extended textual conditioning in text-to-image generation," *arXiv preprint arXiv:2303.09522*, 2023. **11, 13**

- [177] H. Ye, J. Zhang, S. Liu, X. Han, and W. Yang, "Ip-adapter: Text compatible image prompt adapter for text-to-image diffusion models," *arXiv preprint arXiv:2308.06721*, 2023. **11, 13**
- [178] J. Cheng, P. Xie, X. Xia, J. Li, J. Wu, Y. Ren, H. Li, X. Xiao, M. Zheng, and L. Fu, "Resadapter: Domain consistent resolution adapter for diffusion models," *arXiv preprint arXiv:2403.02084*, 2024. **11, 13**
- [179] Y. Wang, R. Gao, K. Chen, K. Zhou, Y. Cai, L. Hong, Z. Li, L. Jiang, D.-Y. Yeung, Q. Xu *et al.*, "Detdiffusion: Synergizing generative and perceptive models for enhanced data generation and perception," in *CVPR*, 2024. **11, 13**
- [180] H. Cai, M. Li, Q. Zhang, M.-Y. Liu, and S. Han, "Condition-aware neural network for controlled image generation," in *CVPR*, 2024. **11, 13**
- [181] J. Ren, M. Xu, J.-C. Wu, Z. Liu, T. Xiang, and A. Toisoul, "Move anything with layered scene diffusion," in *CVPR*, 2024. **11, 14**
- [182] M. Ohanyan, H. Manukyan, Z. Wang, S. Navasardyan, and H. Shi, "Zero-painter: Training-free layout control for text-to-image synthesis," in *CVPR*, 2024. **11, 14**
- [183] S. Mo, F. Mu, K. H. Lin, Y. Liu, B. Guan, Y. Li, and B. Zhou, "Freecontrol: Training-free spatial control of any text-to-image diffusion model with any condition," in *CVPR*, 2024. **11, 14**
- [184] F. Shen, H. Ye, J. Zhang, C. Wang, X. Han, and W. Yang, "Advancing pose-guided image synthesis with progressive conditional diffusion models," *arXiv preprint arXiv:2310.06313*, 2023. **11, 14**
- [185] M. Li, T. Yang, H. Kuang, J. Wu, Z. Wang, X. Xiao, and C. Chen, "Controlnet++ improving conditional controls with efficient consistency feedback," in *ECCV*, 2024. **11, 14**
- [186] B. Peng, J. Wang, Y. Zhang, W. Li, M.-C. Yang, and J. Jia, "Controlnext: Powerful and efficient control for image and video generation," *arXiv preprint arXiv:2408.06070*, 2024. **11, 14**
- [187] O. Bar-Tal, L. Yariv, Y. Lipman, and T. Dekel, "Multidiffusion: Fusing diffusion paths for controlled image generation," 2023. **11, 14**
- [188] X. Wu, Z. Hu, L. Sheng, and D. Xu, "Styleformer: Real-time arbitrary style transfer via parametric style composition," in *ICCV*, 2021. **9, 11, 14**
- [189] Y. Zhang, N. Huang, F. Tang, H. Huang, C. Ma, W. Dong, and C. Xu, "Inversion-based style transfer with diffusion models," in *CVPR*, 2023. **11, 14, 15**
- [190] D.-Y. Chen, H. Tennent, and C.-W. Hsu, "Artadapter: Text-to-image style transfer using multi-level style encoder and explicit adaptation," in *CVPR*, 2024. **11, 15**
- [191] J. Shi, W. Xiong, Z. Lin, and H. J. Jung, "Instantbooth: Personalized text-to-image generation without test-time finetuning," in *CVPR*, 2024. **11, 15**
- [192] H. Cho, J. Lee, S. Chang, and Y. Jeong, "One-shot structure-aware stylized image synthesis," in *CVPR*, 2024. **11, 15**
- [193] T. Qi, S. Fang, Y. Wu, H. Xie, J. Liu, L. Chen, Q. He, and Y. Zhang, "Deadiff: An efficient stylization diffusion model with disentangled representations," in *CVPR*, 2024. **11, 15**
- [194] Q. Wu, Y. Liu, H. Zhao, A. Kale, T. Bui, T. Yu, Z. Lin, Y. Zhang, and S. Chang, "Uncovering the disentanglement capability in text-to-image diffusion models," in *CVPR*, 2023. **9, 11, 14**
- [195] H. Wang, M. Spinelli, Q. Wang, X. Bai, Z. Qin, and A. Chen, "Instantstyle: Free lunch towards style-preserving in text-to-image generation," *arXiv preprint arXiv:2404.02733*, 2024. **11, 15**
- [196] A. Hertz, A. Voynov, S. Fruchter, and D. Cohen-Or, "Style aligned image generation via shared attention," in *CVPR*, 2024. **11, 15**
- [197] G. Ding, C. Zhao, W. Wang, Z. Yang, Z. Liu, H. Chen, and C. Shen, "Freecustom: Tuning-free customized image generation for multi-concept composition," in *CVPR*, 2024. **11, 15**
- [198] Y. Zhang, M. Yang, Q. Zhou, and Z. Wang, "Attention calibration for disentangled text-to-image personalization," in *CVPR*, 2024. **11, 15**
- [199] K. Sueyoshi and T. Matsubara, "Predicated diffusion: Predicate logic-based attention guidance for text-to-image diffusion models," in *CVPR*, 2024. **11, 15**
- [200] M. Brack, F. Friedrich, K. Kornmeier, L. Tsaban, P. Schramowski, K. Kersting, and A. Passos, "Ledits++: Limitless image editing using text-to-image models," in *CVPR*, 2024. **11, 15**
- [201] S. Mahajan, T. Rahman, K. M. Yi, and L. Sigal, "Prompting hard or hardly prompting: Prompt inversion for text-to-image diffusion models," in *CVPR*, 2024. **11, 15**
- [202] H. Chefer, Y. Alaluf, Y. Vinker, L. Wolf, and D. Cohen-Or, "Attend-and-excite: Attention-based semantic guidance for text-to-image diffusion models," *ACM Transactions on Graphics (TOG)*, vol. 42, no. 4, pp. 1–10, 2023. **11, 19, 20**
- [203] H. Cho, J. Lee, S. B. Kim, T.-H. Oh, and Y. Jeong, "Noise map guidance: Inversion with spatial context for real image editing," *arXiv preprint arXiv:2402.04625*, 2024. **11, 15**
- [204] B. Kavar, S. Zada, O. Lang, O. Tov, H. Chang, T. Dekel, I. Mosseri, and M. Irani, "Imagic: Text-based real image editing with diffusion models," in *CVPR*, 2023. **11, 15, 16**
- [205] Z. Zhang, L. Han, A. Ghosh, D. N. Metaxas, and J. Ren, "Sine: Single image editing with text-to-image diffusion models," in *CVPR*, 2023. **11, 15**
- [206] Z. Ma, G. Jia, and B. Zhou, "Adapedit: Spatio-temporal guided adaptive editing algorithm for text-based continuity-sensitive image editing," in *Proceedings of the AAAI Conference on Artificial Intelligence*, vol. 38, no. 5, 2024, pp. 4154–4161. **11, 15**
- [207] Z. Yu, H. Li, F. Fu, X. Miao, and B. Cui, "Accelerating text-to-image editing via cache-enabled sparse diffusion inference," in *Proceedings of the AAAI Conference on Artificial Intelligence*, vol. 38, no. 15, 2024, pp. 16605–16613. **11, 15**
- [208] Y. Qiao, F. Wang, J. Su, Y. Zhang, Y. Yu, S. Wu, and G.-J. Qi, "Baret: Balanced attention based real image editing driven by target-text inversion," in *Proceedings of the AAAI Conference on Artificial Intelligence*, vol. 38, no. 5, 2024, pp. 4560–4568. **11, 15**
- [209] A. Feng, W. Qiu, J. Bai, X. Zhang, Z. Dong, K. Zhou, R. Ying, and L. Tassulas, "An item is worth a prompt: Versatile image editing with disentangled control," *arXiv preprint arXiv:2403.04880*, 2024. **11, 15**
- [210] Z. Wang, Y. Huang, D. Song, L. Ma, and T. Zhang, "Promptcharm: Text-to-image generation through multi-modal prompting and refinement," in *Proceedings of the CHI Conference on Human Factors in Computing Systems*, 2024, pp. 1–21. **11, 15**
- [211] Z. Xue, G. Song, Q. Guo, B. Liu, Z. Zong, Y. Liu, and P. Luo, "Raphael: Text-to-image generation via large mixture of diffusion paths," in *NeurIPS*, 2024. **11, 15**
- [212] S. Zhong, Z. Huang, W. Wen, J. Qin, and L. Lin, "Sur-adapter: Enhancing text-to-image pre-trained diffusion models with large language models," in *Proceedings of the 31st ACM International Conference on Multimedia*, 2023, pp. 567–578. **11, 15**
- [213] Z. Wang, Y. Jiang, Y. Lu, P. He, W. Chen, Z. Wang, M. Zhou *et al.*, "In-context learning unlocked for diffusion models," in *NeurIPS*, 2023. **11, 15**
- [214] X. Liu, D. H. Park, S. Azadi, G. Zhang, A. Chopikyan, Y. Hu, H. Shi, A. Rohrbach, and T. Darrell, "More control for free! image synthesis with semantic diffusion guidance," in *WACV*, 2023. **11, 15**
- [215] S. Xu, Y. Huang, J. Pan, Z. Ma, and J. Chai, "Inversion-free image editing with natural language," *arXiv preprint arXiv:2312.04965*, 2023. **11, 15**
- [216] B. Liu, C. Wang, T. Cao, K. Jia, and J. Huang, "Towards understanding cross and self-attention in stable diffusion for text-guided image editing," in *CVPR*, 2024. **11, 16**
- [217] Q. Guo and T. Lin, "Focus on your instruction: Fine-grained and multi-instruction image editing by attention modulation," in *CVPR*, 2024. **11, 16**
- [218] C. Mou, X. Wang, J. Song, Y. Shan, and J. Zhang, "Diffeditor: Boosting accuracy and flexibility on diffusion-based image editing," in *CVPR*, 2024. **11, 16**
- [219] R. Bodur, B. Bhattarai, and T.-K. Kim, "Prompt augmentation for self-supervised text-guided image manipulation," in *CVPR*, 2024. **11, 16**
- [220] Z. Wu, N. Kolkin, J. Brandt, R. Zhang, and E. Shechtman, "Turboedit: Instant text-based image editing," *arXiv preprint arXiv:2408.08332*, 2024. **11, 16**
- [221] Z. Xu, T. Lin, H. Tang, F. Li, D. He, N. Sebe, R. Timofte, L. Van Gool, and E. Ding, "Predict, prevent, and evaluate: Disentangled text-driven image manipulation empowered by pre-trained vision-language model," in *CVPR*, 2022. **11**
- [222] M. Tao, B.-K. Bao, H. Tang, F. Wu, L. Wei, and Q. Tian, "Denet: Dynamic text-guided image editing adversarial networks," in *AAAI*, 2023. **11**
- [223] E. J. Hu, Y. Shen, P. Wallis, Z. Allen-Zhu, Y. Li, S. Wang, L. Wang, and W. Chen, "Lora: Low-rank adaptation of large language models," *arXiv preprint arXiv:2106.09685*, 2021. **9, 11, 16**
- [224] M. Patel, C. Kim, S. Cheng, C. Baral, and Y. Yang, "Eclipse: A resource-efficient text-to-image prior for image generations," in *CVPR*, 2024. **11, 17, 31**

- [225] X. Liu, X. Zhang, J. Ma, J. Peng *et al.*, "Instaflo: One step is enough for high-quality diffusion-based text-to-image generation," in *The Twelfth International Conference on Learning Representations*, 2023. **11, 17**
- [226] S. Liu, W. Yu, Z. Tan, and X. Wang, "Linfusion: 1 gpu, 1 minute, 16k image," *arXiv preprint arXiv:2409.02097*, 2024. **11, 17**
- [227] J. Lezama, H. Chang, L. Jiang, and I. Essa, "Improved masked image generation with token-critic," in *ECCV*, 2022. **11, 17**
- [228] R. Mokady, A. Hertz, K. Aberman, Y. Pritch, and D. Cohen-Or, "Null-text inversion for editing real images using guided diffusion models," in *CVPR*, 2023. **9, 11, 17**
- [229] E. Xie, L. Yao, H. Shi, Z. Liu, D. Zhou, Z. Liu, J. Li, and Z. Li, "Diffit: Unlocking transferability of large diffusion models via simple parameter-efficient fine-tuning," in *ICCV*, 2023. **11, 17**
- [230] T. Salimans and J. Ho, "Progressive distillation for fast sampling of diffusion models," *arXiv preprint arXiv:2202.00512*, 2022. **11, 17**
- [231] Y. Luo, X. Chen, X. Qu, T. Hu, and J. Tang, "You only sample once: Taming one-step text-to-image synthesis by self-cooperative diffusion gans," *arXiv preprint arXiv:2403.12931*, 2024. **11, 17**
- [232] T. H. Nguyen and A. Tran, "Swiftbrush: One-step text-to-image diffusion model with variational score distillation," in *CVPR*, 2024. **11, 17**
- [233] A. Kodaira, C. Xu, T. Hazama, T. Yoshimoto, K. Ohno, S. Mitsuhori, S. Sugano, H. Cho, Z. Liu, and K. Keutzer, "Streamdiffusion: A pipeline-level solution for real-time interactive generation," *arXiv preprint arXiv:2312.12491*, 2023. **11, 17**
- [234] S. X. Chen, Y. Vaxman, E. Ben Baruch, D. Asulin, A. Moreshet, K.-C. Lien, M. Sra, and P. Sen, "Tino-edit: Timestep and noise optimization for robust diffusion-based image editing," in *CVPR*, 2024. **11, 17**
- [235] H. Li, Y. Zou, Y. Wang, O. Majumder, Y. Xie, R. Manmatha, A. Swaminathan, Z. Tu, S. Ermon, and S. Soatto, "On the scalability of diffusion-based text-to-image generation," in *CVPR*, 2024. **11, 17**
- [236] H. Chang, H. Zhang, J. Barber, A. Maschinot, J. Lezama, L. Jiang, M.-H. Yang, K. Murphy, W. T. Freeman, M. Rubinstein *et al.*, "Muse: Text-to-image generation via masked generative transformers," *arXiv preprint arXiv:2301.00704*, 2023. **11, 16**
- [237] Z. Zhang, J. Ma, C. Zhou, R. Men, Z. Li, M. Ding, J. Tang, J. Zhou, and H. Yang, "Ufc-bert: Unifying multi-modal controls for conditional image synthesis," *Advances in Neural Information Processing Systems*, vol. 34, pp. 27 196–27 208, 2021. **11, 16**
- [238] S. Jayasumana, D. Glasner, S. Ramalingam, A. Veit, A. Chakrabarti, and S. Kumar, "Markovgen: Structured prediction for efficient text-to-image generation," in *Proceedings of the IEEE/CVF Conference on Computer Vision and Pattern Recognition*, 2024, pp. 9316–9325. **11, 16**
- [239] W. Mo, T. Zhang, Y. Bai, B. Su, J.-R. Wen, and Q. Yang, "Dynamic prompt optimizing for text-to-image generation," in *CVPR*, 2024. **11, 17**
- [240] R. Jena, A. Taghibakhshi, S. Jain, G. Shen, N. Tajbakhsh, and A. Vahdat, "Elucidating optimal reward-diversity tradeoffs in text-to-image diffusion models," *arXiv preprint arXiv:2409.06493*, 2024. **11, 17**
- [241] X. Zhang, L. Yang, G. Li, Y. Cai, J. Xie, Y. Tang, Y. Yang, M. Wang, and B. Cui, "Itercomp: Iterative composition-aware feedback learning from model gallery for text-to-image generation," *arXiv preprint arXiv:2410.07171*, 2024. **11, 17**
- [242] F. Wei, W. Zeng, Z. Li, D. Yin, L. Duan, and W. Li, "Powerful and flexible: Personalized text-to-image generation via reinforcement learning," *arXiv preprint arXiv:2407.06642*, 2024. **11, 17**
- [243] Y. Hao, Z. Chi, L. Dong, and F. Wei, "Optimizing prompts for text-to-image generation," in *NeurIPS*, 2024. **11, 17**
- [244] H. Yuan, Z. Chen, K. Ji, and Q. Gu, "Self-play fine-tuning of diffusion models for text-to-image generation," *arXiv preprint arXiv:2402.10210*, 2024. **11, 17**
- [245] H. Li, C. Shen, P. Torr, V. Tresp, and J. Gu, "Self-discovering interpretable diffusion latent directions for responsible text-to-image generation," in *CVPR*, 2024. **9, 11, 18, 30**
- [246] Z. Wu, H. Gao, Y. Wang, X. Zhang, and S. Wang, "Universal prompt optimizer for safe text-to-image generation," *arXiv preprint arXiv:2402.10882*, 2024. **11, 17**
- [247] J. Rando, D. Paleka, D. Lindner, L. Heim, and F. Tramèr, "Red-teaming the stable diffusion safety filter," *arXiv preprint arXiv:2210.04610*, 2022. **11, 17**
- [248] H. Zhang, Y. He, and H. Chen, "Steerdiff: Steering towards safe text-to-image diffusion models," *arXiv preprint arXiv:2410.02710*, 2024. **11, 18, 32**
- [249] Y. Liu, C. Fan, Y. Dai, X. Chen, P. Zhou, and L. Sun, "Metacloak: Preventing unauthorized subject-driven text-to-image diffusion-based synthesis via meta-learning," in *CVPR*, 2024. **11, 18**
- [250] M. D'Incà, E. Peruzzo, M. Mancini, D. Xu, V. Goel, X. Xu, Z. Wang, H. Shi, and N. Sebe, "Openbias: Open-set bias detection in text-to-image generative models," in *CVPR*, 2024. **11, 18, 30, 32**
- [251] M. Lyu, Y. Yang, H. Hong, H. Chen, X. Jin, Y. He, H. Xue, J. Han, and G. Ding, "One-dimensional adapter to rule them all: Concepts diffusion models and erasing applications," in *CVPR*, 2024. **9, 11, 17**
- [252] P. Schramowski, M. Brack, B. Deiseroth, and K. Kersting, "Safe latent diffusion: Mitigating inappropriate degeneration in diffusion models," in *CVPR*, 2023. **11, 17, 25, 26**
- [253] R. Gandikota, J. Materzynska, J. Fiotto-Kaufman, and D. Bau, "Erasing concepts from diffusion models," in *ICCV*, 2023. **11, 17**
- [254] S. Kim, S. Jung, B. Kim, M. Choi, J. Shin, and J. Lee, "SafeGuard text-to-image diffusion models with human feedback inversion," *arXiv preprint arXiv:2407.21032*, 2024. **11, 18, 30**
- [255] C. Gong, K. Chen, Z. Wei, J. Chen, and Y.-G. Jiang, "Reliable and efficient concept erasure of text-to-image diffusion models," *arXiv preprint arXiv:2407.12383*, 2024. **11, 18**
- [256] H. Liu, Y. Wu, S. Zhai, B. Yuan, and N. Zhang, "Riatig: Reliable and imperceptible adversarial text-to-image generation with natural prompts," in *CVPR*, 2023. **11, 18**
- [257] C. Liang, X. Wu, Y. Hua, J. Zhang, Y. Xue, T. Song, Z. Xue, R. Ma, and H. Guan, "Adversarial example does good: Preventing painting imitation from diffusion models via adversarial examples," *arXiv preprint arXiv:2302.04578*, 2023. **9, 11, 18, 19**
- [258] C. Liang and X. Wu, "Mist: Towards improved adversarial examples for diffusion models," *arXiv preprint arXiv:2305.12683*, 2023. **11, 18**
- [259] T. Van Le, H. Phung, T. H. Nguyen, Q. Dao, N. N. Tran, and A. Tran, "Anti-dreambooth: Protecting users from personalized text-to-image synthesis," in *ICCV*, 2023. **11, 18**
- [260] H. Liu, Z. Sun, and Y. Mu, "Countering personalized text-to-image generation with influence watermarks," in *CVPR*, 2024. **11, 18, 31**
- [261] X. Li, Q. Shen, and K. Kawaguchi, "Va3: Virtually assured amplification attack on probabilistic copyright protection for text-to-image generative models," in *CVPR*, 2024. **11, 18, 31**
- [262] F. Wang, Z. Tan, T. Wei, Y. Wu, and Q. Huang, "Simac: A simple anti-customization method for protecting face privacy against text-to-image synthesis of diffusion models," in *CVPR*, 2024. **9, 11, 18, 31**
- [263] Z. Wang, Z. Sha, Z. Ding, Y. Wang, and Z. Tu, "Tokencompose: Grounding diffusion with token-level supervision," *arXiv preprint arXiv:2312.03626*, 2023. **9, 11, 19**
- [264] Q. Phung, S. Ge, and J.-B. Huang, "Grounded text-to-image synthesis with attention refocusing," in *CVPR*, 2024. **9, 11, 19, 20**
- [265] L. Qu, W. Wang, Y. Li, H. Zhang, L. Nie, and T.-S. Chua, "Discriminative probing and tuning for text-to-image generation," in *CVPR*, 2024. **11, 19**
- [266] D. Zhou, Y. Li, F. Ma, X. Zhang, and Y. Yang, "Migc: Multi-instance generation controller for text-to-image synthesis," in *CVPR*, 2024. **11, 20**
- [267] X. Guo, J. Liu, M. Cui, J. Li, H. Yang, and D. Huang, "Initno: Boosting text-to-image diffusion models via initial noise optimization," in *CVPR*, 2024. **11, 20**
- [268] G. Kim, T. Kwon, and J. C. Ye, "Diffusionclip: Text-guided diffusion models for robust image manipulation," in *CVPR*, 2022. **11, 19**
- [269] C. Meng, Y. He, Y. Song, J. Song, J. Wu, J.-Y. Zhu, and S. Ermon, "Sdedit: Guided image synthesis and editing with stochastic differential equations," *arXiv preprint arXiv:2108.01073*, 2021. **11, 19**
- [270] M. Cao, X. Wang, Z. Qi, Y. Shan, X. Qie, and Y. Zheng, "Masactrl: Tuning-free mutual self-attention control for consistent image synthesis and editing," in *ICCV*, 2023. **11, 19**
- [271] C. Liu, X. Li, and H. Ding, "Referring image editing: Object-level image editing via referring expressions," in *CVPR*, 2024. **11, 19**
- [272] Q. Zhangli, J. Jiang, D. Liu, L. Yu, X. Dai, A. Ramchandani, G. Pang, D. N. Metaxas, and P. Krishnan, "Layout-agnostic scene text image synthesis with diffusion models," in *VPR*, 2024. **11, 19**

- [273] Y. Tuo, W. Xiang, J.-Y. He, Y. Geng, and X. Xie, "Anytext: Multilingual visual text generation and editing," *arXiv preprint arXiv:2311.03054*, 2023. **11, 19**
- [274] A. Farshad, Y. Yeganeh, Y. Chi, C. Shen, B. Ommer, and N. Navab, "Scenegenie: Scene graph guided diffusion models for image synthesis," in *ICCV*, 2023. **11, 19**
- [275] G. Couairon, M. Careil, M. Cord, S. Lathuiliere, and J. Verbeek, "Zero-shot spatial layout conditioning for text-to-image diffusion models," in *ICCV*, 2023. **11, 19**
- [276] X. Wu, H. Zhao, L. Zheng, S. Ding, and X. Li, "Adma-gan: Attribute-driven memory augmented gans for text-to-image generation." in *Proceedings of the 30th ACM International Conference on Multimedia*, 2022, pp. 1593–1602. **11, 20**
- [277] Z. Shi, Z. Chen, Z. Xu, W. Yang, and L. Huang, "Athom: Two divergent attentions stimulated by homomorphic training in text-to-image synthesis," in *ACM MM*, 2022. **11, 20**
- [278] Z. Chen, Z. Mao, S. Fang, and B. Hu, "Background layout generation and object knowledge transfer for text-to-image generation," in *ACM MM*, 2022. **11, 20**
- [279] D. Yang, R. Dong, J. Ji, Y. Ma, H. Wang, X. Sun, and R. Ji, "Exploring phrase-level grounding with text-to-image diffusion model," *arXiv preprint arXiv:2407.05352*, 2024. **11, 19**
- [280] J. Lee, H. Cho, Y. Yoo, S. B. Kim, and Y. Jeong, "Compose and conquer: Diffusion-based 3d depth aware composable image synthesis," *arXiv preprint arXiv:2401.09048*, 2024. **11, 20**
- [281] Y. Zhou, D. Zhou, M.-M. Cheng, J. Feng, and Q. Hou, "Storydif-fusion: Consistent self-attention for long-range image and video generation," *arXiv preprint arXiv:2405.01434*, 2024. **11, 20**
- [282] R. Rassin, E. Hirsch, D. Glickman, S. Ravfogel, Y. Goldberg, and G. Chechik, "Linguistic binding in diffusion models: Enhancing attribute correspondence through attention map alignment," in *NeurIPS*, 2024. **11, 20**
- [283] W. Wu, Z. Li, Y. He, M. Z. Shou, C. Shen, L. Cheng, Y. Li, T. Gao, D. Zhang, and Z. Wang, "Paragraph-to-image generation with information-enriched diffusion model," *arXiv preprint arXiv:2311.14284*, 2023. **11, 20**
- [284] T. Hu, L. Li, J. van de Weijer, H. Gao, F. S. Khan, J. Yang, M.-M. Cheng, K. Wang, and Y. Wang, "Token merging for training-free semantic binding in text-to-image synthesis," *arXiv preprint arXiv:2411.07132*, 2024. **11, 20**
- [285] W. Feng, X. He, T.-J. Fu, V. Jampani, A. Akula, P. Narayana, S. Basu, X. E. Wang, and W. Y. Wang, "Training-free structured diffusion guidance for compositional text-to-image synthesis," *arXiv preprint arXiv:2212.05032*, 2022. **11, 20, 25, 26**
- [286] Z. Li, M. R. Min, K. Li, and C. Xu, "Styler2i: Toward compositional and high-fidelity text-to-image synthesis," 2022. **11, 20**
- [287] O. Dahary, O. Patashnik, K. Aberman, and D. Cohen-Or, "Be yourself: Bounded attention for multi-subject text-to-image generation," *arXiv preprint arXiv:2403.16990*, vol. 2, no. 5, 2024. **11, 20**
- [288] X. Song, J. Cui, H. Zhang, J. Chen, R. Hong, and Y.-G. Jiang, "Doubly abductive counterfactual inference for text-based image editing," in *CVPR*, 2024. **11, 20**
- [289] R. Wang, Z. Chen, C. Chen, J. Ma, H. Lu, and X. Lin, "Compositional text-to-image synthesis with attention map control of diffusion models," in *AAAI*, 2024. **11**
- [290] A. Hertz, K. Aberman, and D. Cohen-Or, "Delta denoising score," in *ICCV*, 2023. **11, 20**
- [291] H. Nam, G. Kwon, G. Y. Park, and J. C. Ye, "Contrastive denoising score for text-guided latent diffusion image editing," in *CVPR*, 2024. **11, 20**
- [292] Y. Cui, X. Zhao, G. Zhang, S. Cao, K. Ma, and L. Wang, "Stabledrag: Stable dragging for point-based image editing," *arXiv preprint arXiv:2403.04437*, 2024. **11, 20**
- [293] P. Ling, L. Chen, P. Zhang, H. Chen, Y. Jin, and J. Zheng, "Free-drag: Feature dragging for reliable point-based image editing," in *CVPR*, 2024. **11, 20**
- [294] J. Lu, X. Li, and K. Han, "Regiondrag: Fast region-based image editing with diffusion models," *arXiv preprint arXiv:2407.18247*, 2024. **11, 20**
- [295] A. Chatterjee, G. B. M. Stan, E. Aflalo, S. Paul, D. Ghosh, T. Gokhale, L. Schmidt, H. Hajishirzi, V. Lal, C. Baral *et al.*, "Getting it right: Improving spatial consistency in text-to-image models," in *ECCV*, 2025. **9, 11, 20, 21, 32**
- [296] D. Jiang, G. Song, X. Wu, R. Zhang, D. Shen, Z. Zong, Y. Liu, and H. Li, "Comat: Aligning text-to-image diffusion model with image-to-text concept matching," *arXiv preprint arXiv:2404.03653*, 2024. **9, 11, 21**
- [297] P.-D. Tudosiu, Y. Yang, S. Zhang, F. Chen, S. McDonagh, G. Lampouras, I. Iacobacci, and S. Parisot, "Mulan: A multi layer annotated dataset for controllable text-to-image generation," in *CVPR*, 2024. **11, 21**
- [298] K. Yan, L. Ji, C. Wu, J. Bao, M. Zhou, N. Duan, and S. Ma, "Trace controlled text to image generation," in *ECCV*, 2022. **11, 21**
- [299] Z. Lv, Y. Wei, W. Zuo, and K.-Y. K. Wong, "Place: Adaptive layout-semantic fusion for semantic image synthesis," in *CVPR*, 2024. **11, 21**
- [300] M. Chen, I. Laina, and A. Vedaldi, "Training-free layout control with cross-attention guidance," in *WCV*, 2024. **11, 21**
- [301] C. Jia, M. Luo, Z. Dang, G. Dai, X. Chang, M. Wang, and J. Wang, "Ssmg: Spatial-semantic map guided diffusion model for free-form layout-to-image generation," in *AAAI*, 2024. **11, 21**
- [302] S. Li, J. Fu, K. Liu, W. Wang, K.-Y. Lin, and W. Wu, "Cosmicman: A text-to-image foundation model for humans," in *CVPR*, 2024. **11, 21**
- [303] Y. Jiang, S. Yang, H. Qiu, W. Wu, C. C. Loy, and Z. Liu, "Text2human: Text-driven controllable human image generation," *ACM Transactions on Graphics (TOG)*, vol. 41, no. 4, pp. 1–11, 2022. **11, 22**
- [304] Y. Zhou, R. Zhang, J. Gu, and T. Sun, "Customization assistant for text-to-image generation," in *CVPR*, 2024. **11, 24**
- [305] F. Lin, M. Li, D. Li, T. Hospedales, Y.-Z. Song, and Y. Qi, "Zero-shot everything sketch-based image retrieval, and in explainable style," in *CVPR*, 2023. **11, 22**
- [306] S. Narasimhaswamy, U. Bhattacharya, X. Chen, I. Dasgupta, S. Mitra, and M. Hoai, "Handdiffuser: Text-to-image generation with realistic hand appearances," in *CVPR*, 2024. **11, 22**
- [307] J. Yang, J. Feng, and H. Huang, "Emogen: Emotional image content generation with text-to-image diffusion models," in *CVPR*, 2024. **11, 21, 22**
- [308] L. Pang, J. Yin, H. Xie, Q. Wang, Q. Li, and X. Mao, "Cross initialization for personalized text-to-image generation," *arXiv preprint arXiv:2312.15905*, 2023. **11, 22**
- [309] J. Wang, Z. Sun, Z. Tan, X. Chen, W. Chen, H. Li, C. Zhang, and Y. Song, "Towards effective usage of human-centric priors in diffusion models for text-based human image generation," in *CVPR*, 2024. **11, 22**
- [310] C. Zhang, Q. Wu, C. C. Gambardella, X. Huang, D. Phung, W. Ouyang, and J. Cai, "Taming stable diffusion for text to 360 panorama image generation," in *CVPR*, 2024. **11, 22**
- [311] C. Liu, H. Wu, Y. Zhong, X. Zhang, Y. Wang, and W. Xie, "Intelligent grimm-open-ended visual storytelling via latent diffusion models," in *CVPR*, 2024. **11, 22**
- [312] J. Su, S. Gu, Y. Duan, X. Chen, and J. Luo, "Text2street: Controllable text-to-image generation for street views," *arXiv preprint arXiv:2402.04504*, 2024. **11, 22**
- [313] X. Xing, H. Zhou, C. Wang, J. Zhang, D. Xu, and Q. Yu, "Svgs-dreamer: Text guided svg generation with diffusion model," in *CVPR*, 2024. **11, 22**
- [314] Y. Han, J. Zhu, K. He, X. Chen, Y. Ge, W. Li, X. Li, J. Zhang, C. Wang, and Y. Liu, "Face adapter for pre-trained diffusion models with fine-grained id and attribute control," *arXiv preprint arXiv:2405.12970*, 2024. **11, 22**
- [315] A. Maharana, D. Hannan, and M. Bansal, "Storydall-e: Adapting pretrained text-to-image transformers for story continuation," in *ECCV*, 2022. **11, 22**
- [316] T. Wang and M. Ye, "Textfit: Text-driven fashion image editing with diffusion models," in *AAAI*, 2024. **11, 22**
- [317] L. Yang, B. Zeng, J. Liu, H. Li, M. Xu, W. Zhang, and S. Yan, "Editworld: Simulating world dynamics for instruction-following image editing," *arXiv preprint arXiv:2405.14785*, 2024. **11, 22**
- [318] T.-Y. Cheng, M. Gadelha, T. Groueix, M. Fisher, R. Mech, A. Markham, and N. Trigoni, "Learning continuous 3d words for text-to-image generation," in *CVPR*, 2024. **9, 11, 22**
- [319] T. Wu, Y. Xu, R. Po, M. Zhang, G. Yang, J. Wang, Z. Liu, D. Lin, and G. Wetzstein, "Fiva: Fine-grained visual attribute dataset for text-to-image diffusion models," in *The Thirty-eight Conference on Neural Information Processing Systems Datasets and Benchmarks Track*. **11, 22**
- [320] Y. Li, H. Liu, Q. Wu, F. Mu, J. Yang, J. Gao, C. Li, and Y. J. Lee, "Gligen: Open-set grounded text-to-image generation," in *CVPR*, 2023. **11, 23**

- [321] J. T. Hoe, X. Jiang, C. S. Chan, Y.-P. Tan, and W. Hu, "Interactdiffusion: Interaction control in text-to-image diffusion models," in *CVPR*, 2024. **11, 23**
- [322] R. Parihar, V. Sachidanand, S. Mani, T. Karmali, and R. Venkatesh Babu, "Precisecontrol: Enhancing text-to-image diffusion models with fine-grained attribute control," in *ECCV*, 2024. **11, 23**
- [323] O. Patashnik, D. Garibi, I. Azuri, H. Averbuch-Elor, and D. Cohen-Or, "Localizing object-level shape variations with text-to-image diffusion models," in *ICCV*, 2023. **9, 11, 22**
- [324] D. Geng and A. Owens, "Motion guidance: Diffusion-based image editing with differentiable motion estimators," *arXiv preprint arXiv:2401.18085*, 2024. **11, 23**
- [325] P. Zhang, H. Yin, C. Li, and X. Xie, "Tackling the singularities at the endpoints of time intervals in diffusion models," in *CVPR*, 2024. **11, 23**
- [326] Y. Lu, M. Zhang, A. J. Ma, X. Xie, and J. Lai, "Coarse-to-fine latent diffusion for pose-guided person image synthesis," in *CVPR*, 2024. **11, 23**
- [327] T. Shirakawa and S. Uchida, "Noisecollage: A layout-aware text-to-image diffusion model based on noise cropping and merging," in *CVPR*, 2024. **11, 23**
- [328] G. Kwon, S. Jenni, D. Li, J.-Y. Lee, J. C. Ye, and F. C. Heilbron, "Concept weaver: Enabling multi-concept fusion in text-to-image models," in *CVPR*, 2024. **11, 23**
- [329] D. Li, A. Kamko, E. Akhgari, A. Sabet, L. Xu, and S. Doshi, "Playground v2. 5: Three insights towards enhancing aesthetic quality in text-to-image generation," *arXiv preprint arXiv:2402.17245*, 2024. **11, 22, 23**
- [330] L. Zhang and M. Agrawala, "Transparent image layer diffusion using latent transparency," *arXiv preprint arXiv:2402.17113*, 2024. **11, 23**
- [331] T. H. S. Meral, E. Simsar, F. Tombari, and P. Yanardag, "Conform: Contrast is all you need for high-fidelity text-to-image diffusion models," in *CVPR*, 2024. **11, 23**
- [332] W. Feng, W. Zhu, T.-j. Fu, V. Jampani, A. Akula, X. He, S. Basu, X. E. Wang, and W. Y. Wang, "Layoutgpt: Compositional visual planning and generation with large language models," in *NeurIPS*, 2024. **11, 23**
- [333] A. Zala, H. Lin, J. Cho, and M. Bansal, "Diagrammergpt: Generating open-domain, open-platform diagrams via llm planning," *arXiv preprint arXiv:2310.12128*, 2023. **11, 23**
- [334] W. Wang, C. Zhao, H. Chen, Z. Chen, K. Zheng, and C. Shen, "Autostory: Generating diverse storytelling images with minimal human effort," *arXiv preprint arXiv:2311.11243*, 2023. **11, 24, 29**
- [335] L. Qu, S. Wu, H. Fei, L. Nie, and T.-S. Chua, "Layoutllm-t2i: Eliciting layout guidance from llm for text-to-image generation," in *Proceedings of the 31st ACM International Conference on Multimedia*, 2023, pp. 643–654. **9, 11, 23**
- [336] K. Song, Y. Zhu, B. Liu, Q. Yan, A. Elgammal, and X. Yang, "Moma: Multimodal llm adapter for fast personalized image generation," *arXiv preprint arXiv:2404.05674*, 2024. **11, 24**
- [337] Y. Huang, L. Xie, X. Wang, Z. Yuan, X. Cun, Y. Ge, J. Zhou, C. Dong, R. Huang, R. Zhang *et al.*, "Smartedit: Exploring complex instruction-based image editing with multimodal large language models," in *CVPR*, 2024. **9, 11, 23**
- [338] Y. Yao, C.-F. Hsu, J.-H. Lin, H. Xie, T. Lin, Y.-N. Huang, H.-H. Shuai, and W.-H. Cheng, "The fabrication of reality and fantasy: Scene generation with llm-assisted prompt interpretation," in *ECCV*, 2024. **11, 24**
- [339] J. Liao, X. Chen, Q. Fu, L. Du, X. He, X. Wang, S. Han, and D. Zhang, "Text-to-image generation for abstract concepts," in *AAAI*, 2024. **11, 24**
- [340] X. Hu, R. Wang, Y. Fang, B. Fu, P. Cheng, and G. Yu, "Ella: Equip diffusion models with llm for enhanced semantic alignment," *arXiv preprint arXiv:2403.05135*, 2024. **11, 24**
- [341] M. Huang, Y. Long, X. Deng, R. Chu, J. Xiong, X. Liang, H. Cheng, Q. Lu, and W. Liu, "Dialoggen: Multi-modal interactive dialogue system for multi-turn text-to-image generation," *arXiv preprint arXiv:2403.08857*, 2024. **11, 24**
- [342] T.-J. Fu, W. Hu, X. Du, W. Y. Wang, Y. Yang, and Z. Gan, "Guiding instruction-based image editing via multimodal large language models," *arXiv preprint arXiv:2309.17102*, 2023. **11, 23, 24**
- [343] P. Grimal, H. Le Borgne, O. Ferret, and J. Tourille, "Tiam-a metric for evaluating alignment in text-to-image generation," in *Proceedings of the IEEE/CVF Winter Conference on Applications of Computer Vision*, 2024, pp. 2890–2899. **10, 27, 28**
- [344] Y. Bai, A. Jones, K. Ndousse, A. Askell, A. Chen, N. DasSarma, D. Drain, S. Fort, D. Ganguli, T. Henighan *et al.*, "Training a helpful and harmless assistant with reinforcement learning from human feedback," *arXiv preprint arXiv:2204.05862*, 2022. **10**
- [345] X. Wu, Y. Hao, K. Sun, Y. Chen, F. Zhu, R. Zhao, and H. Li, "Human preference score v2: A solid benchmark for evaluating human preferences of text-to-image synthesis," *arXiv preprint arXiv:2306.09341*, 2023. **11**
- [346] T.-Y. Lin, M. Maire, S. Belongie, J. Hays, P. Perona, D. Ramanan, P. Dollár, and C. L. Zitnick, "Microsoft coco: Common objects in context," in *ECCV*, 2014. **11, 24, 25, 27**
- [347] G. Zheng, X. Zhou, X. Li, Z. Qi, Y. Shan, and X. Li, "Layoutdiffusion: Controllable diffusion model for layout-to-image generation," in *CVPR*, 2023. **12**
- [348] Y. Wang, W. Zhang, J. Zheng, and C. Jin, "High-fidelity person-centric subject-to-image synthesis," in *CVPR*, 2024. **12**
- [349] J. Li, D. Li, S. Savarese, and S. Hoi, "Blip-2: Bootstrapping language-image pre-training with frozen image encoders and large language models," in *ICML*, 2023. **13, 26, 27, 28**
- [350] B. Romera-Paredes and P. Torr, "An embarrassingly simple approach to zero-shot learning," in *ICML*, 2015. **13**
- [351] Y. Lin, Y.-W. Chen, Y.-H. Tsai, L. Jiang, and M.-H. Yang, "Text-driven image editing via learnable regions," in *CVPR*, 2024. **16**
- [352] L. Li, H. Zeng, C. Yang, H. Jia, and D. Xu, "Block-wise lora: Revisiting fine-grained lora for effective personalization and stylization in text-to-image generation," *arXiv preprint arXiv:2403.07500*, 2024. **17**
- [353] D. J. Bartholomew, M. Knott, and I. Moustaki, *Latent variable models and factor analysis: A unified approach*. John Wiley & Sons, 2011. **17**
- [354] C. J. C. H. Watkins, "Learning from delayed rewards," 1989. **17**
- [355] Z. Miao, J. Wang, Z. Wang, Z. Yang, L. Wang, Q. Qiu, and Z. Liu, "Training diffusion models towards diverse image generation with reinforcement learning," in *CVPR*, 2024. **17**
- [356] M. Huang, Z. Mao, P. Wang, Q. Wang, and Y. Zhang, "Dse-gan: Dynamic semantic evolution generative adversarial network for text-to-image generation," in *ACM MM*, 2022. **20**
- [357] S. Yin, C. Fu, S. Zhao, K. Li, X. Sun, T. Xu, and E. Chen, "A survey on multimodal large language models," *arXiv preprint arXiv:2306.13549*, 2023. **23, 24**
- [358] L. Lian, B. Li, A. Yala, and T. Darrell, "Llm-grounded diffusion: Enhancing prompt understanding of text-to-image diffusion models with large language models," *arXiv preprint arXiv:2305.13655*, 2023. **23**
- [359] J. Cho, A. Zala, and M. Bansal, "Visual programming for step-by-step text-to-image generation and evaluation," in *NeurIPS*, 2024. **23**
- [360] L. H. Li, P. Zhang, H. Zhang, J. Yang, C. Li, Y. Zhong, L. Wang, L. Yuan, L. Zhang, J.-N. Hwang *et al.*, "Grounded language-image pre-training," in *CVPR*, 2022. **23**
- [361] A. Brock, "Large scale gan training for high fidelity natural image synthesis," *arXiv preprint arXiv:1809.11096*, 2018. **24**
- [362] T. Karras, S. Laine, M. Aittala, J. Hellsten, J. Lehtinen, and T. Aila, "Analyzing and improving the image quality of stylegan," in *CVPR*, 2020. **24**
- [363] S. Hartwig, D. Engel, L. Sick, H. Kniessel, T. Payer, T. Ropinski *et al.*, "Evaluating text to image synthesis: Survey and taxonomy of image quality metrics," *arXiv preprint arXiv:2403.11821*, 2024. **24, 27**
- [364] M.-E. Nilsback and A. Zisserman, "Automated flower classification over a large number of classes," in *2008 Sixth Indian conference on computer vision, graphics & image processing*. IEEE, 2008, pp. 722–729. **24, 25**
- [365] C. Rashtchian, P. Young, M. Hodosh, and J. Hockenmaier, "Collecting image annotations using amazon's mechanical turk," in *Proceedings of the NAACL HLT 2010 workshop on creating speech and language data with Amazon's Mechanical Turk*, 2010, pp. 139–147. **25**
- [366] V. Ordonez, G. Kulkarni, and T. Berg, "Im2text: Describing images using 1 million captioned photographs," in *NeurIPS*, 2011. **25**
- [367] M. Hodosh, P. Young, and J. Hockenmaier, "Framing image description as a ranking task: Data, models and evaluation metrics," *Journal of Artificial Intelligence Research*, vol. 47, pp. 853–899, 2013. **24, 25**
- [368] R. Vedantam, C. Lawrence Zitnick, and D. Parikh, "Cider: Consensus-based image description evaluation," in *CVPR*, 2015. **25, 26, 27, 28**

- [369] B. A. Plummer, L. Wang, C. M. Cervantes, J. C. Caicedo, J. Hockenmaier, and S. Lazebnik, "Flickr30k entities: Collecting region-to-phrase correspondences for richer image-to-sentence models," in *ICCV*, 2015. [24](#), [25](#)
- [370] X. Chen, H. Fang, T.-Y. Lin, R. Vedantam, S. Gupta, P. Dollár, and C. L. Zitnick, "Microsoft coco captions: Data collection and evaluation server," *arXiv preprint arXiv:1504.00325*, 2015. [24](#), [25](#)
- [371] S. Antol, A. Agrawal, J. Lu, M. Mitchell, D. Batra, C. L. Zitnick, and D. Parikh, "Vqa: Visual question answering," in *ICCV*, 2015. [25](#), [26](#)
- [372] J. Mao, J. Xu, K. Jing, and A. L. Yuille, "Training and evaluating multimodal word embeddings with large-scale web annotated images," in *NeurIPS*, 2016. [25](#)
- [373] R. Krishna, Y. Zhu, O. Groth, J. Johnson, K. Hata, J. Kravitz, S. Chen, Y. Kalantidis, L.-J. Li, D. A. Shamma *et al.*, "Visual genome: Connecting language and vision using crowdsourced dense image annotations," *International journal of computer vision*, vol. 123, pp. 32–73, 2017. [25](#)
- [374] Y. Goyal, T. Khot, D. Summers-Stay, D. Batra, and D. Parikh, "Making the v in vqa matter: Elevating the role of image understanding in visual question answering," in *CVPR*, 2017. [25](#), [26](#)
- [375] Z. Liu, P. Luo, X. Wang, and X. Tang, "Large-scale celebfaces attributes (celeba) dataset," *Retrieved August*, vol. 15, no. 2018, p. 11, 2018. [24](#), [25](#)
- [376] H. Agrawal, K. Desai, Y. Wang, X. Chen, R. Jain, M. Johnson, D. Batra, D. Parikh, S. Lee, and P. Anderson, "Nocaps: Novel object captioning at scale," in *ICCV*, 2019. [25](#)
- [377] R. Zellers, Y. Bisk, A. Farhadi, and Y. Choi, "From recognition to cognition: Visual commonsense reasoning," in *CVPR*, 2019. [25](#), [26](#)
- [378] P. Sharma, N. Ding, S. Goodman, and R. Soiccut, "Conceptual captions: A cleaned, hypernymed, image alt-text dataset for automatic image captioning," in *Proceedings of the 56th Annual Meeting of the Association for Computational Linguistics (Volume 1: Long Papers)*, 2018, pp. 2556–2565. [25](#)
- [379] C. Schuhmann, R. Vencu, R. Beaumont, R. Kaczmarczyk, C. Mullis, A. Katta, T. Coombes, J. Jitsev, and A. Komatsuzaki, "Laion-400m: Open dataset of clip-filtered 400 million image-text pairs," *arXiv preprint arXiv:2111.02114*, 2021. [25](#)
- [380] S. Changpinyo, P. Sharma, N. Ding, and R. Soiccut, "Conceptual 12m: Pushing web-scale image-text pre-training to recognize long-tail visual concepts," in *CVPR*, 2021. [25](#)
- [381] C. Schuhmann, R. Beaumont, R. Vencu, C. Gordon, R. Wightman, M. Cherti, T. Coombes, A. Katta, C. Mullis, M. Wortsman *et al.*, "Laion-5b: An open large-scale dataset for training next generation image-text models," in *NeurIPS*, 2022. [25](#), [27](#), [28](#), [30](#), [32](#)
- [382] Z. J. Wang, E. Montoya, D. Munechika, H. Yang, B. Hoover, and D. H. Chau, "Diffusiondb: A large-scale prompt gallery dataset for text-to-image generative models," *arXiv preprint arXiv:2210.14896*, 2022. [25](#)
- [383] T. Thrush, R. Jiang, M. Bartolo, A. Singh, A. Williams, D. Kiela, and C. Ross, "Winoground: Probing vision and language models for visio-linguistic compositionality," in *CVPR*, 2022. [25](#), [26](#)
- [384] K. Huang, K. Sun, E. Xie, Z. Li, and X. Liu, "T2i-compbench: A comprehensive benchmark for open-world compositional text-to-image generation," in *NeurIPS*, 2023. [25](#), [26](#), [27](#), [28](#)
- [385] J. Cho, A. Zala, and M. Bansal, "Dall-eval: Probing the reasoning skills and social biases of text-to-image generation models," in *ICCV*, 2023. [25](#)
- [386] P. Young, A. Lai, M. Hodosh, and J. Hockenmaier, "From image descriptions to visual denotations: New similarity metrics for semantic inference over event descriptions," *Transactions of the Association for Computational Linguistics*, vol. 2, pp. 67–78, 2014. [24](#)
- [387] H. Dong, J. Zhang, D. McIlwraith, and Y. Guo, "Learning text to image synthesis with textual data augmentation," *arXiv preprint arXiv:1703.06676*, vol. 2, 2017. [26](#)
- [388] C.-B. Zhang, P.-T. Jiang, Q. Hou, Y. Wei, Q. Han, Z. Li, and M.-M. Cheng, "Delving deep into label smoothing," *IEEE TIP*, vol. 30, pp. 5984–5996, 2021. [26](#)
- [389] H. Zhang, "mixup: Beyond empirical risk minimization," *arXiv preprint arXiv:1710.09412*, 2017. [26](#)
- [390] S. Ye and F. Liu, "Data extrapolation for text-to-image generation on small datasets," *arXiv preprint arXiv:2410.01638*, 2024. [26](#)
- [391] N. Dhanachandra, K. Manglem, and Y. J. Chanu, "Image segmentation using k-means clustering algorithm and subtractive clustering algorithm," *Procedia Computer Science*, vol. 54, pp. 764–771, 2015. [26](#)
- [392] X. Yan, J. Yang, K. Sohn, and H. Lee, "Attribute2image: Conditional image generation from visual attributes," in *ECCV*, 2016. [26](#)
- [393] A. Van den Oord, N. Kalchbrenner, L. Espeholt, O. Vinyals, A. Graves *et al.*, "Conditional image generation with pixelcnn decoders," in *NeurIPS*, 2016. [26](#)
- [394] Z. Tan, X. Yang, and K. Huang, "Semantic-aware data augmentation for text-to-image synthesis," in *AAAI*, 2024. [26](#)
- [395] D. Lopez-Paz and M. Oquab, "Revisiting classifier two-sample tests," *arXiv preprint arXiv:1610.06545*, 2016. [27](#)
- [396] T. Kynkäänniemi, T. Karras, S. Laine, J. Lehtinen, and T. Aila, "Improved precision and recall metric for assessing generative models," in *NeurIPS*, 2019. [27](#), [28](#)
- [397] Z. Wang, A. C. Bovik, H. R. Sheikh, and E. P. Simoncelli, "Image quality assessment: from error visibility to structural similarity," *IEEE transactions on image processing*, vol. 13, no. 4, pp. 600–612, 2004. [27](#)
- [398] A. Hore and D. Ziou, "Image quality metrics: Psnr vs. ssim," in *2010 20th international conference on pattern recognition*. IEEE, 2010, pp. 2366–2369. [27](#)
- [399] T. Salimans, I. Goodfellow, W. Zaremba, V. Cheung, A. Radford, and X. Chen, "Improved techniques for training gans," in *NeurIPS*, 2016. [27](#)
- [400] M. Heusel, H. Ramsauer, T. Unterthiner, B. Nessler, and S. Hochreiter, "Gans trained by a two time-scale update rule converge to a local nash equilibrium," in *NeurIPS*, 2017. [27](#)
- [401] C.-Y. Bai, H.-T. Lin, C. Raffel, and W. C.-w. Kan, "On training sample memorization: Lessons from benchmarking generative modeling with a large-scale competition," in *Proceedings of the 27th ACM SIGKDD conference on knowledge discovery & data mining*, 2021, pp. 2534–2542. [27](#)
- [402] M. Bińkowski, D. J. Sutherland, M. Arbel, and A. Gretton, "Demystifying mmd gans," *arXiv preprint arXiv:1801.01401*, 2018. [27](#)
- [403] D. H. Park, S. Azadi, X. Liu, T. Darrell, and A. Rohrbach, "Benchmark for compositional text-to-image synthesis," in *Thirty-fifth Conference on Neural Information Processing Systems Datasets and Benchmarks Track (Round 1)*, 2021. [27](#)
- [404] Y. Kirstain, A. Polyak, U. Singer, S. Matiana, J. Penna, and O. Levy, "Pick-a-pic: An open dataset of user preferences for text-to-image generation," in *NeurIPS*, 2023. [27](#)
- [405] T. Lee, M. Yasunaga, C. Meng, Y. Mai, J. S. Park, A. Gupta, Y. Zhang, D. Narayanan, H. Teufel, M. Bellagente *et al.*, "Holistic evaluation of text-to-image models," in *NeurIPS*, 2024. [27](#), [31](#)
- [406] M. S. Sajjadi, O. Bachem, M. Lucic, O. Bousquet, and S. Gelly, "Assessing generative models via precision and recall," in *NeurIPS*, vol. 31, 2018. [27](#), [28](#)
- [407] Y. Cui, G. Yang, A. Veit, X. Huang, and S. Belongie, "Learning to evaluate image captioning," in *CVPR*, 2018. [27](#), [28](#)
- [408] S. Kolouri, G. K. Rohde, and H. Hoffmann, "Sliced wasserstein distance for learning gaussian mixture models," in *CVPR*, 2018. [27](#), [28](#)
- [409] P. Madhyastha, J. Wang, and L. Specia, "Vifidel: Evaluating the visual fidelity of image descriptions," *arXiv preprint arXiv:1907.09340*, 2019. [27](#), [28](#)
- [410] M. Jiang, Q. Huang, L. Zhang, X. Wang, P. Zhang, Z. Gan, J. Diesner, and J. Gao, "Tiger: Text-to-image grounding for image caption evaluation," *arXiv preprint arXiv:1909.02050*, 2019. [27](#), [28](#)
- [411] H. Lee, S. Yoon, F. Dernoncourt, D. S. Kim, T. Bui, and K. Jung, "Vilbertscore: Evaluating image caption using vision-and-language bert," in *Proceedings of the First Workshop on Evaluation and Comparison of NLP Systems*, 2020, pp. 34–39. [27](#), [28](#)
- [412] T. Hinz, S. Heinrich, and S. Wermter, "Semantic object accuracy for generative text-to-image synthesis," *IEEE TPAMI*, vol. 44, no. 3, pp. 1552–1565, 2020. [27](#), [28](#)
- [413] J. Hessel, A. Holtzman, M. Forbes, R. L. Bras, and Y. Choi, "Clip-score: A reference-free evaluation metric for image captioning," *arXiv preprint arXiv:2104.08718*, 2021. [27](#)
- [414] M. Yuksekogonul, F. Bianchi, P. Kalluri, D. Jurafsky, and J. Zou, "When and why vision-language models behave like bags-of-words, and what to do about it?" *arXiv preprint arXiv:2210.01936*, 2022. [27](#)
- [415] J. Li, D. Li, C. Xiong, and S. Hoi, "Blip: Bootstrapping language-image pre-training for unified vision-language understanding and generation," in *ICML*, 2022. [27](#), [28](#)

- [416] T. Gokhale, H. Palangi, B. Nushi, V. Vineet, E. Horvitz, E. Kamar, C. Baral, and Y. Yang, "Benchmarking spatial relationships in text-to-image generation," *arXiv preprint arXiv:2212.10015*, 2022. [27, 28](#)
- [417] J.-H. Kim, Y. Kim, J. Lee, K. M. Yoo, and S.-W. Lee, "Mutual information divergence: A unified metric for multimodal generative models," 2022. [27, 28](#)
- [418] L. Zhang, Y. Zhou, C. Barnes, S. Amirghodsi, Z. Lin, E. Shechtman, and J. Shi, "Perceptual artifacts localization for inpainting," in *ECCV*, 2022. [27, 28](#)
- [419] H. Singh, P. Zhang, Q. Wang, M. Wang, W. Xiong, J. Du, and Y. Chen, "Coarse-to-fine contrastive learning in image-text-graph space for improved vision-language compositionality," *arXiv preprint arXiv:2305.13812*, 2023. [27](#)
- [420] J. Wang, K. C. Chan, and C. C. Loy, "Exploring clip for assessing the look and feel of images," in *Proceedings of the AAAI Conference on Artificial Intelligence*, vol. 37, no. 2, 2023, pp. 2555–2563. [27](#)
- [421] F. Betti, J. Staiano, L. Baraldi, L. Baraldi, R. Cucchiara, and N. Sebe, "Let's vice! mimicking human cognitive behavior in image generation evaluation," in *Proceedings of the 31st ACM International Conference on Multimedia*, 2023, pp. 9306–9312. [27, 28](#)
- [422] S. Fu, N. Tamir, S. Sundaram, L. Chai, R. Zhang, T. Dekel, and P. Isola, "Dreamsim: Learning new dimensions of human visual similarity using synthetic data," *arXiv preprint arXiv:2306.09344*, 2023. [27, 28](#)
- [423] J. Singh and L. Zheng, "Divide, evaluate, and refine: Evaluating and improving text-to-image alignment with iterative vqa feedback," in *NeurIPS*, 2023. [27, 28](#)
- [424] Y. Hu, B. Liu, J. Kasai, Y. Wang, M. Ostendorf, R. Krishna, and N. A. Smith, "Tifa: Accurate and interpretable text-to-image faithfulness evaluation with question answering," in *ICCV*, 2023. [27, 28](#)
- [425] M. Ku, D. Jiang, C. Wei, X. Yue, and W. Chen, "Viescore: Towards explainable metrics for conditional image synthesis evaluation," *arXiv preprint arXiv:2312.14867*, 2023. [27, 28](#)
- [426] Z. Ma, C. Wang, Y. Ouyang, F. Zhao, J. Zhang, S. Huang, and J. Chen, "Cobra effect in reference-free image captioning metrics," *arXiv preprint arXiv:2402.11572*, 2024. [27, 28](#)
- [427] M. Yarom, Y. Bitton, S. Changpinyo, R. Aharoni, J. Herzig, O. Lang, E. Ofek, and I. Szepkator, "What you see is what you read? improving text-image alignment evaluation," in *NeurIPS*, 2024. [27, 28](#)
- [428] J. Wang, H. Duan, G. Zhai, and X. Min, "Understanding and evaluating human preferences for ai generated images with instruction tuning," *arXiv preprint arXiv:2405.07346*, 2024. [27, 28](#)
- [429] S. Castro, A. Ziai, A. Saluja, Z. Yuan, and R. Mihalcea, "Clove: Encoding compositional language in contrastive vision-language models," *arXiv preprint arXiv:2402.15021*, 2024. [27](#)
- [430] B. Gordon, Y. Bitton, Y. Shafir, R. Garg, X. Chen, D. Lischinski, D. Cohen-Or, and I. Szepkator, "Mismatch quest: Visual and textual feedback for image-text misalignment," in *ECCV*, 2024. [27, 28](#)
- [431] L. Zhang, Z. Xu, C. Barnes, Y. Zhou, Q. Liu, H. Zhang, S. Amirghodsi, Z. Lin, E. Shechtman, and J. Shi, "Perceptual artifacts localization for image synthesis tasks," in *ICCV*, 2023. [28](#)
- [432] Y. Gong, Y. Pang, X. Cun, M. Xia, Y. He, H. Chen, L. Wang, Y. Zhang, X. Wang, Y. Shan *et al.*, "Talecrafter: Interactive story visualization with multiple characters," *arXiv preprint arXiv:2305.18247*, 2023. [29](#)
- [433] B. Yang, S. Gu, B. Zhang, T. Zhang, X. Chen, X. Sun, D. Chen, and F. Wen, "Paint by example: Exemplar-based image editing with diffusion models," in *CVPR*, 2023. [29](#)
- [434] T. Rahman, H.-Y. Lee, J. Ren, S. Tulyakov, S. Mahajan, and L. Sigal, "Make-a-story: Visual memory conditioned consistent story generation," in *CVPR*, 2023. [29](#)
- [435] K. Team, "Kolores: Effective training of diffusion model for photorealistic text-to-image synthesis," 2024. [29, 30, 31, 32](#)
- [436] Y. Skandarani, P.-M. Jodoin, and A. Lalande, "Gans for medical image synthesis: An empirical study," *Journal of Imaging*, vol. 9, no. 3, p. 69, 2023. [30](#)
- [437] Y. Wan, A. Subramonian, A. Ovalle, Z. Lin, A. Suvarna, C. Chance, H. Bansal, R. Pattichis, and K.-W. Chang, "Survey of bias in text-to-image generation: Definition, evaluation, and mitigation," *arXiv preprint arXiv:2404.01030*, 2024. [30](#)
- [438] J. Vice, N. Akhtar, R. Hartley, and A. Mian, "Quantifying bias in text-to-image generative models," *arXiv preprint arXiv:2312.13053*, 2023. [30](#)
- [439] D. Li, S. Wang, J. Zou, C. Tian, E. Nieuwburg, F. Sun, and E. Kanoulas, "Paint4poem: A dataset for artistic visualization of classical chinese poems," *arXiv preprint arXiv:2109.11682*, 2021. [30](#)
- [440] S. Kim, S. Jung, B. Kim, M. Choi, J. Shin, and J. Lee, "Safeguard text-to-image diffusion models with human feedback inversion," in *ECCV*, 2025. [30](#)
- [441] M. A. H. Palash, M. A. Al Nasim, A. Dhali, and F. Afrin, "Fine-grained image generation from bangla text description using attentional generative adversarial network," in *2021 IEEE International Conference on Robotics, Automation, Artificial-Intelligence and Internet-of-Things (RAAICON)*. IEEE, 2021, pp. 79–84. [30](#)
- [442] A. Jha, V. Prabhakaran, R. Denton, S. Laszlo, S. Dave, R. Qadri, C. Reddy, and S. Dev, "Visage: A global-scale analysis of visual stereotypes in text-to-image generation," in *Proceedings of the 62nd Annual Meeting of the Association for Computational Linguistics (Volume 1: Long Papers)*, 2024. [31](#)
- [443] F. Friedrich, K. Hämmerl, P. Schramowski, M. Brack, J. Libovicky, K. Kersting, and A. Fraser, "Multilingual text-to-image generation magnifies gender stereotypes and prompt engineering may not help you," *arXiv preprint arXiv:2401.16092*, 2024. [31](#)
- [444] M. Kim, H. Lee, B. Gong, H. Zhang, and S. J. Hwang, "Automatic jailbreaking of the text-to-image generative ai systems," *arXiv preprint arXiv:2405.16567*, 2024. [31](#)
- [445] A. Gu and T. Dao, "Mamba: Linear-time sequence modeling with selective state spaces," *arXiv preprint arXiv:2312.00752*, 2023. [33](#)
- [446] Y. Sun, X. Li, K. Dalal, J. Xu, A. Vikram, G. Zhang, Y. Dubois, X. Chen, X. Wang, S. Koyejo *et al.*, "Learning to (learn at test time): Rnns with expressive hidden states," *arXiv preprint arXiv:2407.04620*, 2024. [33](#)